Overview of Cordilleran oceanic terranes and their significance for the tectonic evolution of the northern Cordillera

A. Zagorevski[1*], C.R. van Staal[2], J.H. Bédard[3], A. Bogatu[4], D. Canil[5], M. Coleman[6], M. Golding[2], N.L. Joyce[1], C. Lawley[1], S. McGoldrick[5], M.G. Mihalynuk[2], D. Milidragovic[7], A. Parsons[8], and P. Schiarizza[7]

Zagorevski, A., van Staal, C.R., Bédard, J.H., Bogatu, A., Canil, D., Coleman, M., Golding, M., Joyce, N.L., Lawley, C., McGoldrick, S., Mihalynuk, M.G., Milidragovic, D., Parsons, A., and Schiarizza, P., 2021. Overview of Cordilleran oceanic terranes and their significance for the tectonic evolution of the northern Cordillera; in *Northern Cordillera geology: a synthesis of research from the Geo-mapping for Energy and Minerals program, British Columbia and Yukon, (ed.) J.J. Ryan and A. Zagorevski; Geological Survey of Canada, Bulletin 610, p. 21-65. https://doi.org/10.4095/326053*

Abstract: Ophiolite complexes are an important component of oceanic terranes in the northern Cordillera and constitute a significant amount of juvenile crust added to the Mesozoic Laurentian continental margin during Cordilleran orogenesis. Despite their tectonic importance, few systematic studies of these complexes have been conducted. Detailed studies of the pseudostratigraphy, age, geochemistry, and structural setting of ophiolitic rocks in the northern Cordillera indicate that ophiolites formed in Permian to Middle Triassic suprasubduction zone settings and were obducted onto passive margin sequences. Re-evaluation of ophiolite complexes highlights fundamental gaps in the understanding of the tectonic framework of the northern Cordillera. The previous inclusion of ophiolite complexes into generic 'oceanic' terranes resulted in significant challenges for stratigraphic nomenclature, led to incorrect terrane definitions, and resulted in flawed tectonic reconstructions.

Résumé : Les complexes ophiolitiques forment une composante importante des terranes océaniques de la Cordillère septentrionale et représentent une quantité importante de croûte juvénile ajoutée à la marge continentale de la Laurentie du Mésozoïque lors de l'orogenèse de la Cordillère. Malgré leur importance tectonique, peu d'études systématiques de ces complexes ont été menées. Des études détaillées de la pseudostratigraphie, de l'âge, de la géochimie et du cadre structural des roches ophiolitiques dans la Cordillère septentrionale indiquent que les ophiolites se sont formées dans des contextes de suprazone de subduction du Permien au Trias moyen et ont été obductées sur des séquences de marge passive. La réévaluation des complexes ophiolitiques met en évidence des lacunes fondamentales de notre compréhension du cadre tectonique de la Cordillère septentrionale. L'inclusion antérieure des complexes ophiolitiques dans des terranes « océaniques » génériques a entraîné des défis importants pour la nomenclature stratigraphique, a conduit à des définitions incorrectes des terranes et a donné lieu à des reconstitutions tectoniques fautives.

[1]Geological Survey of Canada, 601 Booth Street, Ottawa, Ontario K1A 0E8
[2]Geological Survey of Canada, 625 Robson Street, Vancouver, British Columbia V6B 5J3
[3]Geological Survey of Canada, 490, rue de la Couronne, Québec, Quebec G1K 9A9
[4]Département des sciences de la Terre et de l'atmosphère, Université du Québec à Montréal, C.P. 8888, succ. Centre-Ville, Montréal, Quebec H3C 3P8
[5]School of Earth and Ocean Sciences, University of Victoria, Victoria, British Columbia V8W 3P6
[6]Department of Earth and Environmental Sciences, University of Ottawa, 120 University, Ottawa, Ontario K1N 6N5
[7]British Columbia Geological Survey, 1810 Blanshard Street, Victoria, British Columbia V8T 4J1
[8]Department of Earth Sciences, University of Oxford, South Parks Road, Oxford OX1 3AN, United Kingdom
*Corresponding author: A. Zagorevski (email: alex.zagorevski@nrcan-rncan.gc.ca)

INTRODUCTION

Oceanic terranes in ancient orogenic belts are commonly identified by the presence of ophiolites or remnants thereof. Ophiolites are a ubiquitous and important component of Phanerozoic orogenic belts worldwide, and are fundamental in recognizing old suture or subduction zones. Understanding the origin of ophiolitic rocks has significantly evolved since they were first interpreted as remnants of ancient mid-ocean ridges (*see* review in Dilek, 2003). They are now thought to represent a variety of tectonic environments, including: hyperextended continental margins (e.g. Manatschal et al., 2011) and suprasubduction zone complexes that formed in arc and back-arc settings (e.g. Bédard et al., 1998; Zagorevski et al., 2006; Stern et al., 2012; Dilek and Furnes, 2014; Pearce, 2014). Preservation of normal mid-ocean-ridge ophiolites is extremely rare (Stern et al., 2012; Pearce, 2014), typically occurring as volumetrically minor scraped-off slabs in accretionary complexes (e.g. Kimura and Ludden, 1995).

The majority of ophiolitic rocks in the northern Cordillera are exposed in the Slide Mountain, Cache Creek, and Yukon-Tanana terranes (Fig. 1), where they represent the principal evidence of 'oceanic terranes'. These ophiolites are commonly interpreted as suprasubduction-zone ophiolites (e.g. Nelson, 1993; Piercey et al., 2001, 2004; Murphy et al., 2009), that is, ophiolites formed on the upper plate above a subduction zone; however, the majority of northern Cordilleran tectonic models interpret these ophiolites as vestiges of consumed ocean basins, thus placing them on the subducted plate during Cordilleran orogenesis (e.g. Slide Mountain Ocean: Nelson et al., 2006; Cache Creek Ocean: Mihalynuk et al., 1994, 2004a). This apparent contradiction between an upper plate origin and lower plate designation cannot be resolved without understanding the age and tectonic setting of the individual ophiolite massifs. In this contribution, the authors summarize the pseudostratigraphy, geochemistry, and geochronology of some ophiolite complexes in the Cache Creek, Slide Mountain, and Yukon-Tanana terranes. The authors discuss their significance with

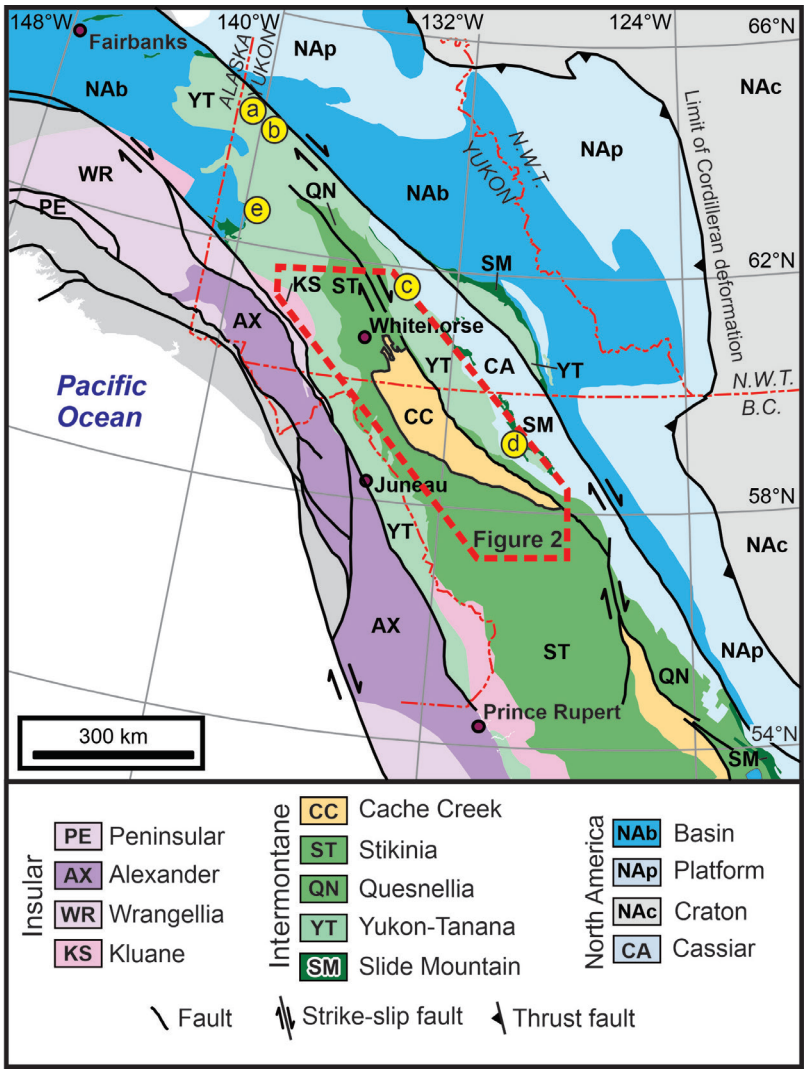

Figure 1. Lithotectonic map of northern Cordillera (Colpron and Nelson, 2011). a = Clinton Creek, b = Midnight Dome, c = Dunite Peak, d = Cassiar Mountains, e = Harzburgite Peak. Dashed red line is outline of Figure 2 geology map.

regard to the tectonic framework and genetic models of the northern Cordillera and then identify directions for future research.

OPHIOLITIC COMPLEXES IN YUKON AND BRITISH COLUMBIA

Many ophiolites are characterized by a pseudostratigraphy of ultramafic mantle rocks, ultramafic cumulate rocks, mafic cumulate rocks, isotropic gabbro, sheeted dykes, basalt, and overlying oceanic sediments (Anonymous, 1972). This classic Penrose-style pseudostratigraphy is not developed in some ophiolites due to low spreading rates, low magma productivity, and/or localization of strain along tectonic detachments (e.g. Miranda and Dilek, 2010). Alternatively, Penrose stratigraphy can be structurally disrupted during orogenesis. As such, ophiolites are commonly identified on the basis of a combination of some of the components, most characteristically, the presence of mantle tectonite and basalt. In this contribution, the authors discuss ophiolitic rocks and some juvenile arc sequences that form part of the Cache Creek, Slide Mountain, and Yukon-Tanana terranes (Fig. 1, 2). The Slide Mountain and Cache Creek terranes are defined as oceanic terranes and are generally interpreted as a peri-Laurentian back-arc basin and Panthalassa ocean floor, respectively, which were emplaced onto adjacent terranes during subduction and eventual collision (e.g. Nelson et al., 2013). Ophiolitic mafic-ultramafic complexes that are interpreted to have formed during the early stages of rifting of the Yukon-Tanana terrane from the Laurentian margin, and those that do not easily fit the model that was developed for the evolution of the Slide Mountain terrane (e.g. Colpron et al., 2006, 2007; Murphy et al., 2006) have been previously included in the Yukon-Tanana terrane as the Devonian to Mississippian Finlayson assemblage mafic-ultramafic complexes (Yukon Geological Survey, 2019).

Recent work by the present authors, summarized below, demonstrates that the existing terrane framework is at odds with recent data. In this paper, the authors contend that a radical reorganization of the terrane framework is needed in order to accurately reconstruct how the northern Cordillera formed. In the following sections, the geological relationships in the northern Cordillera are summarized, which constrain internal relationships within 'oceanic' terranes. These relationships indicate widespread preobduction, extensional tectonism in the Permo-Triassic suprasubduction zone ophiolites. The relationships between ophiolites and their adjacent terranes indicate that Permo-Triassic ophiolites were obducted onto adjacent terranes along shallow-dipping suture zones. These suture zones were not recognized in previous studies as terrane-bounding faults.

CACHE CREEK AND ATLIN TERRANES

The Cache Creek terrane was defined as a belt of 'oceanic' rocks that originated far outboard of the Laurentian margin in the Panthalassa Ocean (e.g. Monger and Ross, 1971; Monger, 1977a, b; Orchard et al., 2001). The most widely accepted model of the Cache Creek terrane postulates that subduction of Panthalassa ocean floor beneath the Stikinia-Quesnellia arc led to accretion of an exotic carbonate platform and obduction of the ophiolites, Kutcho-Sitlika arc, and oceanic sedimentary sequences from the subducting plate (e.g. Mihalynuk et al., 1994, 2004a). Detailed re-evaluation of the Cache Creek terrane indicated that the Paleozoic carbonate platform is a distinct terrane from the Permian to Middle Triassic ophiolites (Fig. 3; Zagorevski et al., 2015, 2016; cf. English and Johnston, 2005). Both terranes are overlapped by a Middle to Late Triassic assemblage comprising chert, siliciclastic rocks, and limestone (Fig. 3).

Previous assignment of ophiolitic rocks to the same terrane as the carbonate platform was based on a model in which ophiolites formed the basement to seamounts and carbonate platforms and/or atolls (Fig. 4; Monger, 1975; Monger et al., 1991); however, more recent studies conclusively demonstrate that these ophiolites are Middle Permian to Middle Triassic (Gordey et al., 1998; Devine, 2002; Mihalynuk et al., 2003) and are much too young to be the basement to the Early Carboniferous to Late Permian carbonate platform (Fig. 4b). Since much of the definition of the Cache Creek terrane and its origins hinges on the Paleozoic carbonate platform that contains warm-water (Tethyan) fossils (e.g. Monger and Ross, 1971; Sano et al., 2001), this paper retains the Cache Creek terrane for the Paleozoic carbonate platform. In northern British Columbia and southern Yukon, this carbonate platform comprises the Horsefeed and Teslin formations as well as interbedded mafic volcanic rocks of the French Range Formation (Monger, 1975; Mihalynuk and Smith, 1992; Mihalynuk and Cordey, 1997; Mihalynuk et al., 2003, 2004a). Discontinuous volcanic horizons within the Horsefeed Formation do not constitute a regionally mappable formation on their own; as such they are herein included within the Horsefeed Formation (*see* Appendix A).

Middle Permian to Middle Triassic ophiolitic rocks formed in a distinctly different tectonic setting than the Cache Creek terrane carbonate platform (*see* 'Geochemical characteristics of ophiolites' below). Hence, they are herein excluded from the Cache Creek terrane and instead included in the Atlin terrane. The Atlin terrane was one of the early synonyms for the Cache Creek Group and the Cache Creek terrane (Monger, 1975), but was subsequently abandoned. The present authors use Atlin as the type locality for the Atlin terrane ophiolitic rocks because excellent exposures are relatively easily accessed on Monarch and Union mountains, near the town of Atlin. Atlin terrane ophiolites typically form very large (tens to hundreds of square kilometres),

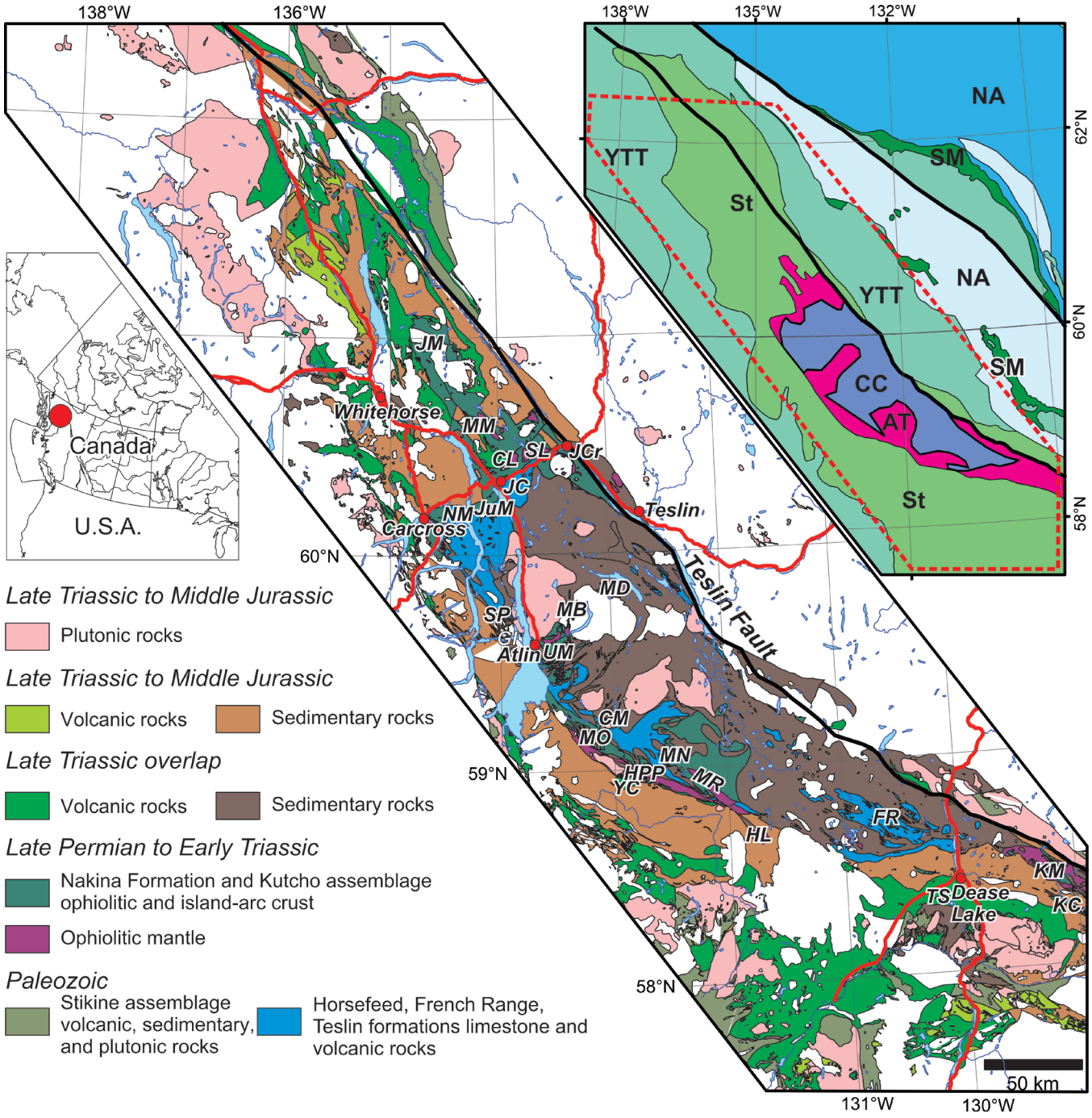

Figure 2. Simplified geology of the Atlin and Cache Creek terranes and their overlap assemblages (*modified from* Cui et al., 2017; Yukon Geological Survey, 2019; terrane map *modified from* Colpron and Nelson, 2011). Dashed red outline on terrane map shows area of geology map. CL = Cabin Lake, CM = Chikoida Mountain, FR = French Range, GI = Graham Inlet, HL = Haitin Lake, HPP = Hardluck and Peridotite peaks, JC = Jake's Corner, JCr = Johnson's Crossing, JM = Joe Mountain, JuM = Jubilee Mountain, KC = Kutcho Creek, KM = King Mountain, MB = Mount Barham, MD = Marble Dome, MM = Mount Michie, MN = Nimbus Mountain, MO = Mount O'Keefe, MR = Menatatuline Range, NM = Nares Mountain, SL = Squanga Lake, SP = Sunday Peak, TS = Tsaybahe, UM = Union and Monarch mountains, YC = Yeth Creek, YTT = Yukon-Tanana terrane, St = Stikinia, NA = North America, SM = Slide Mountain terrane, CC = Cache Creek terrane (revised), AT = Atlin terrane (new).

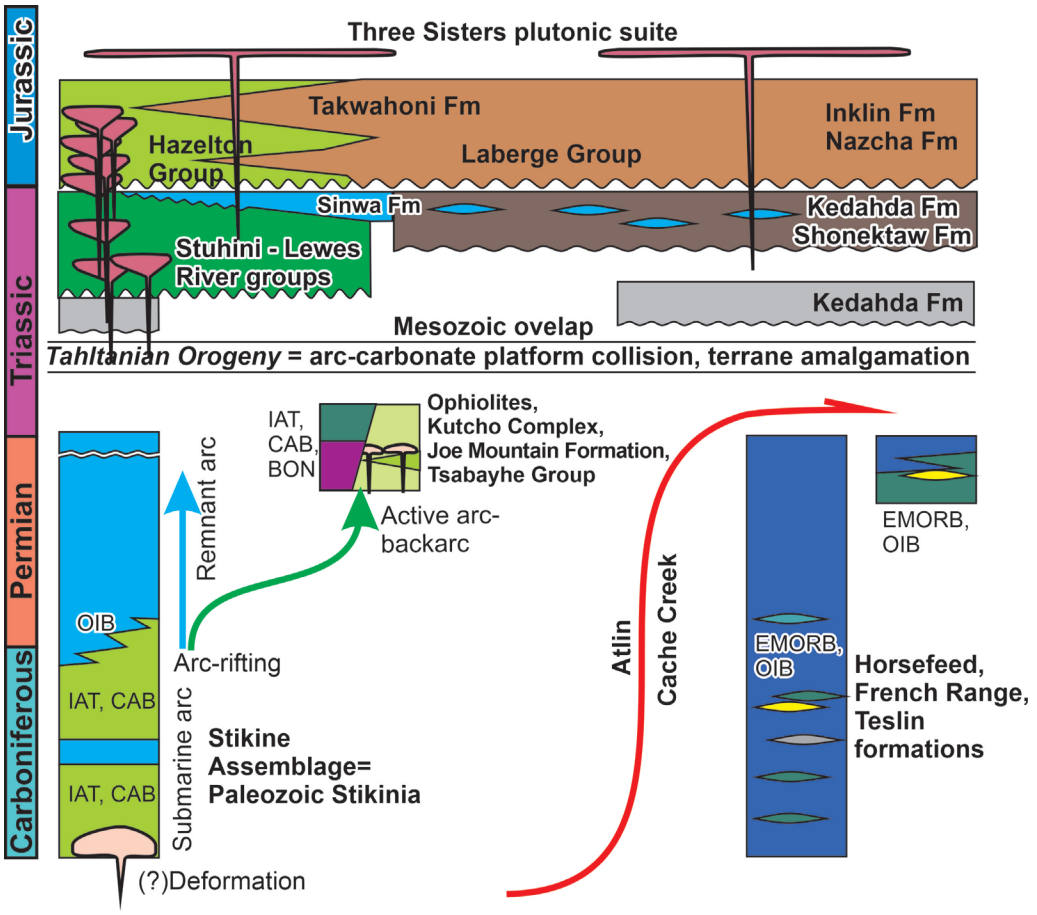

Figure 3. Simplified tectonostratigraphy of the Atlin and Cache Creek terranes and their overlap assemblages (cf. Fig. 8.75 in Monger et al., 1991). IAT = island-arc tholeiite, CAB = calc-alkaline basalt, BON = boninite, E-MORB = enriched mid-ocean-ridge basalt, OIB = ocean-island basalt

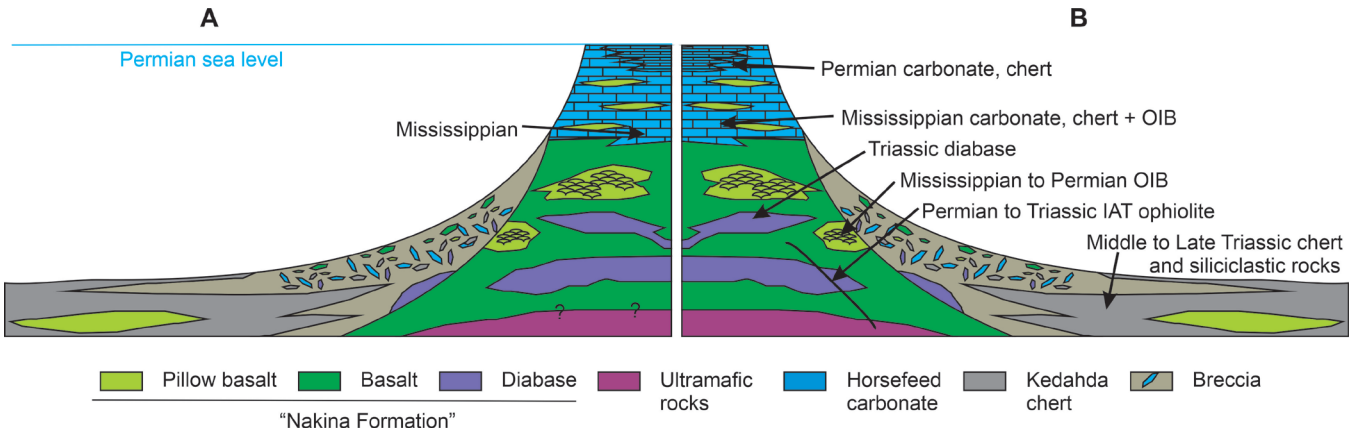

Figure 4. Schematic diagram showing relationships between various oceanic components in the Cache Creek terrane as interpreted by Monger et al. (1991) (A). New data indicate that this model is ultimately incorrect because it groups distinct tectonic settings across different ages (B). Modified from Monger et al. (1991). OIB = ocean-island basalt, IAT = island-arc tholeiite

discontinuous massifs structurally lying above the Jurassic Nahlin Fault, and isolated massifs and slivers elsewhere. Previously recognized Kutcho–Sitlika–Joe Mountain arc rocks occur to the southwest of the Nahlin Fault in British Columbia and north of the Cache Creek terrane carbonate platform in Yukon (Jobin-Bevans, 1995; Hart, 1997; English et al., 2010; Schiarizza, 2012; Bickerton, 2013; Bickerton et al., 2013; Bordet, 2017, 2018; Bordet et al., 2019). These arc rocks were previously included in the Cache Creek (Kutcho-Sitlika) and Stikinia (Joe Mountain) terranes. They are herein included in the Atlin terrane. In the following sections, the present authors briefly summarize geological relationships within the Atlin terrane, between the Atlin and Cache Creek terranes, and between these terranes and their overlap assemblage, starting in the King Mountain area.

King Mountain area

The King Mountain (Fig. 2) area preserves the most complete, albeit structurally disrupted, ophiolite succession in the northern Cordillera, including mantle tectonite, layered mafic-ultramafic cumulate rocks, layered mafic cumulate rocks, isotropic gabbro, and sheeted dyke zones (Fig. 5) of a Penrose-style ophiolite (Anonymous, 1972). The mantle zone comprises strongly serpentinized massive harzburgite, foliated refractory harzburgite tectonite, with minor pyroxenite, and dunite dykes and pods (Fig. 5a). Mantle rocks can be difficult to distinguish from the ultramafic cumulate rocks, which typically comprise strongly layered dunite, harzburgite, and locally abundant websterite (Fig. 5b), gabbro-norite, and gabbro pegmatite.

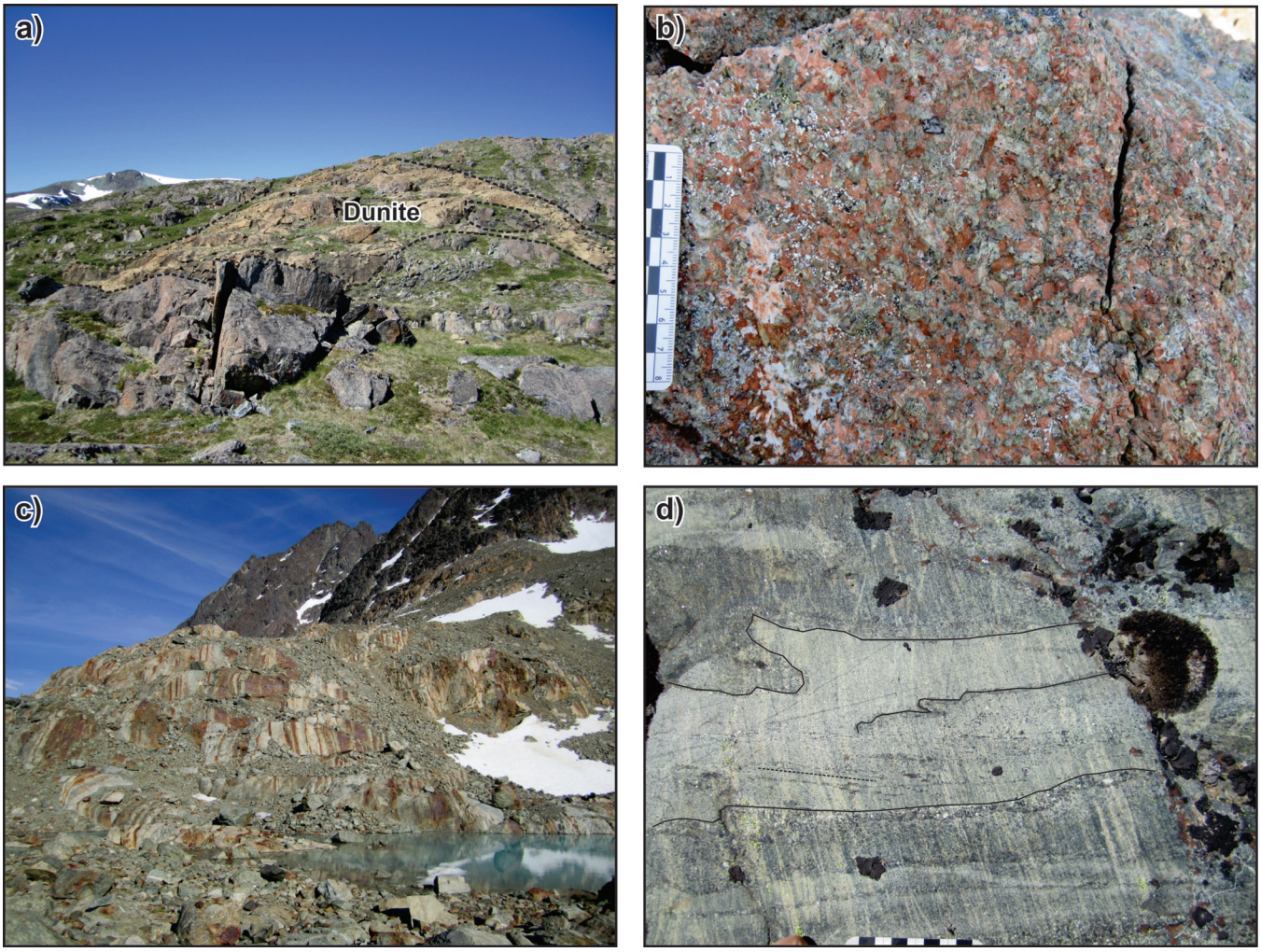

Figure 5. Representative photographs of the Atlin terrane in the King Mountain area. **a)** Mantle harzburgite cut by dunite (outlined by dashed line). NRCan photo 2019-681. **b)** Websterite from layered ultramafic cumulate zone; scale in centimetres. NRCan photo 2019-682. **c)** Layered cumulate gabbro on King Mountain, notice that the layering is not visible in the surrounding weathered peaks. NRCan photo 2019-683. **d)** Ductile deformation in layered gabbro. Foliation is oblique to cumulate layering (indicated by solid lines). Axial-planar foliation is indicated by dashed line; scale in centimetres. NRCan photo 2019-684

Figure 5. (cont.) Representative photographs of the Atlin terrane in the King Mountain area. **e)** Gabbro-sheeted dyke transition zone characterized by coarse- to fine-grained gabbro dykes; mountaineering axe for scale approximately 3 cm across the wider axis. NRCan photo 2019-685. **f)** Typical exposure of the sheeted dyke complex near Dozy Marmot Ridge characterized by blocky, aphanitic mafic boulders; marmot is approximately 50 cm long. NRCan photo 2019-686. Inset: dyke contacts (solid lines) in sheeted dyke complex; red Sharpie™ is 14 cm long. NRCan photo 2019-687. **g)** Jurassic imbrication of Triassic suture zone. Suture is characterized by emplacement of mantle over carbonate platform. Jurassic thrusts imbricate the suture and pre-existing thrust stack (blue D_1 thrust) and are commonly characterized by young over old, or deep over shallow relationships (red D_2 thrusts). NRCan photo 2019-688. **h)** Jurassic imbrication of ophiolite emplaces sheeted dyke complex over ultramafic cumulate zone along steeply north-northeast-dipping thrust faults (red line). NRCan photo 2019-689. All photographs by A. Zagorevski.

The layered mafic cumulate zone is spectacularly exposed on the north side of King Mountain (Fig. 5c, d; Gabrielse, 1998; Bédard et al., 2016; Zagorevski et al., 2016). Layered gabbro-norite grades into isotropic gabbro with minor tonalite and trondhjemite pods and dykes (ca. 255 Ma crystallization age: N. Joyce, unpub. data, 2020). Gabbroic rocks are cut by and grade into fine-grained gabbro and diabase (Fig. 5e, f), which were previously mapped as basalt intruded by gabbro (Gabrielse, 1998). Careful re-examination of alpine exposures northeast of Letain Lake revealed numerous dyke contacts where vesicular basalt, basalt, diabase, and gabbro intrude each other (Fig. 5e, f). Alpine weathering and frost heaving fractured the rock along dyke contacts, making them difficult to measure, but on outcrop scale, the dyke contacts are subparallel, indicating that these rocks represent the sheeted dyke zone of an ophiolite. Although coherent sheeted dyke complex is exposed in several areas, extrusive ophiolitic basaltic rocks and ocean-floor sediments are poorly exposed in this area.

Many ultramafic rocks are highly depleted, typical of mantle harzburgite. Strongly layered ultramafic cumulate rocks, including websterite, have higher trace-element concentrations that are consistent with cumulate origin. Gabbroic rocks from the layered mafic cumulate zone are commonly characterized by extremely low trace-element abundances and have a boninitic affinity (not shown; Bédard et al.,

2016; Zagorevski, 2018). Fine-grained gabbro, diabase, and basalt dykes have a variety of geochemical characteristics (Fig. 6a), ranging from depleted U-shaped normal mid-ocean-ridge normalized profiles characteristic of boninites to flat normal mid-ocean-ridge basalt normalized rare-earth element (REE) profiles with strong Nb depletion characteristic of island-arc and back-arc tholeiites.

Subophiolite basement

Tectonostratigraphic relationships are complex, but are locally well exposed in the King Mountain area. The Atlin terrane ophiolites, Cache Creek terrane carbonate rocks, and younger rocks overlap sediments that are imbricated by at least two generations of thrust faults in this area. Although few age constraints are available on the strongly deformed and recrystallized Cache Creek terrane carbonate platform in this area, low-strain lenses preserve recrystallized coral, crinoid ossicles, fusulinids, as well as Serpukhovian to Moscovian conodonts (M. Golding, unpub. GSC Paleontological Report 4-MG-2019, 2019). Volcanic rocks that are locally interbedded with Paleozoic carbonate rocks are characterized by ocean-island basalt and enriched mid-ocean-ridge basalt (E-MORB) trace-element geochemical profiles, and are distinctly different from the Atlin terrane (Zagorevski, 2018). Chert and siliciclastic sediments of the Kedahda Formation (*see* Appendix A) are commonly imbricated with the ophiolite and carbonate platform; however, stratigraphic relationships are poorly exposed. Kedahda Formation siliciclastic rocks yielded Late Triassic to Early Jurassic youngest detrital zircon populations (N. Joyce, unpub. data, 2020), indicating that they form part of the Mesozoic overlap sequence, which was imbricated with the Atlin and Cache Creek terranes during the Early to Middle Jurassic D_2 deformation.

The D_1 thrusts are only locally preserved within the D_2 (or later) thrust panels. Shallowly dipping D_1 thrusts emplace Atlin terrane mantle tectonites onto the Cache Creek terrane carbonate platform. The D_1 thrusts are marked by variably wide zones of phyllonite and scaly serpentinite. South-directed D_2 thrust faults largely control the distribution of the rock units and define the main structural grain of this area, including the Nahlin and King Salmon faults. The D_2 thrusts imbricate Atlin terrane ophiolitic lithologies, Cache Creek terrane carbonate platform, and Mesozoic overlap assemblages (Fig. 5f). In general, D_2 thrust faults are characterized by steep, narrow zones of phyllonite and scaly serpentinite. The D_2 thrusts are difficult to distinguish from D_1 thrusts, but they are commonly steeper, preserve Mesozoic sedimentary rocks in their footwall (e.g. Nahlin Fault: Gabrielse, 1998), or display out-of-sequence relationships (e.g. sheeted dykes tectonically overlying mantle). Regional relationships suggest that the southwest-directed D_2 thrusts have the opposite vergence to the D_1 fold and thrust belt, which emplaced ophiolites over the carbonate platform (Fig. 5 in Zagorevski et al., 2015).

Nakina area

The Nakina area exposes the Hardluck Peak–Peridotite Peak massif and two ophiolitic outliers to the southwest of the Nahlin Fault (Yeth Creek and Hatin Lake; Fig. 2). The Hardluck Peak–Peridotite Peak massif comprises extensive exposures of mantle peridotite and hypabyssal to supracrustal rocks (Fig. 7). Mantle tectonite is characterized by weakly to strongly deformed, orthopyroxene porphyroclastic harzburgite that is interlayered with dunite and orthopyroxenite (Fig. 7a, b, c). Dunite and orthopyroxenite also form crosscutting dykes and pods. Dunite locally forms extensive replacive channels ranging from tens of metres to 100 m wide (Canil et al., 2006; McGoldrick et al., 2018). Lherzolite is present locally, and clinopyroxenite locally forms along orthopyroxenite dyke contacts (Fig. 7d). The transition from mantle to cumulate zones has been documented only in the Hardluck Peak area (Canil et al., 2004). There, the refractory mantle harzburgite grades up into a narrow dunite transition zone, followed by a well layered poikilitic harzburgite, websterite, gabbro-norite, and leucogabbro cumulates of tholeiitic affinity cut by diorite veins.

Elsewhere, this transition is marked by ductile boudins of gabbro in mantle tectonite, and reticulated cumulate gabbro dykes and vein sets that intrude variably serpentinized to fresh peridotite (Fig. 7e, f). A sample of cumulate gabbro collected from this area yielded a ca. 264 Ma U-Pb zircon crystallization age (N. Joyce, unpub. data, 2020), constraining the age of peridotite exhumation and mafic magmatism (Fig. 7f). In the Mount O'Keefe area, variably serpentinized and carbonatized mantle peridotite is intruded by fine-grained gabbro and diabase, and is structurally overlain by hypabyssal rocks (Fig. 7g). This indicates that this mantle was exhumed and cooled prior to emplacement of hypabyssal rocks.

Similar relationships are preserved in the Peridotite Peak area, where the mantle to upper crust transition is marked by a narrow interval of varitextured gabbro and brecciated hypabyssal rocks (Fig. 7h). Although fine-grained mafic rocks in the Peridotite Peak area have been generally mapped as extrusive basalt, many localities are composed of phaneritic diabase and microgabbro dykes. These observations indicate that the hypabyssal section of the ophiolite is more extensive than previously thought, and that there was at least local development of a true sheeted sill or dyke complex. Overall, the general lack of plutonic lower to middle ophiolitic crust, together with the common occurrence of hypabyssal mafic intrusive rocks within and above mantle rocks, are consistent with tectonic exhumation of the mantle coeval with magmatism in an oceanic core complex.

Cumulate ultramafic and gabbroic rocks (Zagorevski, 2018) yielded suprasubduction zone tholeiitic melts. Hypabyssal and volcanic rocks, including mafic dykes that cut mantle rocks, are characterized by flat to light rare-earth element (LREE)–enriched normalized trace-element profiles with Th enrichment and Nb depletion, characteristic of

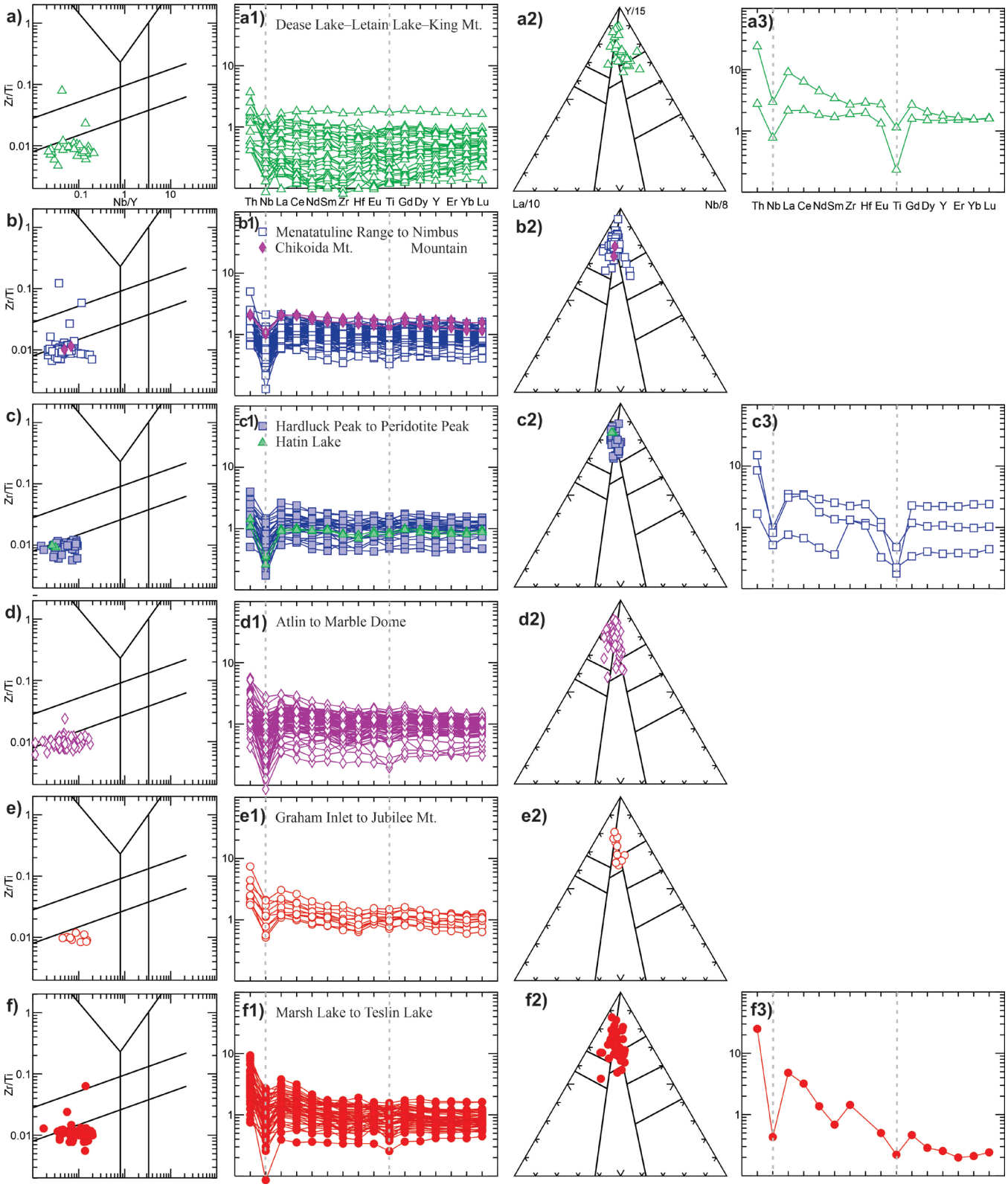

Figure 6. Geochemical characteristics of the Atlin terrane arranged southeast (top) to northwest (bottom). **a)** Dease Lake, Letain Lake, and King Mountain area. Rock-type discrimination plot (Pearce, 1996, 2014). **a1)** normal mid-ocean-ridge basalt normalized extended trace-element plot of mafic rocks (normalization: Sun and McDonough, 1989). **a2)** Basalt discrimination plot (Cabanis and Lecolle, 1989). **a3)** normal mid-ocean-ridge basalt normalized extended trace-element plot of felsic rocks (normalization: Sun and McDonough, 1989). **b)**, **b1)**, **b2)** Menatatuline Range, Nimbus Mountain, and Chikoida Mountain areas. **c)**, **c1)**, **c2)**, **c3)** Hardluck and Peridotite peaks and Hatin Lake areas. **d)**, **d1)**, **d2)** Atlin, Mount Barham, and Marble Dome areas. **e)**, **e1)**, **e2)** Graham Inlet, Turtle Lake, Nares Mountain, and Jubilee Mountain areas. **f)**, **f1)**, **f2)**, **f3)** Marsh Lake to Teslin Lake area.

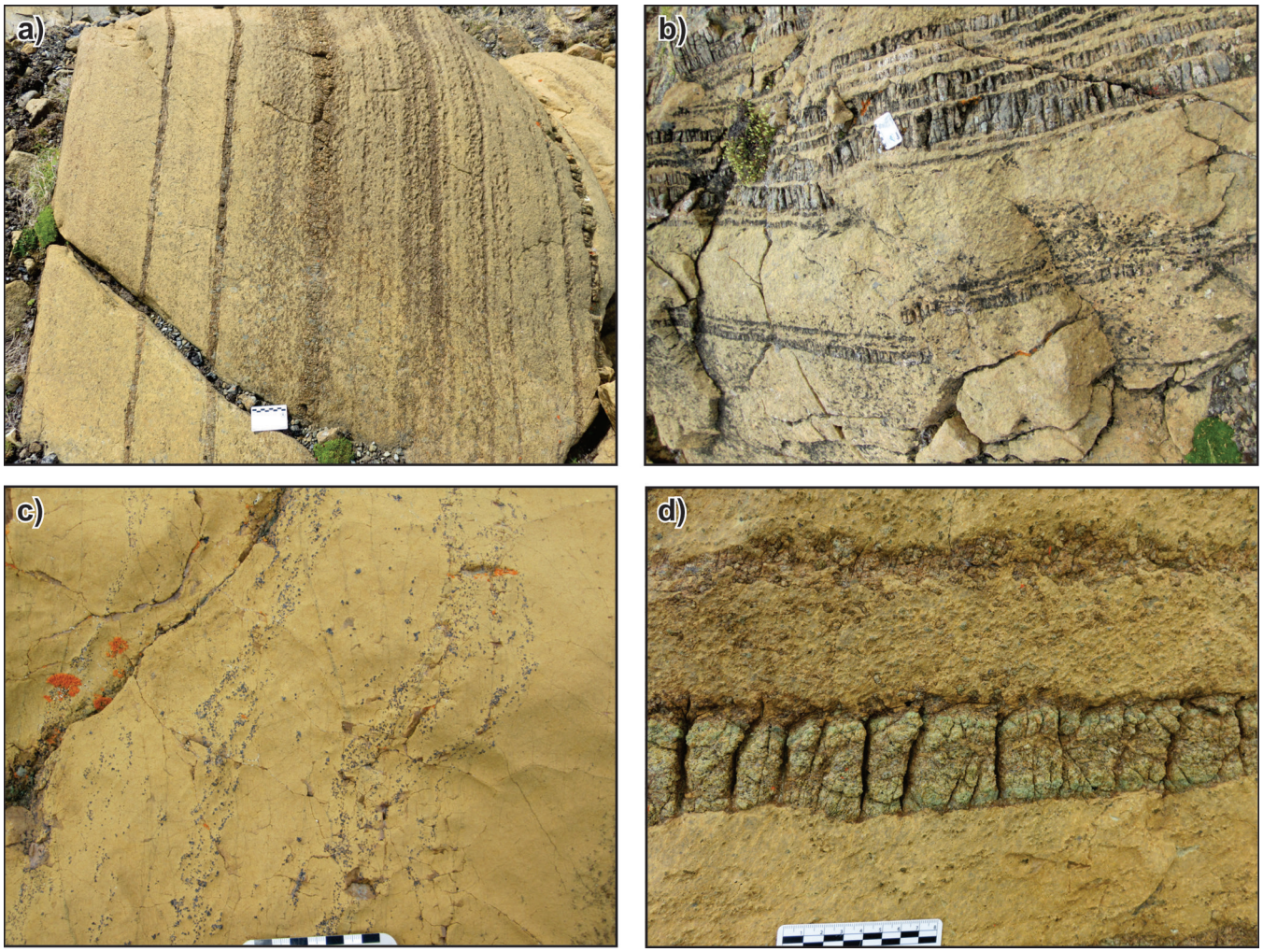

Figure 7. Representative photographs of the Atlin terrane in Hardluck Peak–Peridotite Peak massif. **a)** Typical mantle section consisting of transposed orthopyroxenite, dunite, and harzburgite; card for scale is in centimetres. NRCan photo 2019-690. **b)** Brittle faulting in mantle peridotite. Some pyroxenite bands are offset, whereas others are continuous; card for scale is in centimetres. NRCan photo 2019-691. **c)** Dunite with wisps of chromite records protracted history of melt-peridotite interaction; card for scale is in centimetres. NRCan photo 2019-692. **d)** Rare lherzolite and clinopyroxenite; card for scale is in centimetres. NRCan photo 2019-693

island-arc tholeiite and back-arc-basin basalt environments (Fig. 6c). Lithological relationships within the ophiolite and the chemical signatures suggest that the oceanic core complex formed in a suprasubduction zone ridge environment (McGoldrick et al., 2017).

Subophiolite basement

Clear subophiolitic basement relationships between ophiolite and Cache Creek terrane carbonate rocks are not preserved. In the Mount O'Keefe area, Paleozoic carbonate rocks as well as Middle to Late Triassic chert and siliciclastic rocks (Mihalynuk et al., 2003) are imbricated together with the ophiolitic rocks, presumably along D_2 or later thrust faults and late steep faults. Overall the relationships suggest that the Hardluck Peak–Peridotite Peak ophiolite was first structurally emplaced (obducted) onto the Cache Creek terrane carbonate platform (D_1) and subsequently re-imbricated (D_{2+}).

Yeth Creek and Hatin Lake areas

Outliers of the Atlin terrane ophiolites occur in Yeth Creek and Hatin Lake areas, to the southwest of the Nahlin Fault (Fig. 2). Previous interpretations suggested that the Nahlin Fault marks the terrane boundary with Stikinia in this region; however, the presence of ophiolitic rocks of the Atlin terrane on both sides of the Nahlin Fault indicate that it is not a terrane boundary (e.g. English, 2004). The Yeth Creek area lies structurally below the Nahlin Fault and is characterized by back-arc-basin basalt (Fig. 6, 8a, English et al., 2010). The Hatin Lake area was only briefly visited during regional

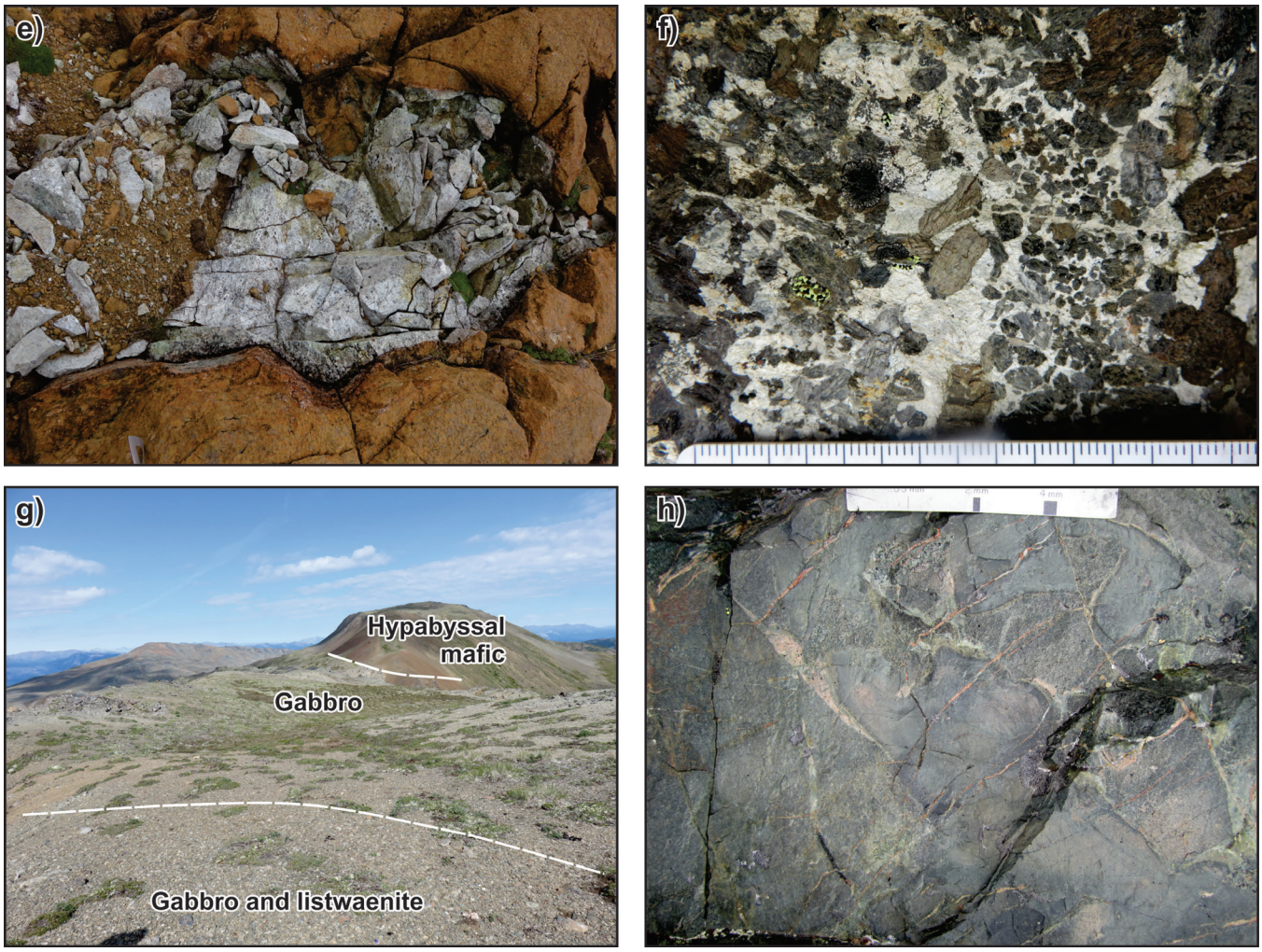

Figure 7. (cont.) Representative photographs of the Atlin terrane in Hardluck Peak–Peridotite Peak massif. **e)** Boudin of cumulate gabbro in mantle tectonite. Note scalloped margin, indicating ductile deformation in fresh harzburgite; tip of adze for scale is 1.5 cm across. NRCan photo 2019-694. **f)** Permian gabbro pegmatite intrudes Hardluck Peak–Peridotite Peak massif along the southern margin; smallest measure in scale is millimetres. NRCan photo 2019-695. This sample yielded ca. 264 Ma U-Pb zircon crystallization age (N. Joyce, unpub. data, 2020). **g)** View toward Mount O'Keefe; mafic unit is approximately 150 m high. NRCan photo 2019-696. Foreground is underlain by gabbro that intrudes serpentinize and listwaenite. Peak in the background is underlain by very fine-grained gabbro and basaltic dykes with screens of basalt and limestone. **h)** Hypabyssal breccia near the contact with varitextured gabbro and mantle hazrburgite, Peridotite Peak area. NRCan photo 2019-697. All photographs by A. Zagorevski.

reconnaissance and comprises harzburgite, dunite, and hypabyssal to extrusive mafic rocks (Fig. 8b). Mafic rocks yield island-arc tholeiite to back-arc-basin basalt trace-element profiles (Fig. 6c).

Subophiolite basement

Ophiolitic rocks occur as isolated inliers within the Jurassic Laberge Group sediments to the southwest of the Nahlin Fault. The structural basement to the ophiolitic inliers is not exposed.

Menatatuline Range–Nimbus Mountain area

A regionally extensive ophiolite massif comprising voluminous mantle peridotite, minor gabbro, hypabyssal rocks, and basalt is exposed in the Menatatuline Range and Nimbus Mountain area (Fig. 2). Menatatuline Range peridotite is characterized by abundant variably tectonized harzburgite, dunite, and orthopyroxenite (Fig. 9a–e; Terry, 1977; McGoldrick et al., 2018). Fine-grained mafic rocks are abundant and have been generally mapped as extrusive Nakina suite basalt (*see* Appendix A; Monger, 1975; Mihalynuk et al., 2003), even though some of these rocks are demonstrably intrusive (Fig. 9c, d, e). The transition from the mantle to the crustal section is best exposed on Nimbus Mountain,

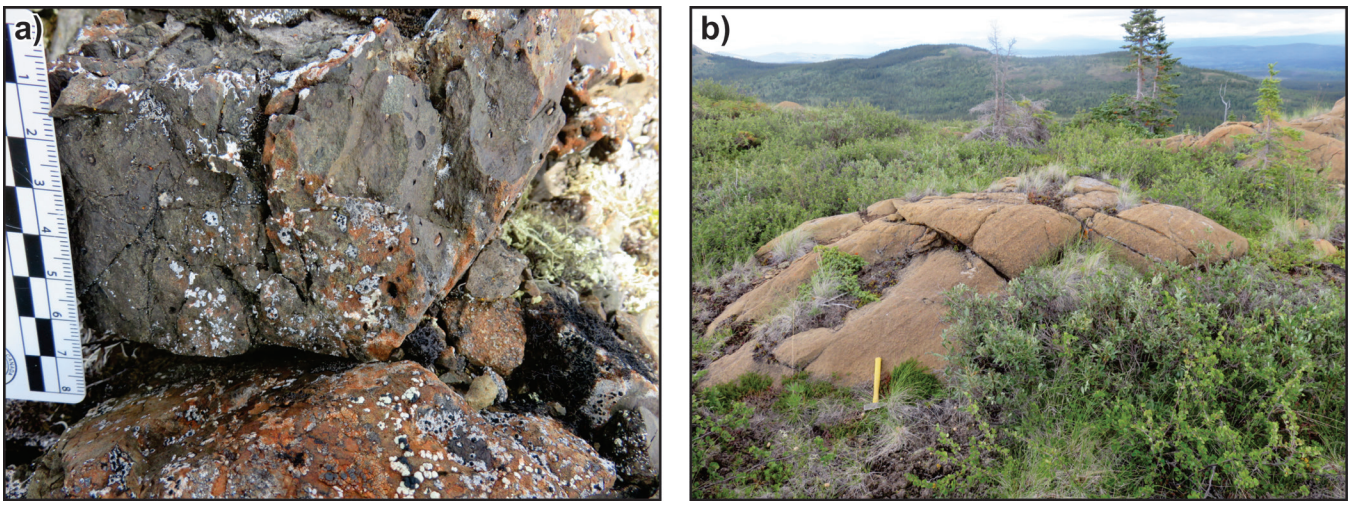

Figure 8. Representative photographs of the Atin terrane below the Nahlin Fault. **a)** Vesicular basalt breccia structurally below Nahlin Fault (Yeth Creek formation of Mihalynuk et al., 2004a); scale is in centimetres. NRCan photo 2019-698. **b)** Faint layering in Hatin Lake harzburgite; hammer handle for scale is 35 cm. NRCan photo 2019-699. All photographs by A. Zagorevski.

where variably serpentinized mantle peridotite is intruded by diabase and gabbro, which locally reacted to form rodingite (Fig. 9f). Deformation of gabbro and diabase dykes in the serpentinite has resulted in boudinage of the more competent mafic rocks within 'scaly' serpentinite and led to their interpretation as a subduction zone mélange (e.g. Mihalynuk et al., 2003); however, primary intrusive relationships between mafic intrusive rocks and peridotite can be observed in several localities where peridotite is relatively fresh, including on the flanks of Nimbus Mountain and on Nahlin Mountain. These intrusive relationships indicate that the mélange-like appearance is the result of deformation of units of radically different competency. As such, these rocks are best described as a 'broken formation' (Raymond, 1984) and they do not represent a subduction zone mélange. Crustal rocks on Nimbus Mountain intrude into and overlie the mantle section (Fig. 9g) and comprise medium- to fine-grained gabbro and diabase. Gabbroic rocks in Tseta Creek and on Nimbus Mountain have yielded ca. 261 Ma and 255 Ma U-Pb zircon ages constraining the age of mafic magmatism in the ophiolite (Devine, 2002; Mihalynuk et al., 2003). The middle and lower ophiolitic crust is not preserved (Fig. 9g), suggesting that the Menatatuline Range and Nimbus Mountain likely form part of an oceanic core complex, similar to other areas of the Atlin terrane.

Hypabyssal and volcanic rocks, including geochemically similar mafic dykes that cut mantle harzburgite, are characterized by flat to LREE-enriched normal mid-ocean-ridge basalt normalized trace-element profiles with Th enrichment and a negative Nb anomaly characteristic of island-arc tholeiite and back-arc-basin basalt (Fig. 6). Lithological relationships within the ophiolite and chemical characteristics of the basalt indicate a suprasubduction zone spreading ridge environment (McGoldrick et al., 2017).

Subophiolite basement

Similar to the King Mountain–Letain Lake area, Menatatuline Range and Nimbus Mountain areas are imbricated by several generations of thrusts, commonly leading to complex and confusing relationships; however, Nimbus Mountain does appear to preserve the early D_1 tectonic relationship between Permo-Triassic ophiolite and its underthrust Paleozoic Horsefeed Formation footwall (Fig. 9g). In this area, serpentinized mantle tectonite is thrust above massive Horsefeed Formation limestone, which yielded Serpukhovian and Bashkirian conodont ages (M. Golding, unpub. report, 2020). Limestone is interbedded with ocean-island basalt breccia that also contains blocks of limestone (Devine, 2002). The structural position of the ophiolite above the carbonate and ocean-island basalt platform indicates that the Atlin terrane was obducted onto the Horsefeed Formation carbonate platform. Nearby sedimentary rocks comprise interbedded chert and fine-grained siliciclastic rocks. These sedimentary rocks were previously interpreted as Paleozoic; however, they contain Late Triassic zircon crystals, indicating they are part of the unconformably overlying Mesozoic overlap assemblage (Devine, 2002; Breitsprecher and Mortensen, 2004; N. Joyce, unpub. data, 2020). The presence of Late Triassic sedimentary rocks requires that some thrust imbrication is Late Triassic or younger.

Atlin area

The Atlin area exposes several large ophiolite massifs and, similar to other areas described herein, is imbricated by several generations of thrusts. Nonetheless, Union Mountain, Mount Barham, and Marble Dome massifs display key relationships critical to understanding the regional tectonostratigraphy. Variably serpentinized ultramafic rocks,

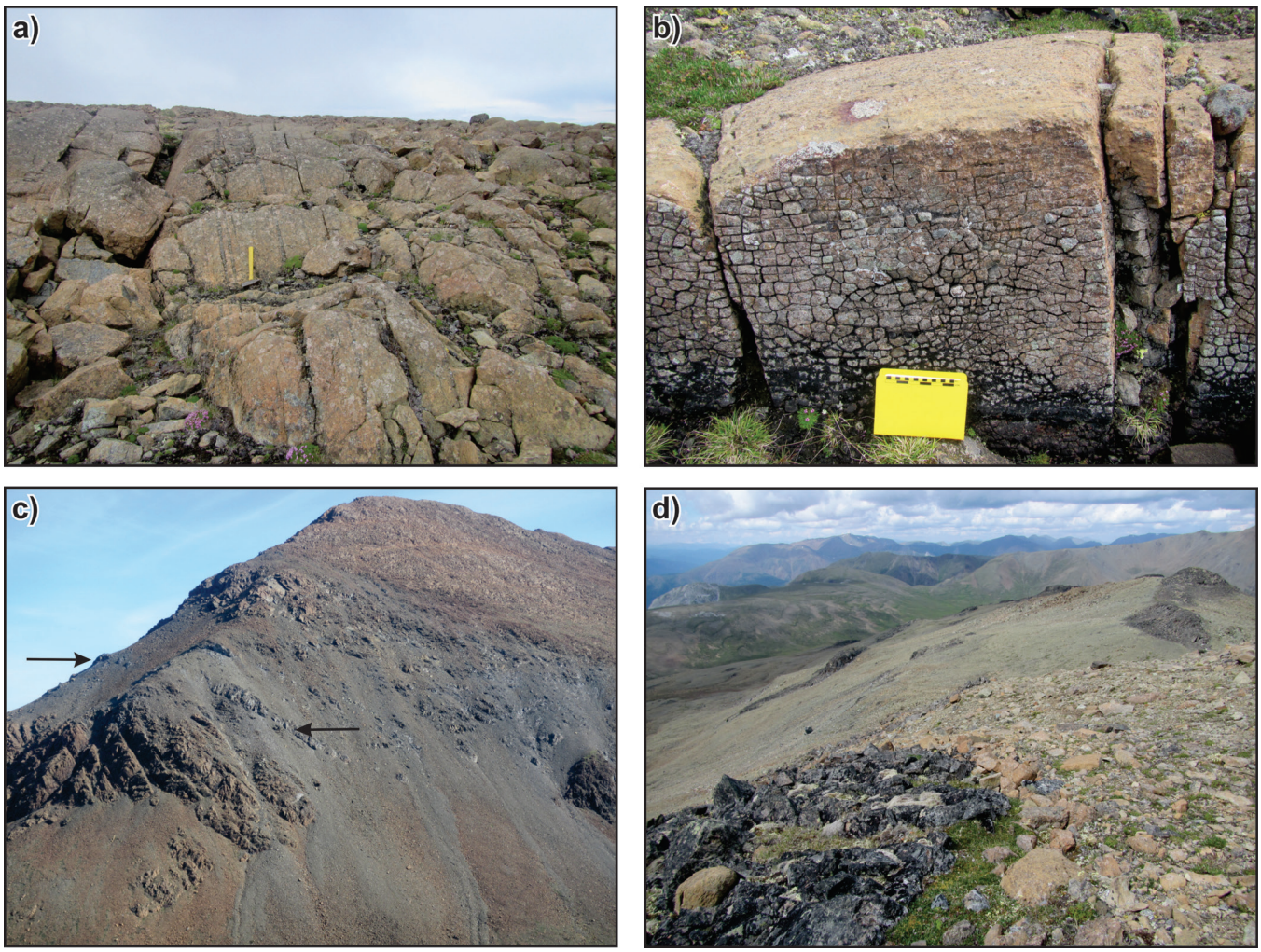

Figure 9. Representative photographs of the Atlin terrane in the Menatatuline Range–Nimbus Mountain area. **a)** Typical mantle section consisting of transposed orthopyroxenite, dunite, and harzburgite; hammer handle is 35 cm. NRCan photo 2019-700. **b)** Characteristic chocolate-tablet texture of pyroxenite dyke along its margin. Serpentinization results in volume gain in the host peridotite, and pyroxenite dykes are extended as a result. Long edge of book for scale is 20 cm NRCan photo 2019-701. **c)** Variably serpentinized mantle with gabbroic dykes (arrows). Elevation change from base of photo to top is about 200 m. NRCan photo 2019-702. **d)** Resistant dark grey gabbro dykes intruding dun mantle. In areas where mantle is extensively serpentinized, these dykes can be confused with basalt knockers in serpentinite mélange. Foreground at bottom of photo approximately 3 m wide. NRCan photo 2019-703

hypabyssal mafic rocks, and minor basalt are exposed on Union Mountain and Mount Barham (Fig. 10a, b, c). Ultramafic rocks comprise harzburgite, dunite, and orthopyroxenite (e.g. Ash, 1994), all of which are intruded by diabase and gabbro dykes (Fig. 10b). Structurally overlying crustal rocks comprise very fine-grained sheeted gabbro and diabase sill or dyke complexes with minor screens of intervening basalt (Fig. 10d) and chert. The contact between crust and mantle is locally marked by a 'mélange'–block-in-matrix unit comprising clasts of mantle and crustal lithologies in a serpentinite matrix (Fig. 10c, e). Since this mélange occurs at the contact between mantle and upper crust (Fig. 10a), it either represents a tectonic mélange that formed along a fault or detachment or a sedimentary mélange (olistostrome) that formed following exhumation of the mantle onto the seafloor. The presence of hypabyssal dykes in the mantle section is consistent with either interpretation as it requires exhumation and cooling of the host peridotites prior to intrusion by gabbro and diabase. The apparent absence of a cumulate crustal section is consistent either with a very slow spreading environment, and/or with tectonic excision in an oceanic core complex. Age constraints on the mafic magmatism are poor, but a screen of chert in the sill complex on Union Mountain yielded Late Permian radiolaria (F. Cordey, unpub. report, 2017).

A previous study of the Atlin area (Ash, 1994) inferred a mid-ocean-ridge paleotectonic setting; however, at the time of that study, the detection limits for key high field-strength

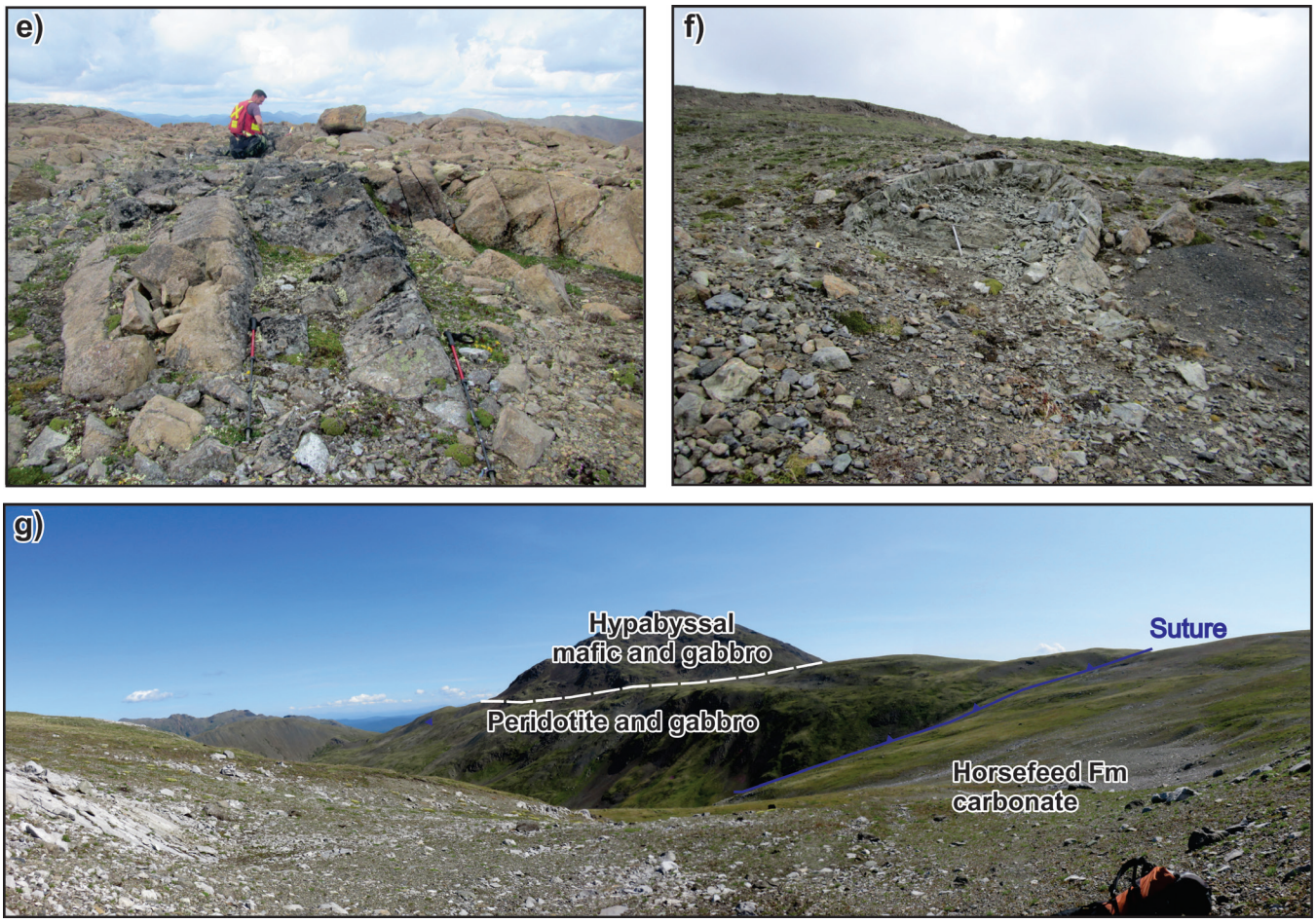

Figure 9. (cont.) Representative photographs of the Atlin terrane in the Menatatuline Range–Nimbus Mountain area. **e)** Well defined margins on a gabbro dyke indicate that the host mantle was cold at the time of the dyke emplacement. Hammer in front of geologist is 35 cm. NRCan photo 2017-704. **f)** Egg-shaped, rogingitized gabbro intrusion in serpentinized mantle can be mistaken for a knocker in serpentinite mélange matrix. The length of the shaft on the mountaineering axe is 60 cm. NRCan photo 2019-705. **g)** Nimbus Mountain exposes Permian ophiolite that was emplaced on top of Paleozoic Horsefeed Formation limestone and basalt. This contact is likely a reactivated suture zone. The ophiolite in this area comprises serpentinized mantle that is intruded by gabbro and diabase and is overlain by microgabbro and fine-grained hypabyssal mafic rocks. The transition from mantle to upper crustal lithologies suggests that this part of the ophiolite formed in an oceanic core complex. Mafic unit is approximately 200 m. Composite of NRCan photographs 2019-706, 2019-708, 2019-709. Photographs by S. McGoldrick (a–d) and A. Zagorevski (e–g).

elements (HFSE: e.g. Th and Nb) were too high to allow their use as reliable paleotectonic setting indicators (Pearce, 2014). The present authors' new analyses indicate that hypabyssal and volcanic rocks, including mafic dykes that cut the mantle section, are characterized by flat to LREE-enriched normal mid-ocean-ridge basalt normalized trace-element profiles with Th enrichments and negative Nb anomalies characteristic or island-arc tholeiite and back-arc-basin basalt (Fig. 6). The chemical characteristics of basalts and dykes in the Atlin area thus indicate a suprasubduction zone ridge environment.

Subophiolite basement

Whereas Mount Barham and Union Mountain preserve good relationships within the crustal section of the ophiolite, Marble Dome preserves the tectonic relationship between the ophiolite and its Cache Creek terrane structural basement. Despite its name, Marble Dome is mainly characterized by imbricated serpenitinized peridotite, hypabyssal mafic rocks, and minor basalt. Massive marble occurs at lower elevations and structurally underlies ophiolitic rocks (Fig. 10f, g). This marble is correlated with the Permian Teslin Formation limestone, exposed to the east along Hall Lake (Monger, 1975; Mihalynuk and Cordey, 1997). The base of the ophiolite section on the northeast flank of the Marble Dome is marked by a thin (about 50 m maximum

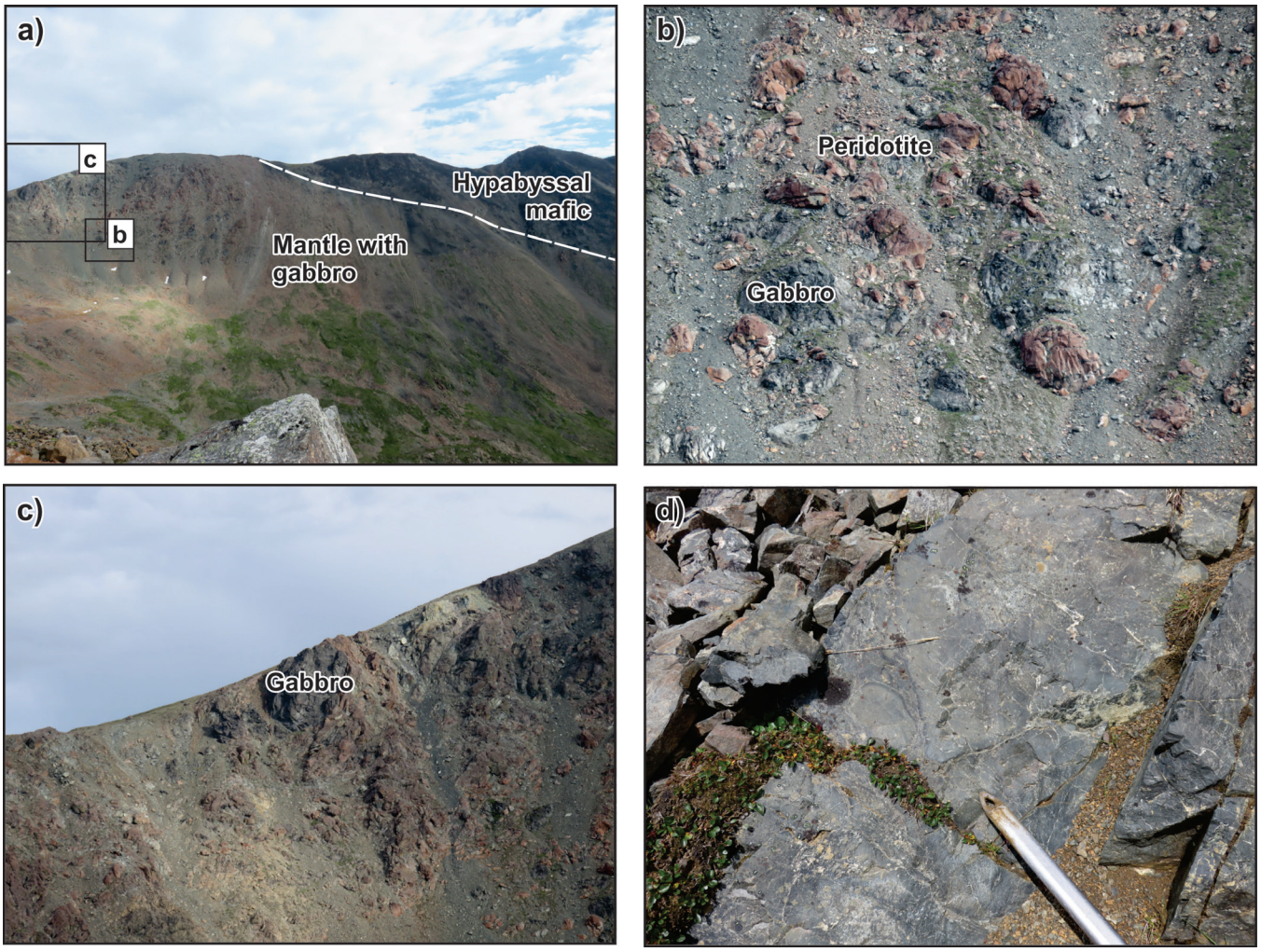

Figure 10. Representative photographs of the Atlin terrane in Atlin area. **a)** Crust-mantle transition near Mount Barham. Ridge in the background is about 1.5 km across. NRCan photo 2019-710. **b)** Harzburgite is intruded by fine- to medium-grained gabbro (width of field of view at bottom of photo 80 m across; NRCan photo 2019-711) and **c)** grades into gabbro-peridotite-serpentinite breccia (approximate length of section of ridge is 275 m; NRCan photo 2019-712) and **d)** is overlain by hypabyssal to volcanic rocks of the Nakina suite (shaft of tool is 3 cm wide; NRCan photo 2019-713).

thickness; Fig. 10h) unit of amphibolite mylonite with an ocean-island basalt geochemical signature. The ocean-island basalt–like geochemical signature suggests that the amphibolite mylonite was originally associated with the Cache Creek terrane volcanic rocks, such as the French Range Formation (Mihalynuk and Cordey, 1997). The higher metamorphic grade of the amphibolite relative to the nearby units suggests that the amphibolite forms part of a discontinuous sole to the Atlin terrane ophiolites.

Graham Inlet to Jubilee Mountain

The northwestern edge of the Cache Creek and Atlin terranes preserves scarce exposures of ophiolitic rocks near Graham Inlet, Sunday Peak, and at Nares and Jubilee mountains. The Graham Inlet and Sunday Peak areas contain several fault-bounded slivers of peridotite (Fig. 11a, b), diabase dykes, and massive to pillowed basalt (Fig. 11c), which are unconformably overlain by the Cretaceous Windy Table Group volcanic rocks (Zagorevski et al., 2017; Mihalynuk et al., 2018). Relationships between crustal and mantle rocks are obscured by Cretaceous faulting. Mihalynuk et al. (1999) suggested a minimum Middle Triassic age for the basalt units based on poorly preserved radiolaria in overlying chert with volcanogenic wacke interbeds. A previous study of the Graham Inlet area inferred a mid-ocean-ridge paleotectonic setting (Mihalynuk et al., 1999); however, at the time of that study, the detection limits for key high field-strength elements (HFSE; e.g. Th and Nb) were too high to allow their use as paleotectonic setting indicators (Pearce, 2014). Recent analyses of volcanic and hypabyssal rocks indicate that they are characterized by flat to LREE-enriched normal mid-ocean-ridge basalt normalized trace-element profiles

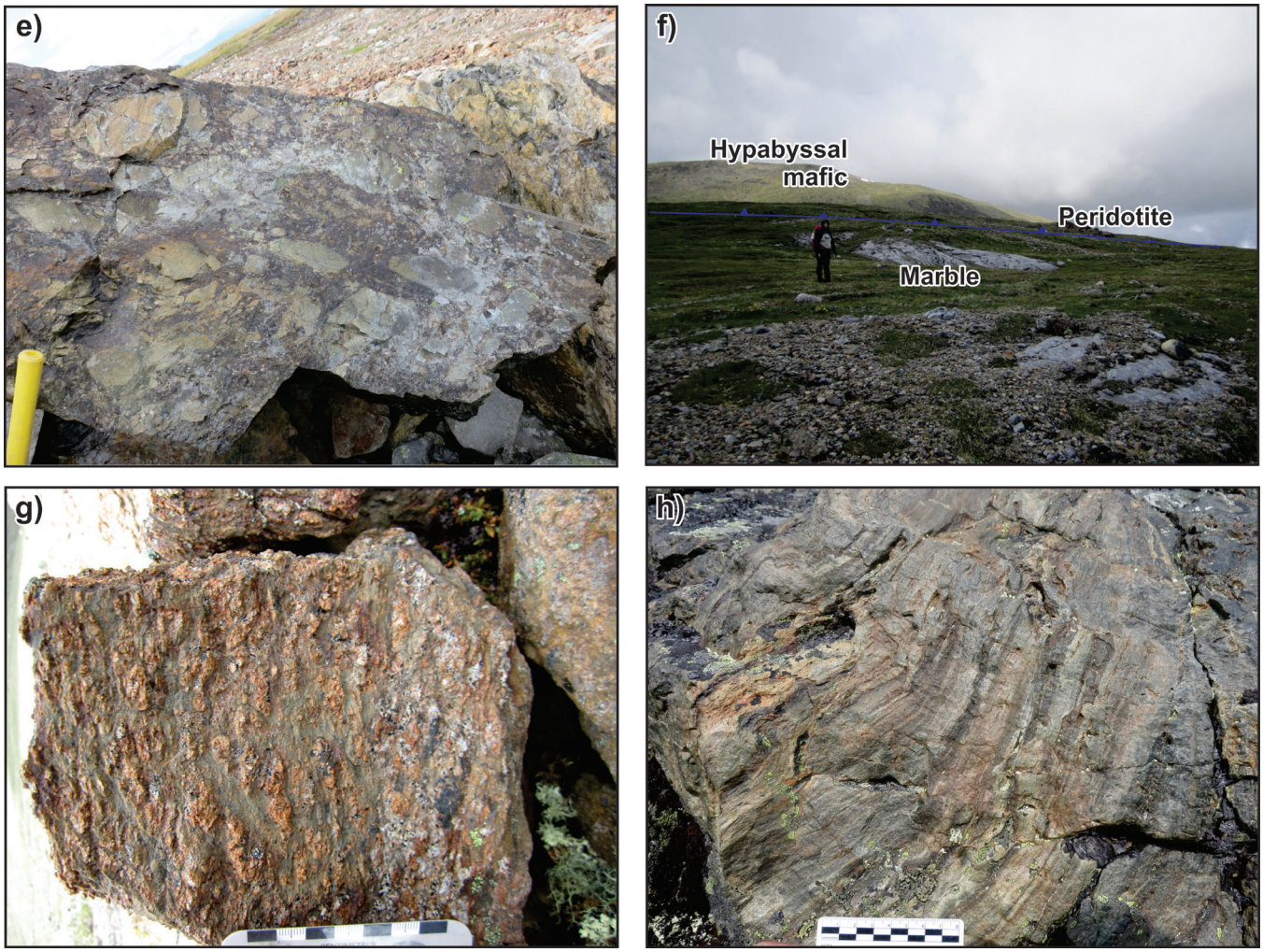

Figure 10. (cont.) Representative photographs of the Atlin terrane in Atlin area. **e)** Harzburgite breccia at the crust-mantle contact on Union Mountain, Atlin; handle for scale is 3.5 cm across. NRCan photo 2019-714. **f)** Ophiolite-footwall relationship on Marble Dome. Geologist is about 170 cm. NRCan photo 2019-715. **g)** Marble derived from Paleozoic Teslin Formation is structurally overlain by deformed and serpentinized harzburgite, which is intruded by gabbro and structurally imbricated with Nakina suite volcanic and hypabyssal basalt. Scale in centimetres. NRCan photo 2019-716. **h)** The contact between marble and harzburgite is locally marked by amphibolite mylonite with ocean-island basalt chemistry. Scale in centimetres. NRCan photo 2019-717. All photographs by A. Zagorevski.

with Th enrichment and a negative Nb anomaly characteristic of island-arc tholeiite and back-arc-basin basalt (Fig. 6; Zagorevski et al., 2017; Mihalynuk et al., 2018).

Nares Mountain was only sampled during regional reconnaissance, and clear contact relationships could not be established. Nares Mountain is underlain by limestone, chert, minor ultramafic rocks, and cumulate gabbro. Gabbro is LREE depleted, as is typical of cumulate gabbro in suprasubduction zone ophiolites (e.g. Lissenberg et al., 2004).

Jubilee Mountain is underlain by a structurally disrupted ophiolite sequence with locally well preserved mantle harzburgite, dunite, and pyroxenite. In other areas on Jubilee Mountain, ultramafic rocks are characterized by scaly or mylonitic serpentinite with centimetre- to decametre-scale clasts and blocks of peridotite, gabbro, and chert (Fig. 11d). The peak of Jubilee Mountain is underlain by hypabyssal rocks that form a sheeted dyke or sill complex (Fig. 11e). The local presence of ultramafic rocks within the sheeted dykes suggests that the dykes were directly emplaced into exhumed serpentinitized mantle or a serpentinite regolith. Hypabyssal rocks and gabbro within the serpentinite are characterized by flat to LREE-enriched normal mid-ocean-ridge basalt normalized trace-element profiles with Th enrichment and a negative Nb anomaly characteristic of island-arc tholeiite and back-arc-basin basalt (Fig. 6). This suggests that this area also formed in a suprasubduction environment.

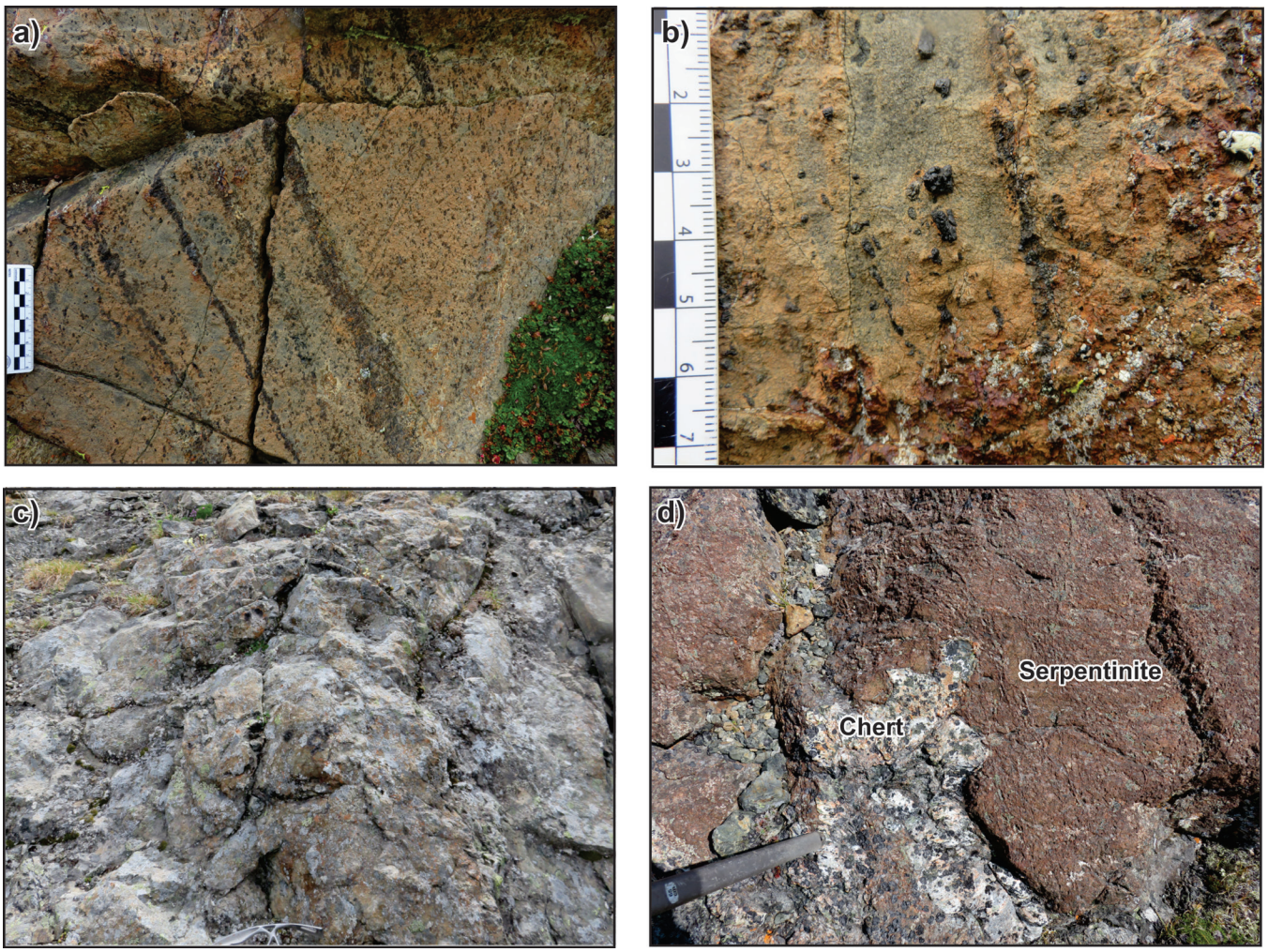

Figure 11. Representative photographs of the Atlin terrane in Graham Inlet to Jubilee Mountain area; **a)** Transposed pyroxenite dykes in mantle harzburgite, Sunday Peak; scale in centimetres. NRCan photo 2019-718. **b)** Detail of coarse chromite in dunite; scale in centimetres. NRCan photo 2019-719. **c)** Island-arc tholeiite–back-arc-basin basalt environments pillow basalt adjacent to mantle harzburgite. Mountaineering axe head is 27 cm. NRCan photo 2019-720. On Sunday Peak, the contact is a Late Cretaceous fault. **d)** Fluidal block of chert in serpentine matrix. Mountaineering axe shaft is 3 cm across. NRCan photo 2019-721

Subophiolite basement

Similar to other areas described herein, the relationships between Atlin and Cache Creek terranes are ambiguous due to several generations of faulting. In the Sunday Peak area, late, steep faults (Mihalynuk et al., 2018) juxtapose ophiolitic rocks with Carboniferous to Permian Horsefeed Formation limestone. Horsefeed Formation in this area locally contains tuffaceous beds which yielded ca. 310 Ma to 285 Ma zircon crystals (Mihalynuk et al., 2018). On Jubilee Mountain, ophiolitic rocks form a klippe above the Cache Creek terrane carbonate platform (Fig. 11f). Paleozoic Horsefeed Formation limestone and volcanic rocks are exposed at the base of Jubilee Mountain and in the surrounding plateaus. Northeast of the Jubilee Mountain peak, Horsefeed Formation pillow basalt is imbricated together with the ophiolite. The Horsefeed Formation pillow basalts are characterized by ocean-island basalt geochemical signature and an interpillow limestone yielded a Pennsylvanian conodont (M. Golding, unpub. GSC Paleontological Report 4-MG-2019, 2019; Fig. 11g, h). These volcanic rocks are the same age and chemistry as volcanic rocks intercalated with the Pennsylvanian Horsefeed Formation to the south at Alfred Butte (Monger, 1975; Golding et al., 2017; Zagorevski et al., 2018; M. Golding and N. Joyce, unpub. data, 2020). Relationships between Atlin and Cache Creek terranes on Jubilee Mountain strongly suggest that the Atlin terrane ophiolites were obducted onto the areally extensive Cache Creek terrane carbonate platform early in the structural history.

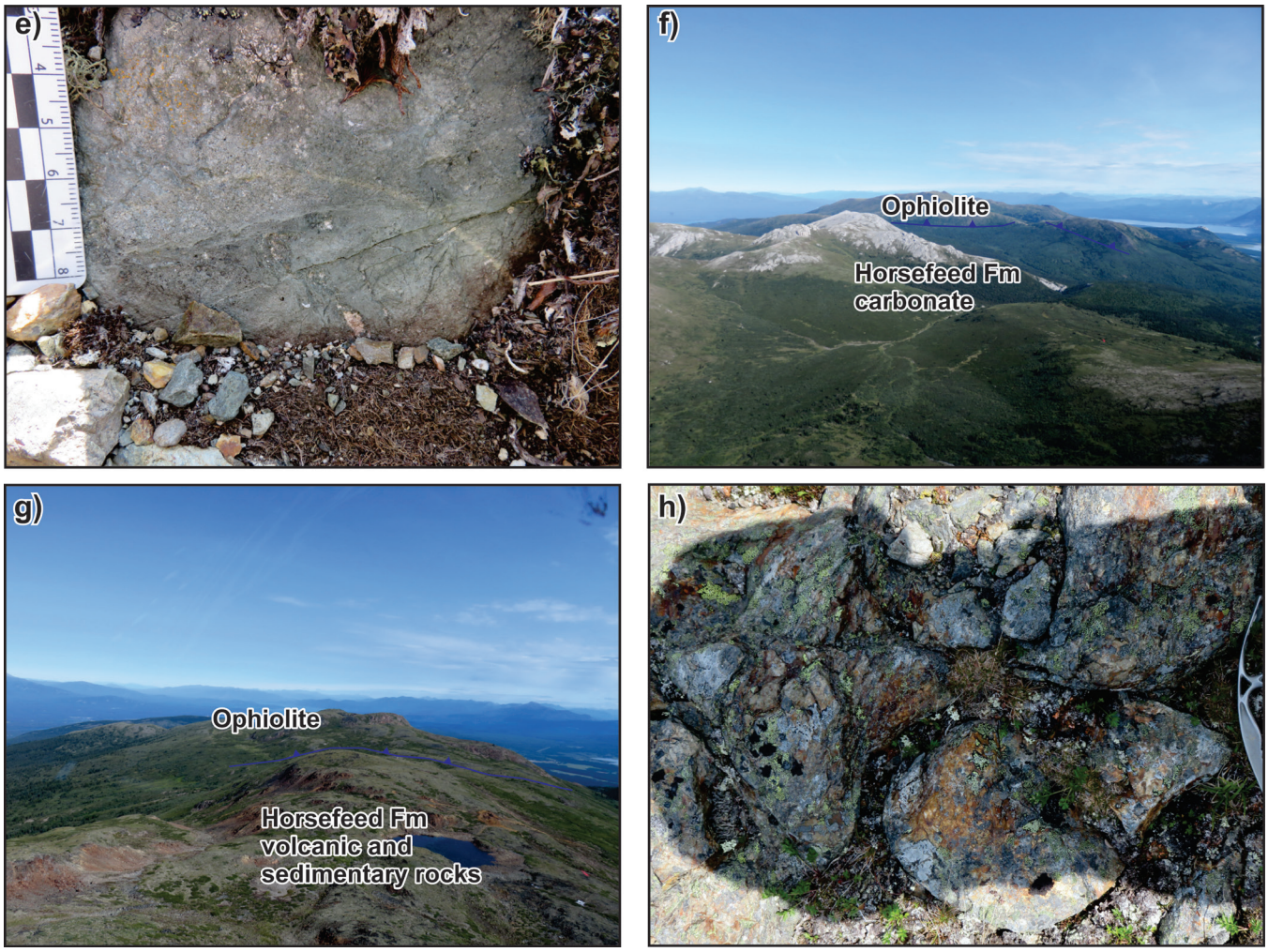

Figure 11. (cont.) Representative photographs of the Atlin terrane in Graham Inlet to Jubilee Mountain area; **e)** Detail of dyke contact in fine-grained gabbro; scale in centimetres. NRCan photo 2019-722. **f)** Overview of ophiolite-carbonate platform relationship in the Jubilee Mountain area. Carbonate platform in the foreground extends through the lowland and is exposed beneath ophiolite. Blue line represents thrust contact between ophiolite and Horsefeed Formation. NRCan photo 2019-723. **g)** Overview of ophiolite footwall relationships north of Jubilee Mountain Peak. Blue line represents thrust contact between ophiolite and Horsefeed Formation. NRCan photo 2019-724. The foreground comprises **h)** Carboniferous ocean-island pillow basalt (mountaineering axe head is 20 cm; NRCan photo 2019-725), rhyolite, and sedimentary rocks. These rocks are structurally overlain by serpentinite mélange comprising blocks of peridotite, chert, gabbro, and basalt in highly deformed serpentinite matrix, and mantle peridotite and gabbro dykes. All photographs by A. Zagorevski.

Marsh Lake to Teslin Lake

The northernmost extent of the Atlin terrane ophiolites and Cache Creek terrane carbonate rocks occur in the Teslin Lake and Whitehorse areas (Fig. 2). To the east, these terranes are juxtaposed with the Upper Triassic Shonektaw Formation (part of Quesnellia) to the east along the Cretaceous Teslin Fault (Gabrielse et al., 2006). To the north and west, the contacts with Upper Triassic Lewes River Group and Jurassic Laberge Group (part of Stikinia) are marked by Jurassic thrust faults (e.g. Bickerton, 2013) and younger normal faults (Fig. 12a), such as the Crag Lake Fault. Ophiolitic rocks occur on both sides of the Crag Lake Fault, exposing different structural levels, which allowed establishment of the ophiolite pseudostratigraphy to the north, and footwall relationships to the south. Ophiolitic rocks are preserved as alpine exposures between Jakes Corner and Squanga Lake. Mantle peridotites south of Cabin Lake and near Mount Michie are fresh and comprise harzburgite, dunite, pyroxenite, and lherzolite (Fig. 12a, b, c). Serpentinization is more extensive to the east, where ultramafic rocks are intruded by gabbro and locally contain podiform chromite (Yukon Mineral Occurrence 105C 012, <https://data.geology.gov.yk.ca/Compilation/24> [accessed December 25, 2019]). South of Cabin Lake, the degree of serpentinization increases drastically to the south along the contact with gabbro, diabase, and Nakina suite basalt (Fig. 12d). The crust-mantle contact in this area is characterized by sheared serpentinite

Figure 12. Representative photographs of the Atlin terrane in Marsh Lake to Teslin Lake area. **a)** Ultramafic rocks in this area are exposed in large massifs and comprise harzburgite, lherzolite, and dunite (lighter dun colour). Ridge in the background is underlain by Norian limestone and volcanic rocks of the Lewes River Group, but the suture between terranes has not been identified. Field of view in foreground is about 3 m. NRCan photo 2019-726. **b)** Clinopyroxene-bearing harzburgite and lherzolite are common in this area; finger for scale about 1.5 cm. NRCan photo 2019-727. **c)** Harzburgite cut by vein with dunite core and coarse clinopyroxene rim; finger for scale is about 1.5 cm. NRCan photo 2019-728. **d)** Detachment zone in the Squanga Lake zone juxtaposes mantle harzburgite-lherzolite with upper crustal lithologies. Width of field of view in foreground about 5 m. NRCan photo 2019-729

mélange that contains decimetre- to metre-sized knockers of hornblende gabbro and olivine gabbro cumulate rocks of tholeiitic affinity (Bédard et al., 2016). The tectonic mélange is intruded by several generations of variably amphibolitized gabbro dykes, locally also including numerous trondhjemite veins (Fig. 12e, f). Gabbro samples from this contact yielded ca. 249 Ma and 245 Ma U-Pb zircon crystallization ages, constraining the age of mafic magmatism and the age of the detachment (R. Friedman and A. Bogatu, unpub. data, 2020). Gabbroic rocks above the mélange rapidly grade into fine-grained gabbro, diabase, and basaltic rocks (Fig. 12g). The relationships here suggest the crust-mantle contact is a synmagmatic, intraophiolitic detachment fault, which exhumed ophiolitic mantle to a shallow crustal level within an oceanic core complex.

Volcanic, hypabyssal rocks and gabbro within serpentinite are characterized by flat to LREE-enriched normal mid-ocean-ridge basalt normalized trace-element profiles with Th enrichment and negative Nb anomaly characteristic of island-arc tholeiite and back-arc-basin basalt (Fig. 6). This indicates a suprasubduction zone environment.

Atlin terrane ophiolites extend further north where they are unconformably overlain by the Jurassic Laberge Group and are interpreted to be in structural contact with the Upper Triassic Lewes River Group (Gordey and Stevens, 1994; Bickerton, 2013). Similar to other areas, Atlin terrane ultramafic rocks in this area are characterized by variably porphyroclastic harzburgite, dunite, and pyroxenite (Fig. 12c; Jobin-Bevans, 1995). Some exposures of

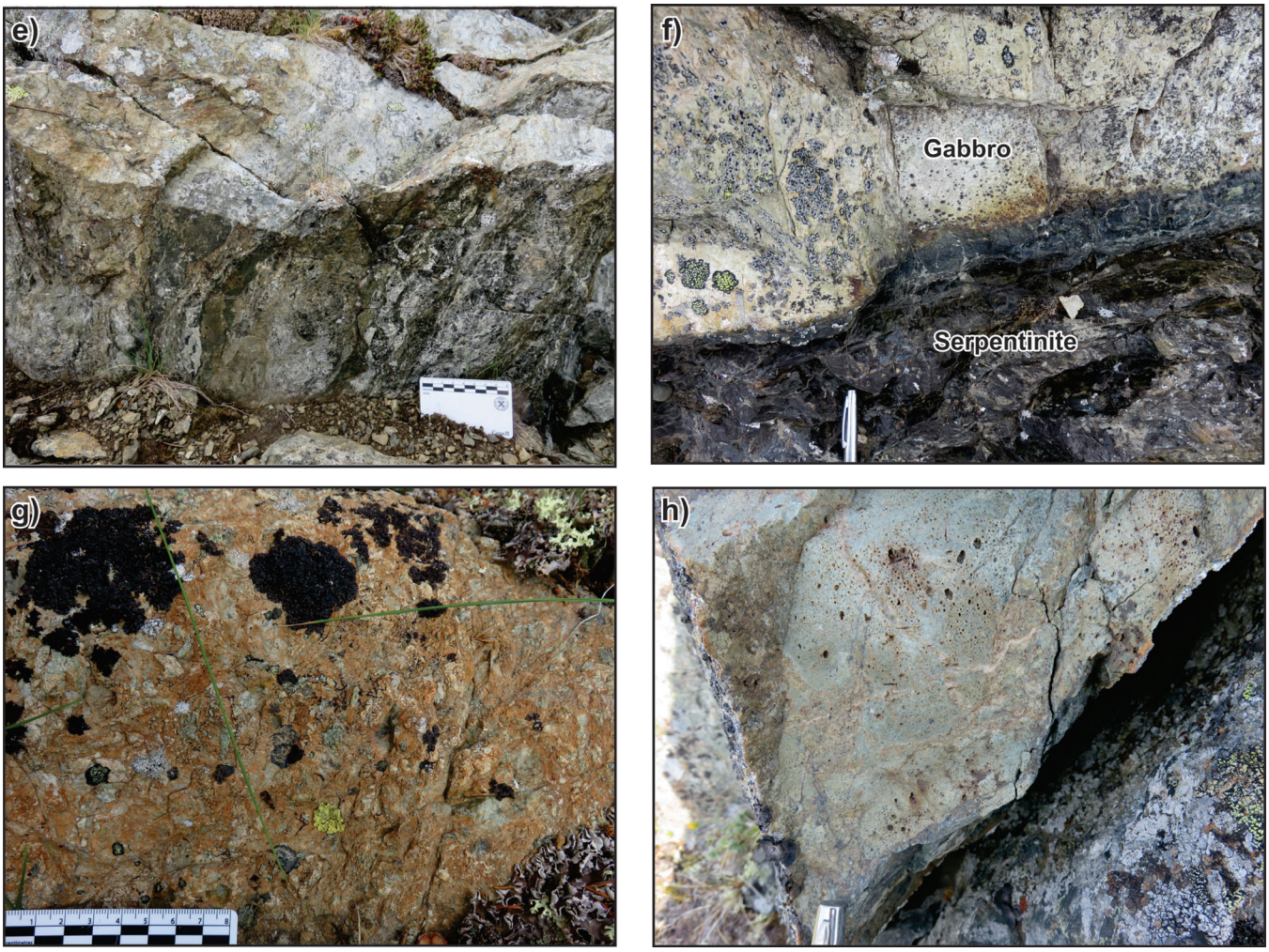

Figure 12. (cont.) Representative photographs of the Atlin terrane in Marsh Lake to Teslin Lake area. **e)** Gabbro at the contact between crust and mantle is locally highly deformed. Scale in centimetres. NRCan photo 2019-730. **f)** Gabbro at the contact between crust and mantle also preserves intrusive relationships with serpentinite; section of pen showing is 6 cm long. NRCan photo 2019-731. **g)** Typical rubbly volcanic rocks of the Nakina suite basalt. Scale in centimetres. NRCan photo 2019-732. **h)** Vesicular Nakina suite basalt near Mount Michie; tip of pen for scale about 1 cm. NRCan photo 2019-733. Photographs by A. Zagorevski.

harzburgite are relatively massive and homogenous with cumulate textures (Jobin-Bevans, 1995). Ultramafic rocks are imbricated with basalt of the Nakina suite by Jurassic thrusts (Fig. 10h). Ultramafic rocks have been dated at Streak Mountain, where a peridotite sample yielded 245.4 ± 0.8 Ma U-Pb zircon crystallization age (Gordey et al., 1998). This age is within error of the ages obtained along the detachment south of Cabin Lake, and is interpreted as representative of the terminal stages of oceanic core complex development in Atlin terrane ophiolites in this area.

Exposures of the Atlin terrane ophiolitic rocks in the Marsh Lake and Mount Michie areas were investigated by Bickerton et al. (2013) and Bickerton (2013), who identified two distinct geochemical suites of volcanic rocks in this area. One suite is characterized by island-arc tholeiite to back-arc-basin basalt trace-element signatures similar to other Nakina suite volcanic rocks in this area. The second suite is characterized by calc-alkaline trace-element signatures. The present study's reconnaissance sampling in this area revealed similar suites. Hypabyssal and volcanic rocks near the Cretaceous Marsh Lake intrusive complex (Yukon Geological Survey, 2019) yielded calc-alkaline geochemical characteristics. The similarity of these geochemical characteristics and proximity to the Marsh Lake intrusive complex (Bickerton, 2013), as well as local occurrence of pristine dunite xenoliths suggest that these calc-alkaline rocks may form part of the Cretaceous Carmacks Group. In contrast, east of Mount Michie, amygdaloidal basalt units structurally below peridotite units yielded back-arc-basin basalt trace-element signatures, typical of Nakina suite. Bickerton (2013) also identified a suite of volcaniclastic rocks, which he included in the new Michie Formation. These volcaniclastic rocks yielded 245.85 ± 0.07 Ma and 244.64 ± 0.08 Ma unimodal U-Pb zircon provenance (Bickerton, 2013). These ages are within error of Streak Mountain peridotite (Gordey

et al., 1998) and gabbro in the detachment south of Cabin Lake (*see* above). These ages indicate that island-arc tholeiite–back-arc-basin basalt magmatism in this area was coeval with eruption of more evolved, felsic to intermediate lavas. Felsic magmatism can be abundant in some ophiolite belts (Rollinson, 2009; Cutts et al., 2012).

On the east side of Teslin Lake (Fig. 2), Gordey and Stevens (1994) identified several bodies of harzburgite, pyroxenite, dunite, and gabbro within the Late Triassic Shonektaw Formation sediments and volcaniclastic rocks. Re-examination of these localities indicates that these rocks are imbricated with the Shonektaw Formation. Gabbro in this area is geochemically similar to gabbroic rocks on Nares Mountain and other cumulate gabbro units in the Atlin terrane (*see* Fig. 6). The Late Triassic Shonektaw Formation volcaniclastic rocks are locally characterized by anomalously high Cr concentrations and contain altered ultramafic clasts (Zagorevski et al., 2018). This suggests that the Late Triassic Shonektaw Formation unconformably overlies the Atlin terrane peridotites in this area, and incorporated clasts of the underlying peridotite units through either volcanic or sedimentary processes (Zagorevski et al., 2018).

Subophiolite basement

The relationship between Atlin terrane ophiolites and their structural basement are not clear north of the Crag Lake Fault. Late Devonian to Early Carboniferous conodonts were recovered between Cabin and Summit lakes, suggesting that the ophiolite is structurally above the Cache Creek terrane in this area, however, the present authors were not able to examine this relationship in detail. To the south of the Crag Lake Fault, Gordey and Stevens (1994) identified ophiolitic ultramafic and gabbroic rocks on top of carbonate rocks of the Paleozoic Horsefeed Formation, suggesting similar relationship to the Jubilee Mountain area (*see* 'Graham Inlet to Jubilee Mountain').

Joe Mountain Formation

The Joe Mountain Formation is exposed to the east of Lake Laberge and is unconformably overlain by the Upper Triassic Lewes River Group volcanic and sedimentary rocks (Hart, 1997; Bordet, 2018). The Joe Mountain Formation comprises massive to pillowed basalt, calcareous siliciclastic rocks, mafic volcaniclastic rocks, and volcanogenic conglomerate. Volcanic sandstone yielded a 244.74 ± 0.09 Ma U-Pb zircon depositional age (Bordet, 2018) consistent with the previously collected Ladinian conodonts (Hart, 1997). Although the Joe Mountain Formation was included in Stikinia, Hart (1997) noted its similarity to the ophiolitic rocks of the Atlin terrane.

Joe Mountain Formation volcanic rocks are characterized by flat to LREE-enriched normal mid-ocean-ridge basalt normalized trace-element profiles with Th enrichment and negative Nb anomalies characteristic of island-arc tholeiite, back-arc-basin basalt, and calc-alkaline basalt (Fig. 13a). The geochemical compositional range and juvenile Nd isotopes have been interpreted to represent a juvenile rifted arc complex (Bordet, 2018). The age and geochemical characteristics of the Joe Mountain Formation are similar to the corresponding rocks in the adjacent Atlin terrane (Gordey et al., 1998; Bickerton, 2013), suggesting that Joe Mountain Formation is an along- or across-strike equivalent of the same Middle Triassic arc–back-arc system as the Atlin terrane, rather than representing a completely separate terrane.

Kutcho complex

Kutcho complex is exposed to the south of the King Mountain, structurally below the Nahlin Fault (Gabrielse, 1998; Schiarizza, 2012). In this area, the Nahlin Fault emplaces Atlin terrane ophiolites and Cache Creek terrane carbonate rocks over the sedimentary strata of the Jurassic Laberge Group (Gabrielse, 1998). Laberge Group unconformably overlies the Kutcho complex (Gabrielse, 1998; Schiarizza, 2012). The Kutcho complex comprises a heterogeneous succession of variably altered and sheared felsic and mafic volcanic rocks, consanguineous intrusions, and volcanogenic massive-sulphide lenses (Gabrielse, 1998; Schiarizza, 2012). Schiarizza (2012) subdivided the Kutcho complex into northern, central, and southern divisions, which he interpreted to broadly represent a stratigraphic succession. The structurally and stratigraphically lowest unit (southern division) is characterized by poorly bedded to massive quartz-phyric felsic tuff, breccia, and epiclastic rocks overlain by rhyolite and related volcaniclastic rocks, and by mafic volcanic rocks locally interlayered with felsic volcanic rocks. The middle unit (central division) is also characterized by interdigitating felsic and mafic rocks, but contains significantly more coherent rhyolite and related rocks than the underlying division, and is extensively intruded by tonalite and diorite. The youngest unit (northern division), is characterized by felsic lithic and crystal tuff, related epiclastic and sedimentary rocks, and massive-sulphide lenses.

The base of the Kutcho complex is not dated. The middle unit is intruded by 251.71 ± 0.48 Ma tonalite, indicating that some of the Kutcho magmatism is older than ca. 252 Ma. Felsic rocks near the stratigraphic top of the Kutcho complex yielded a 242 ± 1 Ma U-Pb zircon age. The Kutcho complex is cut by the (?) Late Triassic Sumac Creek gabbro. The Kutcho complex is overlain by a conglomerate that grades into the Late Triassic Sinwa Formation limestone. The age range of the Kutcho complex overlaps the age range of the Atlin terrane ophiolites (ca. 264–244 Ma: Gordey

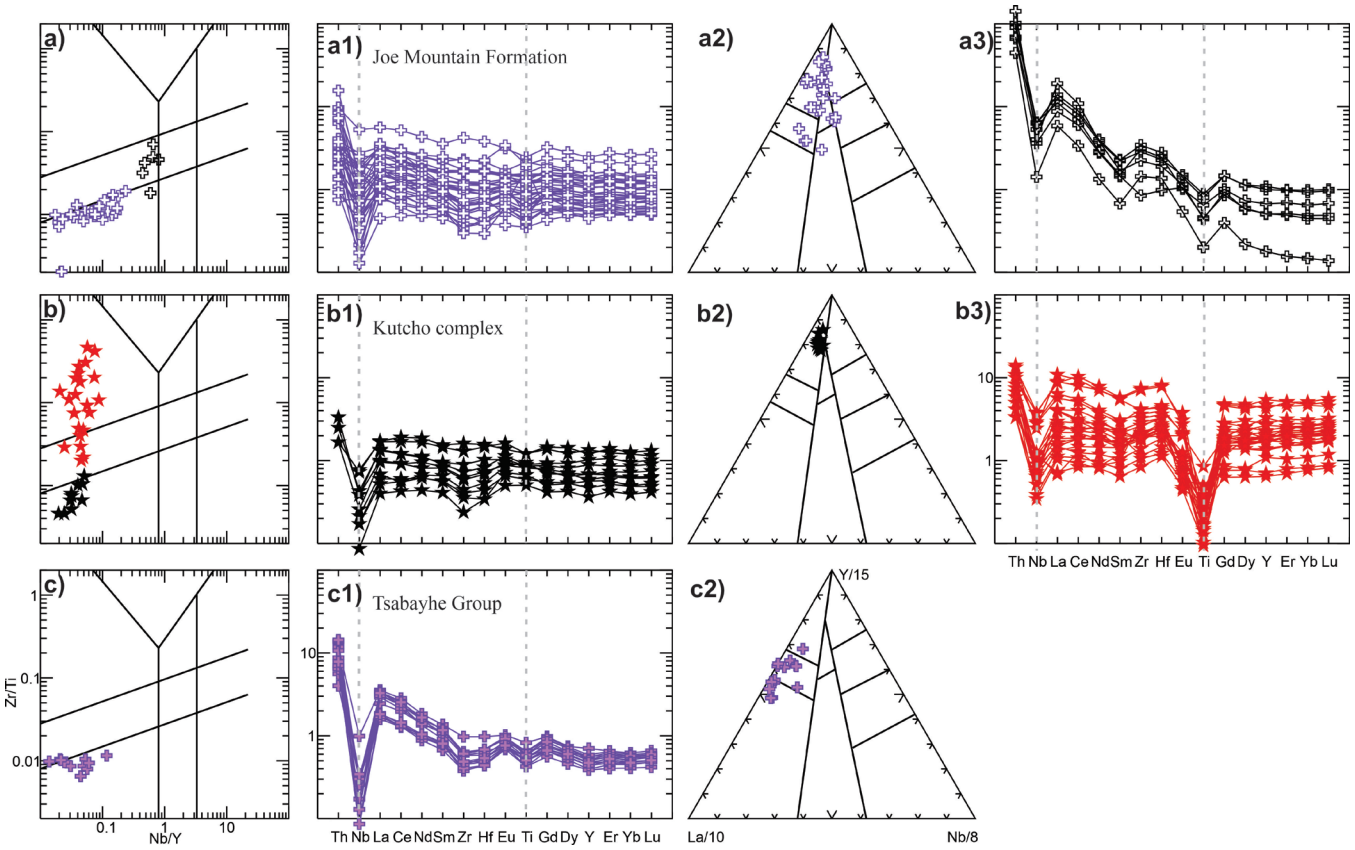

Figure 13. Geochemical characteristics of the Late Permian to Middle Triassic arc rocks adjacent to Atlin terrane ophiolites. **a)** Joe Mountain Formation (Bordet et al., 2019); purple cross = mafic, black cross = felsic. **b)** Kutcho complex (Schiarizza, 2012; Schiarizza, unpub. data, 2019) black star = mafic, red star = felsic. **c)** Tsabayhe Group (Logan and Iverson, 2013); all samples mafic.

et al., 1998; Mihalynuk et al., 2003; Bickerton, 2013; N. Joyce, unpub. data, 2020) and Joe Mountain Formation in Yukon (ca. 244 Ma: Bordet, 2017).

The Kutcho complex mafic volcanic rocks are characterized by flat to LREE-enriched normal mid-ocean-ridge basalt normalized trace-element profiles with Th enrichment and negative Nb anomalies characteristic of island-arc tholeiite and back-arc-basin basalt (Fig. 13b). The much more voluminous felsic rocks have similarly flat to LREE-enriched normal mid-ocean-ridge basalt normalized trace-element profiles, but with significant negative Eu and Ti anomalies, and positive Zr-Hf anomalies. The Kutcho complex is interpreted to have formed in a juvenile arc or back-arc setting (Childe and Thompson, 1997; Schiarizza, 2012).

Tsaybahe Group

The Tsaybahe Group unconformably overlies the deformed Paleozoic Stikine assemblage and is an accepted component of the Triassic Stikinia terrane (Read, 1984; Gabrielse, 1998). The Tsaybahe Group is characterized by chert, fine-grained siliciclastic rocks, augite porphyritic mafic volcanic and epiclastic rocks, and Middle Triassic limestone (Read, 1984). Gabrielse (1998) identified Tsaybahe Group equivalents in the Dease Lake area. He included these in the Stuhini Group, due to their petrographic similarity and poor exposure of sedimentary rocks that are characteristic of the Tsaybahe Group. The present authors retain Tsaybahe Group for the purposes of discussion in this paper as it aids comparison with other Middle Triassic and older sequences. The Tsaybahe Group yielded Lower Triassic to Anisian conodonts (Read, 1984; Golding et al., 2017), making it temporally equivalent to the Kutcho complex (Schiarizza, 2012), Joe Mountain Formation (Bordet et al., 2019), Michie Formation (Bickerton, 2013), and youngest Atlin terrane ophiolites (Gordey et al., 1998; Mihalynuk et al., 1999).

The mafic rocks of the Tsaybahe Group are characterized by LREE-enriched normal mid-ocean-ridge basalt normalized trace-element profiles with Th enrichment and negative Nb anomalies characteristic of arc magmas (Fig. 13c; Logan and Iverson, 2013). Tsabayhe Group is significantly more LREE enriched than adjacent Kutcho, Joe Mountain, or Atlin terrane ophiolites (Fig. 13).

Summary of the Atlin terrane and related rocks

The Atlin terrane is characterized by suprasubduction zone ophiolites (Fig. 6) that range from Middle Permian to Middle Triassic (ca. 264–245 Ma). The majority of these ophiolite massifs in the Atlin terrane exhibit a pseudostratigraphy that is consistent with formation in a suprasubduction zone spreading ridge (island-arc tholeiite to back-arc-basin basalt magmatism) with phases of tectonically accommodated spreading that exhumed mantle tectonites to upper crustal levels or onto the ocean floor (Fig. 14). The only exception to this occurs in the King Mountain area where a boninite-rich ophiolite is characterized by structurally disrupted, but well defined Penrose-style pseudostratigraphy (Fig. 14; Anonymous, 1972), including the presence of a sheeted dyke complex that indicates a robust magma budget (Robinson et al., 2008).

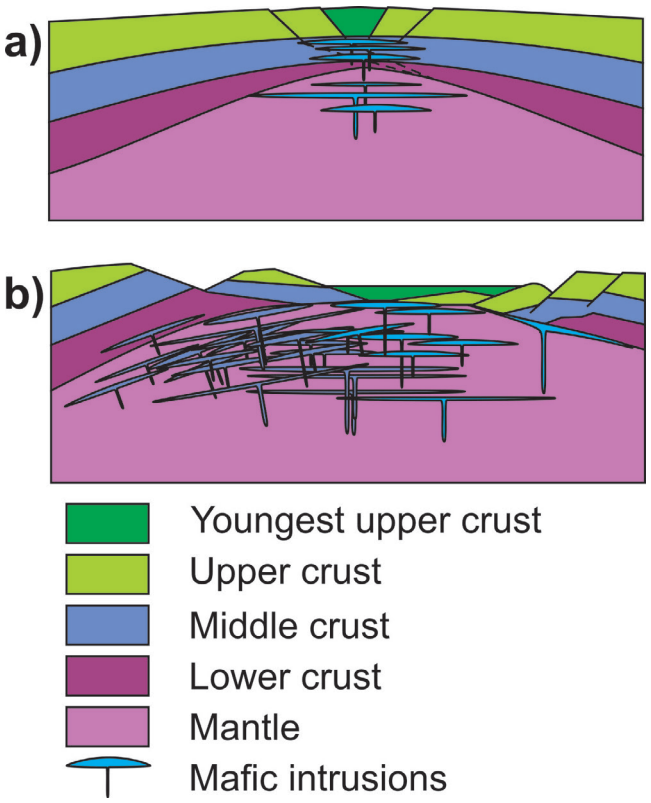

Figure 14. Schematic differences in pseudostratigraphy of ophiolites. **a)** Magmatically accommodated extension produces well defined Penrose ophiolites with mafic-ultramafic cumulates (lower crust), isotropic gabbro (middle crust), and sheeted dykes and basalts (upper crust). **b)** Tectonically accommodated extension produces poorly defined ophiolite pseudostratigraphy characterized by juxtapositions of mantle with lower, middle, and upper crust, exhumation of mantle onto the ocean floor and intrusions of gabbro and diabase in exhumed mantle. Complete exhumation of mantle onto the ocean floor forms oceanic core complexes characterized by megamullions.

The relationships between Atlin terrane ophiolites and their structurally underlying basement are typically poorly constrained; however, several localities indicate that the Atlin terrane ophiolites were obducted onto the Cache Creek terrane carbonate platform. The contact is rarely marked by a metamorphic sole, consisting of amphibolite derived from an ocean-island basalt protolith. Rare high-pressure rocks are locally preserved within volcanic rocks associated with the Cache Creek terrane carbonate platform (Mihalynuk et al., 2004a), though they yield Middle Jurassic Ar-Ar ages that were likely disturbed by the Middle Jurassic Three Sisters plutonic suite (Mihalynuk et al., 1992). In the Nakina area, the presence of omphacite and garnet in stream sediments without an obvious nearby source rock suggests that high-pressure soles are either largely eroded or very poorly exposed (Canil et al., 2004). The vast majority of 'oceanic' (i.e. marine) sediments that are imbricated with the Atlin and Cache Creek terranes are not a subduction zone mélange. Rather, they form part of an extensive Late Triassic to Early Jurassic overlap assemblage that is partly derived from the Late Triassic Stikinia and/or Quesnellia terranes (Zagorevski et al., 2018).

Early to Middle Triassic volcanic successions that were previously included in Stikinia (Joe Mountain Formation and Tsabayhe Group; Logan and Iverson, 2013; Bordet, 2017, 2018; Bordet et al., 2019) formed in an arc setting and are coeval with Atlin terrane ophiolites and Atlin terrane arc sequences (e.g. Kutcho complex: Schiarizza, 2012; Fig. 15). Terrane boundaries (i.e. Nahlin and King Salmon faults) have been inferred to exist between these Stikinia-related volcanic arc sequences and the Atlin terrane; however, recent data indicate that the Nahlin and King Salmon faults are postaccretionary faults (e.g. Zagorevski et al., 2018). The correlation between of the Atlin terrane and parts of Stikinia have been previously suggested for the Kutcho complex (Fig. 8.75 in Monger et al., 1991) and for Atlin terrane ophiolites (Hart, 1997; English and Johnston, 2005). As such, the Middle Triassic rocks of Stikinia and the Middle Triassic rocks of the Atlin terrane are most simply interpreted to form part of the same extensional arc system (Fig. 3, 16). This arc system likely collided with the Cache Creek terrane carbonate platform by the Middle Triassic (Fig. 3, 16).

SLIDE MOUNTAIN AND YUKON-TANANA TERRANES

Ophiolite complexes in the Slide Mountain and Yukon-Tanana terranes occur along the boundary with the parautochthonous North America to the east and west of the Yukon-Tanana terrane, as well as imbricated with the Yukon-Tanana terrane (Fig. 1; e.g. Yukon Geological Survey, 2019). Similar to the Cache Creek and Atlin terrane relationships, these ophiolite massifs comprise peridotite and basalt that are commonly imbricated with chert-siliciclastic-limestone 'oceanic' sequences (Nelson, 1993; Nelson and Bradford,

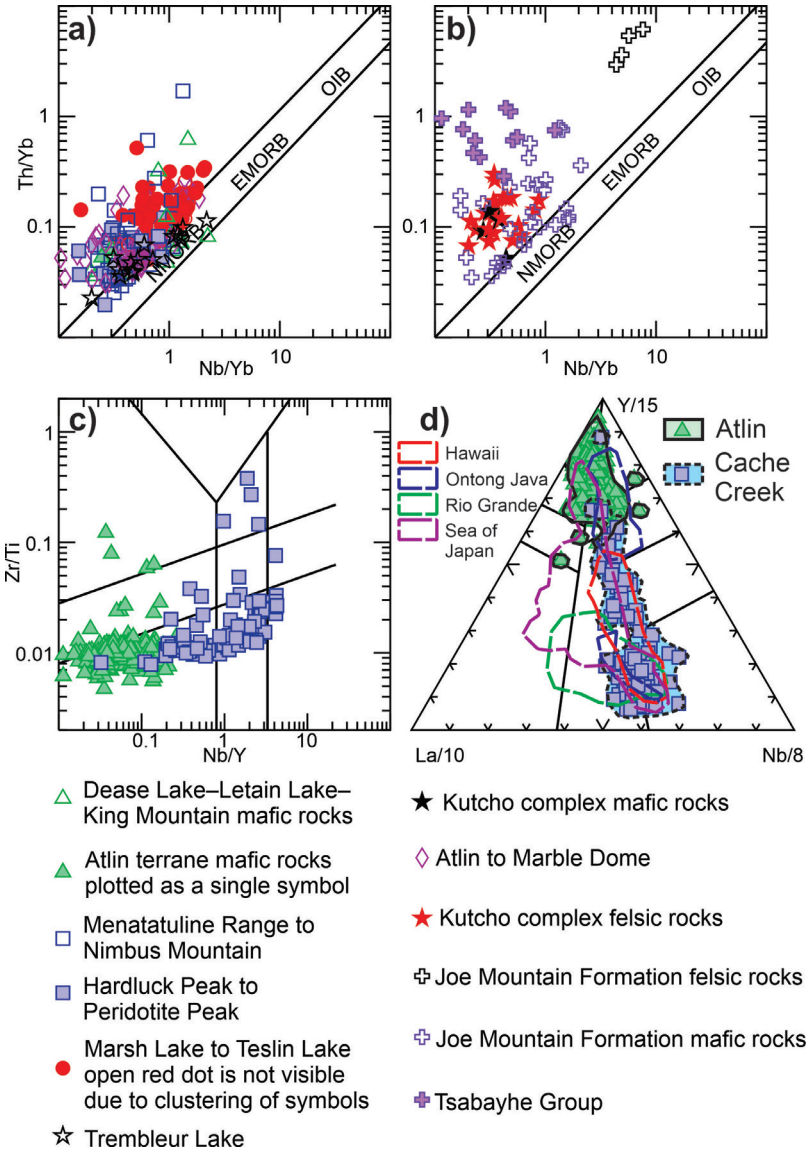

Figure 15. Geochemical characteristics of the Late Permian to Middle Triassic arc rocks of the Atlin and Cache Creek terranes. All compositions are plotted for reference. **a)** Atlin terrane ophiolites plot above the mantle array, suggesting subduction zone contribution (Pearce, 2014). **b)** Joe Mountain Formation, Kutcho complex, and Tsabayhe Group overlap Atlin terrane ophiolites, but generally indicate greater subduction zone component (symbols same as in Fig. 13. **c)**, **d)** Comparison of basaltic rocks from the Atlin and Cache Creek terranes. Cache Creek terrane basalt units are characterized by higher Nb/Y and La/Nb ratios and plot in enriched mid-ocean-ridge basalt–ocean-island basalt and continental rift fields on basalt discrimination plot (Cabanis and Lecolle, 1989). Each terrane is assigned one symbol for clarity. Fields for Hawaii, Ontong Java, Rio Grande, and Sea of Japan are plotted for reference (data were downloaded from the PetDB Database (www.earthchem.org/petdb) [accessed July 30, 2019] using the following parameters: feature name = Hawaii, Ontong Java, Rio Grande, and Sea of Japan and rock classification = basalt (as suggested by database server); Ryan et al., 2009). NMORB = normal mid-ocean-ridge basalt, EMORB = enriched mid-ocean-ridge basalt, OIB = ocean-island basalt

1993; Colpron et al., 2005, 2006; Murphy et al., 2006; Nelson and Colpron, 2007). In general, these ophiolite complexes and oceanic rocks are interpreted to have formed during and following the rifting of the Yukon-Tanana terrane from the Laurentian margin and during the development of the Slide Mountain Ocean marginal basin (e.g. Murphy et al., 2006; Piercey et al., 2006, 2012). Many models interpret these ophiolite complexes and oceanic sedimentary sequences to represent the vestiges of the subducting Slide Mountain Ocean that were emplaced over the Laurentian margin and Yukon-Tanana terrane during collisional orogenesis (e.g. Nelson and Colpron, 2007; Nelson et al., 2013).

Harzburgite Peak complex

The Harzburgite Peak complex and correlative Eikland Mountain complex are the westernmost ophiolites in the Slide Mountain terrane (Fig. 1). The lithological and structural setting of the Harzburgite Peak complex has been described in detail in Canil and Johnston (2003), who identified northeast-directed thrusting within the ophiolite, marked by emplacement of mantle peridotite over gabbro and diabase (Ryan et al., 2014). The Harzburgite Peak complex contains a section of harzburgite tectonite in structural contact with cumulate gabbro and diabase (Canil and Johnston, 2003; Canil et al., 2019). Rare trondhjemite dykes that cut the cumulate gabbro yielded a ca. 285 Ma crystallization age, constraining the timing of Harzburgite Peak complex magmatism (N. Joyce, unpub. data, 2020). Stepped sill to dyke contacts in the diabase zone indicate upward and lateral migration of basaltic melts; however, an organized sheeted dyke zone was not observed during the present study (Ryan et al., 2013b, 2014). Extrusive volcanic rocks have not been identified. Overall, the Harzburgite Peak complex lacks ultramafic and layered mafic cumulate zones and is much too thin for a typical Penrose-style (Anonymous,

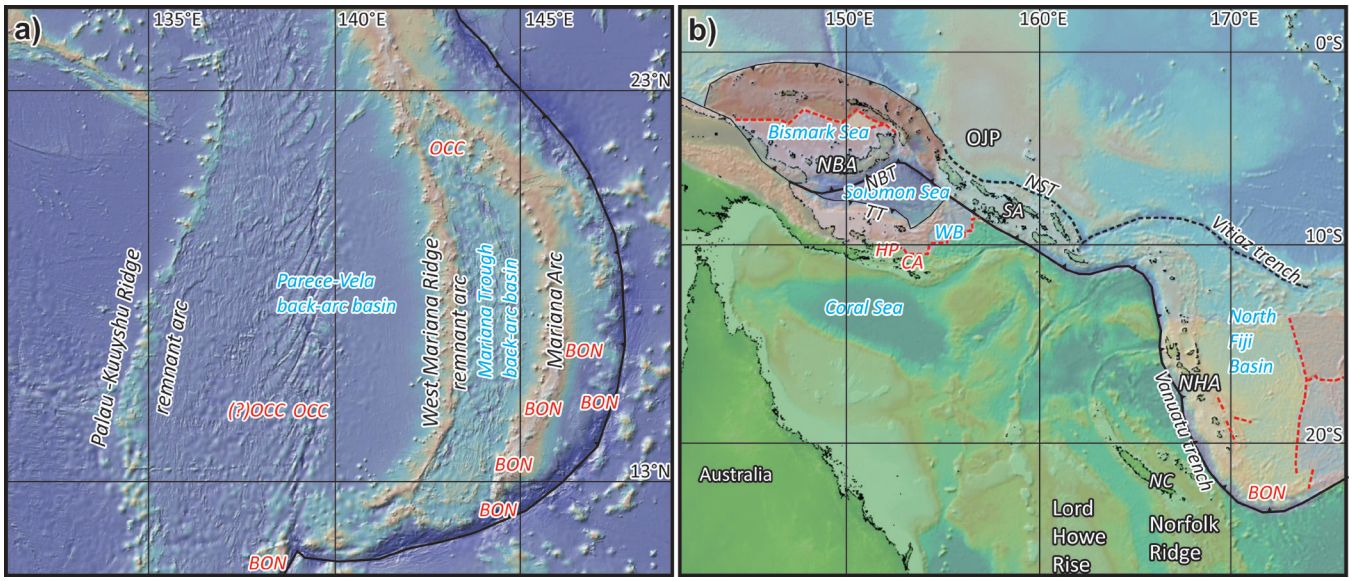

Figure 16. Possible modern analogues of Stikinia–Atlin–Cache Creek terranes (background image generated from <http://www.geomapapp.org>; [accessed July 12, 2019]; Ryan et al., 2009). **a)** Izu-Bonin-Mariana arc–back-arc system forms a good analogue for the various components of the Atlin terrane. Both the Parece-Vela and Mariana Trough back-arc basins have evidence of detachment faulting (?OCC) and formation of oceanic core complexes (OCC; Stern et al., 1996; Ohara et al., 2003). Eocene to Oligocene boninite (BON) occurrences are shown for reference (Deschamps et al., 2003). **b)** Australia-Pacific plate boundary provides a good analogue for interaction of New Hebrides–Solomon–New Britain extensional arc system (equivalent to Atlin terrane and Paleozoic Stikinia or parts of Slide Mountain–Yukon-Tanana; *modified from* van Staal et al., 2018) with Australian continental margin, microcontinental slivers and overlying carbonate platforms (Lord Howe Rise and Norfolk Ridge, equivalent to Laurentia and Cache Creek terrane, respectively). Boninites are generated in the southern termination of the New Hebrides arc (Monzier et al., 1993), which will collide with New Caledonia (NC) in the near future, providing an excellent analogue for obduction of Atlin terrane boninitic ophiolite onto Cache Creek terrane shallow-marine sequences. North Fiji Basin forms a good analogue for various components of the Atlin terrane. OJP = Ontong-Java Plateau, NBA = New Britain Arc, NBT = New Britain Trench, TT = Trobriand Trough, WB = Woodlark Basin, HP = High-pressure metamorphism, CA = Calc-alkaline magmatism, NHA = New Hebrides Arc, SA = Solomon Arc

1972) ophiolite. The thermal history of the peridotites indicates that mantle peridotites were rapidly cooled, implying either rapid exhumation along an intraoceanic detachment or by rapid cooling along a transform fault (Canil et al., 2019).

Ultramafic rocks are highly depleted mantle harzburgite typical of ophiolites (Canil et al., 2019), whereas the gabbro is characterized by a flat normal mid-ocean-ridge basalt normalized trace-element profiles with depletions of Ti, Zr, and Hf, typical of cumulate rocks. The compositions of diabase and trondhjemite are typical of island-arc and back-arc ophiolites (Fig. 17a).

The correlative Eikland Mountain complex comprises ultramafic rocks, gabbro, diabase, basalt, and chert (Murphy et al., 2008). The age of the Eikland Mountain complex is constrained to be ca. 276 Ma (Yukon Geological Survey, 2019). Preliminary analyses of Ekland Mountain complex mafic rocks yielded only MORB signatures (Murphy et al., 2008); however, subsequently analyzed samples yielded calc-alkaline basalt, island-arc tholeiite, and back-arc-basin basalt characteristics indicative of a suprasubduction zone setting (Murphy et al., 2009).

Subophiolite basement

The Harzburgite Peak complex structurally overlies metavolcanic and metasedimentary rocks of the Late Devonian White River assemblage above a shallowly dipping fault and forms several klippen (Murphy et al., 2009; Ryan et al., 2013b, 2014). A subophiolitic emplacement-related fault is in part obscured by the Middle Cretaceous Whitehorse plutonic suite to the north and the upper Cretaceous Carmacks Group to the southeast (Ryan et al., 2013a, 2014). Where exposed, the subophiolitic fault rocks comprise scaly serpentinite derived from mantle tectonites. The structurally underlying Late Devonian White River assemblage comprises ca. 365 Ma (Murphy et al., 2009; N. Joyce, unpub. data, 2020) felsic and mafic volcanic rocks, and related plutonic rocks. These are interlayered with continentally derived pebble conglomerate, quartz arenite, siltstone, and shale (Murphy et al., 2009; N. Joyce, unpub. data, 2020). Sedimentary rocks are generally metamorphosed to quartzite and mica schist. Volcanic rocks are characterized by enriched mid-ocean-ridge basalt chemistry (Ryan et al., 2018), which, considering the association with continental-derived sedimentary rocks, is consistent

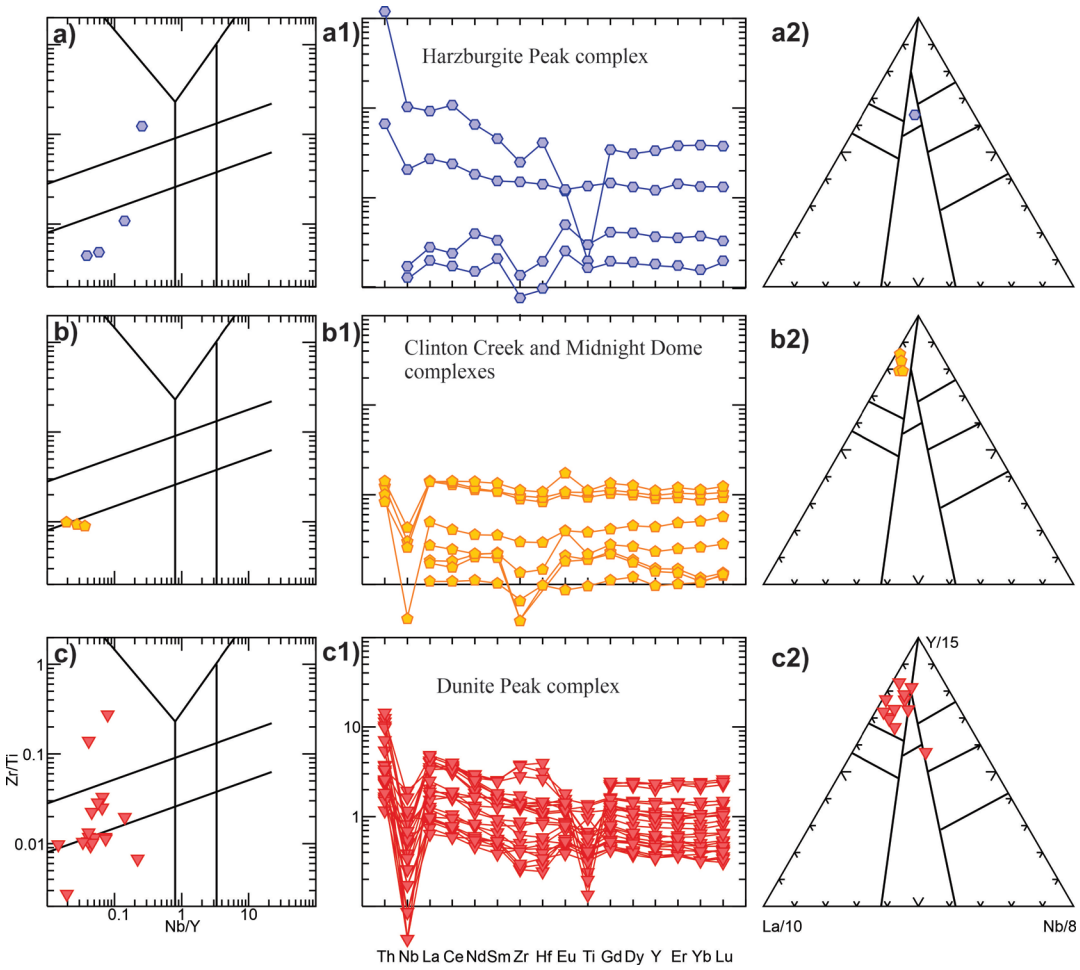

Figure 17. Geochemical characteristics of Slide Mountain terrane ophiolites. **a)** Harzburgite Peak complex. Cumulate gabbro is plotted for reference. **b)** Clinton Creek and Midnight Dome complexes (van Staal et al., 2018). Cumulate gabbro is plotted for reference. **c)** Dunite Peak complex including tonalite, diorite, and gabbro (Parsons et al., 2019).

with a continental rift setting. The Late Triassic Snag Creek suite gabbro intrudes the White River assemblage, but has not been identified within the Harzburgite Peak complex (Ryan et al., 2013b, 2014), suggesting that the final age of emplacement of the ophiolite is Late Triassic or younger.

Clinton Creek and Midnight Dome

The Clinton Creek complex (Fig. 1) comprises strongly altered ultramafic rocks with minor mafic intrusive rocks (Abbott, 1983; van Staal et al., 2018). These rocks generally occur as shallowly dipping, sheared lenses within weakly metamorphosed sedimentary rocks. Primary geological relationships are poorly preserved, but indicate that gabbro intruded the ultramafic rocks following their serpentinization. The correlative Midnight Dome complex (Fig. 1; Mortensen, 1990; van Staal et al., 2018) comprises similarly deformed and altered ultramafic rocks with minor mafic intrusive rocks. The Clinton Creek and Midnight Dome complexes yielded 265 ± 3 Ma and 264 ± 4 Ma crystallization ages that constrain the age of magmatism and provide a minimum age on the exhumation and alteration of the host harzburgite (van Staal et al., 2018).

Ultramafic rocks are highly depleted mantle harzburgite. Gabbroic rocks are characterized by a flat normal mid-ocean-ridge basalt (N-MORB) normalized profile with strong Nb depletion (Fig. 17b). Diabase has a flat N-MORB normalized profile with strong Nb depletion on an N-MORB normalized trace-element plot, characteristic of island-arc tholeiite (van Staal et al., 2018).

Subophiolite basement

Clear relationships between the ophiolite and its basement have not been established at Clinton Creek, and Abbott (1983) only described the imbrication of ophiolitic

rocks and Late Triassic sedimentary rocks. These sedimentary rocks yielded a Norian fauna (Orchard et al., 2006) and a ca. 228 Ma youngest detrital zircon (Beranek and Mortensen, 2011) and have been interpreted to form part of a regionally extensive Triassic overlap assemblage (Beranek and Mortensen, 2011). This indicates Late Triassic or younger imbrication in this area. Late Triassic sedimentary rocks and the Clinton Creek complex are imbricated with Devono-Mississippian volcano-sedimentary rocks of the Yukon-Tanana terrane (Yukon Geological Survey, 2019). To the southeast, ophiolitic rocks at Midnight Dome are imbricated with Devonian to Early Carboniferous sedimentary rocks, which contain ca. 358 Ma tuff (Yukon Geological Survey, 2019). These relationships suggest that the Clinton Creek and Midnight Dome complexes record significant Late Triassic or younger deformation, similar to the Harzburgite Peak complex. The occurrence of these complexes above the Devono-Mississippian volcano-sedimentary rocks suggests that they were originally emplaced on top of the Yukon-Tanana terrane (van Staal et al., 2018).

Dunite Peak complex

The Dunite Peak complex ophiolite (Fig. 1) preserves ultramafic, cumulate gabbro to tonalite, gabbro, and minor hypabyssal and volcanic rocks (de Keijzer et al., 1999; Parsons et al., 2017b, 2019). The ultramafic section is the structurally highest unit and comprises variably serpentinized harzburgite, dunite, orthopyroxenite, minor lherzolite, and gabbro (Parsons et al., 2019). The structurally underlying crustal section is characterized by interlayered cumulate gabbro, layered gabbro, leucogabbro, and finer grained epidote-amphibolite facies hypabyssal and volcanic rocks. All crustal rocks are pervasively sheared. A coarse-grained gabbro yielded a 265 ± 4 Ma crystallization age, which constrains the age of magmatism (Parsons et al., 2019).

Mafic rocks are characterized by LREE-enriched normal mid-ocean-ridge basalt normalized profiles with strong Nb depletion and Th enrichment (Fig. 17c). Some cumulate rocks have positive Eu and/or Ti anomalies, indicative of plagioclase and/or Fe-Ti accumulation. More evolved compositions are characterized by Ti depletion and enrichment of Zr and Hf. Dunite Peak complex crustal rocks yielded high $\varepsilon_{Nd(265\ Ma)}$ ranging from +7.2 to +9.0, indicative of juvenile mantle sources (Parsons et al., 2019).

Subophiolite basement

The Dunite Peak ophiolite structurally overlies a thin unit comprising limestone and graphitic sedimentary rocks, with rare pillow basalt, which yielded an enriched mid-ocean-ridge basalt geochemical signature that is distinctly different and unrelated to the Dunite Peak complex (Parsons et al., 2017b, 2019). The top of the graphitic siliciclastic unit comprises rare interbedded chert and volcaniclastic layers with an island-arc tholeiite chemistry, geochemically similar to that displayed by rocks from the crustal section of the Dunite Peak ophiolite (Parsons et al., 2017a). Devonian to Early Carboniferous marble, quartzite, and garnet-kyanite-mica schist of continental derivation structurally underlie the enriched mid-ocean-ridge basalt unit and Dunite Peak ophiolite. To the southeast, correlative marble and siliciclastic sedimentary rocks are intruded by Mississippian granodiorite and metamorphosed to eclogite and blueschist facies (Colpron et al., 2017; Gilotti et al., 2017).

OTHER MAFIC-ULTRAMAFIC COMPLEXES

Northern British Columbia and Yukon contain many other mafic-ultramafic complexes. It is beyond the scope of this manuscript to discuss these in detail; however, it is useful to highlight that not all mafic-ultramafic complexes are ophiolitic. In central Yukon, the Buffalo Pitts and Schist Creek complexes comprise peridotite, including mantle harzburgite, pyroxenite, hornblendite, and gabbro. Detailed study of the Buffalo Pitts complex indicates that it is an orogenic peridotite (i.e. exhumed continental lithospheric mantle) that was emplaced during the Permian into the extending Yukon-Tanana continental crust (Canil et al., 2003; Johnston et al., 2007). As such, it formed in a continental rift setting similar to Zabargad Island, Red Sea (Canil et al., 2003; Brooker et al., 2004), and is distinct from the Slide Mountain and Atlin terrane ophiolites. The Middle Permian Schist Creek complex (Ryan et al., 2016) likely also formed in a similar continental rift setting.

In the western Yukon, slivers of mafic-ultramafic rocks intercalated with the Kluane schist represent highly altered cumulate rocks, which are likely related to the Late Triassic Stikine plutonic suite (Canil et al., 2015). Similar cumulate rocks are exposed in central Yukon, where they comprise pyroxenite, hornblendite, and gabbro (Pyroxene Mountain suite: Ryan et al., 2013a). In British Columbia, mafic-ultramafic cumulate rocks associated with Late Triassic to Early Jurassic calc-alkaline and alkaline magmatism (formerly included in the now obsolete Polaris suite) comprise dunite, olivine pyroxenite, clinopyroxenite, hornblendite, and gabbro (Milidragovic et al., 2017). With the exception of the highly altered types, such as those imbricated with the Kluane schist (Canil et al., 2015), these mafic-ultramafic complexes tend to be pyroxene- and hornblende-rich and are distinctly different from the ophiolitic rocks in the Atlin and Slide Mountain terranes.

DISCUSSION

Pseudostratigraphy of ophiolites

The classic, Penrose-type ophiolites are characterized by a coherent pseudostratigraphy of ultramafic mantle rocks, ultramafic cumulate rocks, mafic cumulate rocks, isotropic gabbro, sheeted dykes, basalt, and overlying oceanic sedimentary rocks (Anonymous, 1972). With the exception of the King Mountain area (*see* 'King Mountain area'), most northern Cordilleran ophiolites are characterized by a non-Penrose pseudostratigraphy of voluminous mantle tectonite, diabase, and basalt, but with only a minor proportion of gabbro and mafic-ultramafic cumulate rocks (Fig. 14). The non-Penrose pseudostratigraphy was previously recognized in the Cassiar Mountains and attributed to development along a transform or in an oceanic core complex at an ultra-slow spreading centre (Nelson, 1993). In this section, oceanic core complexes are briefly reviewed, and implications for ophiolite pseudostratigraphy and ridge development are discussed.

In classic Penrose-type ophiolites, ongoing extension is accommodated by emplacement of magmas into the crust (Fig. 14a), most spectacularly forming sheeted dyke complexes (e.g. Baragar, 1954; Robinson et al., 2008). In contrast, oceanic core complexes accommodate extension by tectonic exhumation of gabbro and variably serpentinized mantle peridotite onto the ocean floor, forming characteristic megamullion structures (Fig. 14b; e.g. MacLeod et al., 2009). Earlier studies inferred that oceanic core complexes form during periods of very low magma productivity at slow and ultra-slow spreading mid-ocean ridges; however, recent investigations indicate that oceanic core complexes also form during periods of enhanced magma productivity (e.g. Ildefonse et al., 2007), are common at moderate spreading rates (5 cm/a to 7.6 cm/a: Tucholke et al., 2008), and can form within ridges that are otherwise characterized by magmatically accommodated extension (Ohara et al., 2003). Investigation of modern and ancient oceanic core complexes (e.g. Tremblay et al., 2009) indicated that they develop a pseudostratigraphy that is distinctly different from classic Penrose ophiolites. In oceanic core complexes, magmas are often emplaced directly into exhuming mantle (Ildefonse et al., 2007; Tucholke et al., 2008; Cannat et al., 2009; MacLeod et al., 2009), resulting in numerous gabbro intrusions within the mantle section (Fig. 14b; 'plum pudding' of Ildefonse et al., 2007), and generally lack the thick plutonic (layered gabbro–isotropic gabbro) and sheeted dyke sections of the classic Penrose-style ophiolite. Magmatic products that make it onto the ocean floor erupt instead directly onto exhumed mantle (Fig. 14b). As a result, the pseudostratigraphy of oceanic core complexes and slow spreading ridges may comprise mantle sections that are pervasively intruded by cumulate gabbro, isotropic gabbro, and diabase. Although megamullion structures characterize oceanic core complexes, not all detachments lead to exhumation of mantle onto the ocean floor and development of megamullions. Depending on the degree of extension and where the décollement roots, detachments within ophiolitic crust may juxtapose different levels of ophiolitic crust or juxtapose mantle with hypabyssal and volcanic rocks (Fig. 14b).

The majority of ophiolites in the northern Cordillera appear to have formed during tectonically accommodated extension, with local exhumation of the mantle to the ocean floor. This is indicated by clear evidence of emplacement of gabbro and diabase directly into mantle peridotite (Fig. 7e, f, g, 9c–g, 10b, 12f; e.g. McGoldrick et al., 2017; van Staal et al., 2018), common structural contacts between mantle and upper crust (Fig. 9g, 12d), and the local presence of ophicalcite and serpentinite-matrix breccia (e.g. Nelson, 1993). Where tholeiitic cumulate rocks occur, they only form thin, commonly structurally bound packages. These relationships indicate that a classic Penrose-type stratigraphy cannot be applied to most north Cordilleran ophiolites. These relationships also indicate that detachment faulting is extensive in north Cordilleran ophiolites, and occurred in a suprasubduction zone setting (Fig. 18). Atlin terrane ophiolites appear to exhibit detachment faulting as the dominant spreading mechanism over about 300 km strike length during a ca. 20 Ma period (264 Ma to 245 Ma; *see* descriptions above), whereas isolated massifs of the northern Slide Mountain terrane ophiolites exhibit detachment faulting over at least 800 km strike length between ca. 269 Ma and 264 Ma (Gabrielse et al., 1993; van Staal et al., 2018; Parsons et al., 2019)

Geochemical characteristics of ophiolites

Ophiolitic rocks in the Cordillera have been generally investigated either very locally (e.g. Ash, 1994; Piercey et al., 2001) or thematically on a very broad scale (e.g. Lapierre et al., 2003; Canil et al., 2006). Systematic evaluation of ophiolitic belts on a regional scale has been generally lacking. Many studies of northern Cordilleran ophiolites concluded that they represent either MORB or MORB-like environments (e.g. Murphy et al., 2006; Piercey et al., 2012). In some studies, this conclusion stemmed from the best available analytical methodology of the time, which could not effectively discriminate between arc and mid-ocean-ridge settings. Once analytical methodologies improved, many studies still failed to effectively discriminate between an arc–back-arc and mid-ocean-ridge settings. This problem in part stemmed from the significant overlap between island-arc tholeiite, back-arc-basin basalt, and mid-ocean-ridge basalt fields on tectonic discrimination plots (e.g. Shervais, 1982; Cabanis and Lecolle, 1989). In addition, the common practice of using primitive mantle-normalized extended trace-element plots for tectonic discrimination can lead to significant errors because they de-emphasize differences. It is much more effective to directly compare unknown samples to MORB by plotting them on normal mid-ocean-ridge

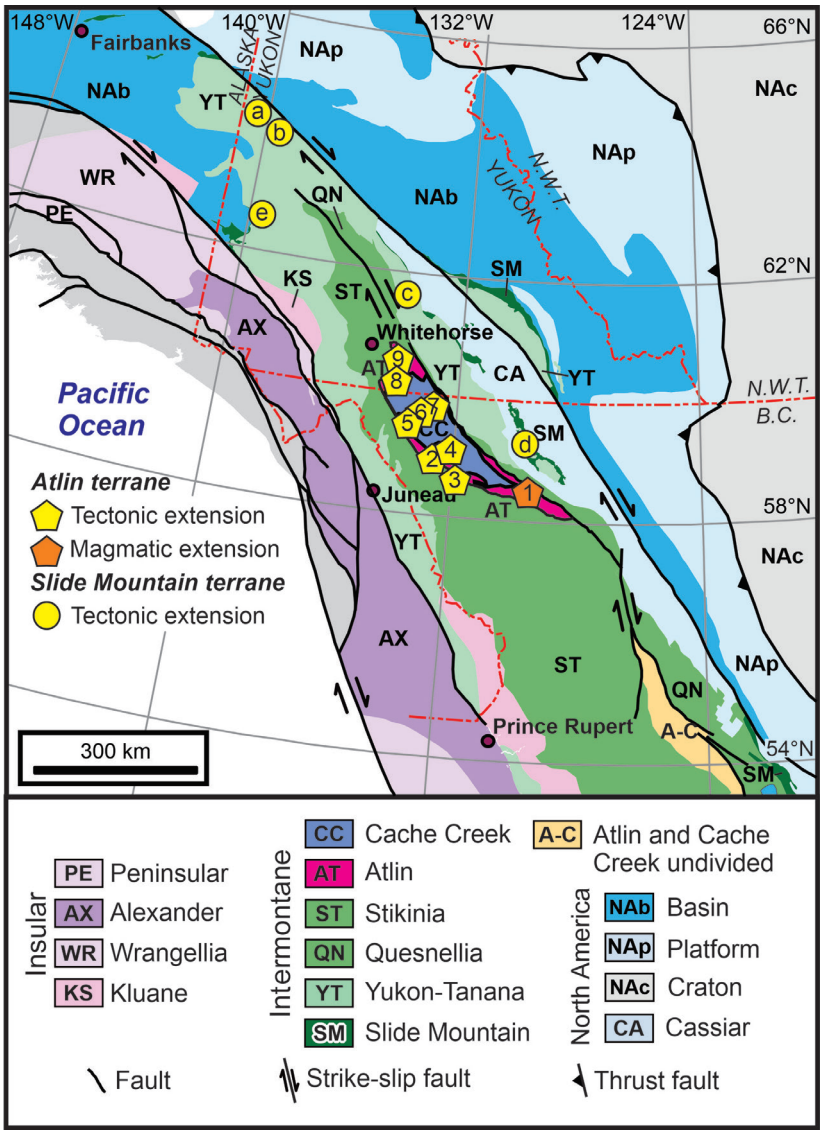

Figure 18. Distribution of tectonically and magmatically accommodated spreading modes in Middle Permian to Middle Triassic ophiolites in the northern Cordillera (terrane map *modified from* Colpron and Nelson, 2011). Atlin terrane: 1 = King Mountain, 2 = Hardluck and Peridotite Peaks, 3 = Hatin Lake, 4 = Menatatuline Range to Nimbus Mountain, 5 = Union Mountain, 6 = Mount Barham, 7 = Marble Dome, 8 = Jubilee Mountain, 9 = Squanga Lake. Slide Mountain terrane: a = Clinton Creek, b = Midnight Dome, c = Dunite Peak, d = Cassiar Mountains, e = Harzburgite Peak. Ophiolite formation styles are not evaluated herein for the Finlayson district or south of 58°N.

basalt normalized extended trace-element plots, as this method emphasizes the differences in Th-Nb-La contents (Fig. 6, 13, 15), which otherwise are, at best, ambiguous.

The present investigation of the Atlin terrane ophiolites clearly demonstrate that they formed in arc-related settings (island-arc tholeiite, back-arc tholeiite, and boninite). The crustal magmatic rocks plot on and above the mantle array of the Th/Yb-Nb/Yb plot, indicating minor to significant subduction-zone influence (Fig. 15a: Pearce et al., 2008). The suprasubduction zone signatures of these ophiolites are similar to the adjacent, and partly coeval, Early to Middle Triassic volcanic rocks of the Kutcho complex, Joe Mountain Formation, and Tsabayhe Group, suggesting that they belong to the same arc–back-arc system (Fig. 15b). The realization that ophiolites do not represent a mid-ocean-ridge setting has significant implications to tectonic reconstructions as it requires them to have occupied the upper plate, not the lower plate, during subduction and likely during collision.

Previous studies of the Atlin- and Cache Creek-terrane–correlative rocks in central and southern British Columbia suggested that ophiolitic rocks are characterized by normal mid-ocean-ridge basalt geochemical signatures and likely formed the basement of oceanic plateaus (Tardy et al., 2001; Lapierre et al., 2003). Evaluation of these models and data sets reveals several problems. Most importantly, ophiolitic rocks are younger (Late Permian: Struik et al., 2001) than the oceanic sequences of the plateaus (Carboniferous to Permian: Orchard et al., 2001; Sano et al., 2001). As such, these ophiolites cannot form the basement to older plateaus. In addition, there are significant problems with the available geochemical data and interpretations. The volcanic and intrusive components of the ophiolites in these previous studies have pronounced positive Zr-Hf anomalies, suggesting either incomplete dissolution of samples and/or chemical compositions dominated by cumulate processes

(Fig. 19a), which makes these samples generally unsuitable for tectonic discrimination (Pearce, 1996). In any case, the inferred normal mid-ocean-ridge basalt setting is inconsistent with the fact that many samples have significant negative Nb anomalies, indicating subduction-zone influence (Fig. 19a). These samples are also distinctly different from the Cache Creek terrane 'plateaus' volcanic samples, characterized by enriched mid-ocean-ridge basalt to ocean-island basalt chemical composition (Fig. 19a).

Detailed investigation of rocks correlative with the Atlin and Cache Creek terranes in the area around Trembleur Lake indicated the presence of a significant volume of island-arc tholeiite and back-arc-basin basalt within ophiolitic rocks (Fig. 19b; Milidragovic et al., 2018; Milidragovic and Grundy, 2019). Furthermore, harzburgites and strongly serpentinized ultramafic rocks from the Trembleur Lake area have relatively high SiO_2 contents (Milidragovic and Grundy, 2019) characteristic of subarc mantle (Bénard et al., 2017). This area also contains a significant volume of Paleozoic ocean-island basalt (Fig. 19b; Milidragovic and Grundy, 2019), likely associated with the Cache Creek terrane. As such, the relationships established herein between the Atlin terrane ophiolites (island-arc tholeiite, back-arc-basin basalt, and boninite) and the Cache Creek terrane carbonate platform (ocean-island basalt and enriched mid-ocean-ridge basalt) appear to be regionally valid.

Similar to the Atlin terrane, the Slide Mountain terrane ophiolites (Harzburgite Peak, Clinton Creek, Midnight Dome, and Dunite Peak: *see* 'Slide Mountain and Yukon-Tanana terranes') show minor to significant subduction-zone influence (Fig. 17), indicating that they formed in an arc–back-arc setting. Extrapolation of these conclusions to the existing interpretations of the Slide Mountain and Yukon-Tanana terranes is difficult because many of these ophiolitic rocks have been interpreted to be in stratigraphic continuity with continental arcs and rifts (Murphy et al., 2006). The correlatives of these ophiolites in northern British Columbia are exposed in the Sylvester allochthon, where they form structurally dismembered ophiolite massifs that were previously interpreted as MORB or back-arc-basin basalt (marginal basin; Nelson, 1993). The re-analysis of samples from that area by the present authors indicated that there is a significant volume of island-arc tholeiite (Fig. 19c), and that Harzburgite Peak, Clinton Creek, and Midnight Dome ophiolites formed in a back-arc ridge environment that was in close proximity to a Middle Permian subduction zone. Although these data do not change the interpretation of the origin of the Slide Mountain terrane as a back-arc basin, they do indicate that these ophiolites were not part of the subducting Slide Mountain Ocean, but rather formed part of the Middle Permian overriding arc system (e.g. van Staal et al., 2018; Parsons et al., 2019). Further south, geochemical investigations of the Slide Mountain terrane also indicate significant component of island-arc tholeiite and back-arc-basin basalt, including in the type locality on Sliding Mountain (Fig. 19d). Similar to the problematic "Cache Creek terrane" as previously defined, the Slide Mountain terrane combines rock assemblages that formed in distinctly different tectonic settings and/or on different tectonic plates (Fig. 19e).

Longevity of ophiolites

In the simplest terms, ophiolites represent fragments of oceanic lithosphere generated along spreading centres (Fig. 14). They can form in a variety of environments, including in advanced intercontinental rifts, along hyperextended continental margins, in back-arc spreading centres, and along mid-ocean ridges (e.g. Bédard et al., 1998; Zagorevski et al., 2006; Manatschal et al., 2011; Stern et al., 2012; van Staal et al., 2013; Dilek and Furnes, 2014; Pearce, 2014). Irrespective of their exact tectonic setting, the development of spreading centres necessitates formation of new oceanic crust at the ridge and its movement away from the ridge over time (Fig. 14). Crustal accretion can be symmetrical or highly asymmetrical across a ridge (Fig. 14). Once the crust moves away from the ridge, it also moves away from the axial melt lens and ridge-related magmatism ceases as hydrothermal cells propagate deeper in the section and stabilize the suboceanic lithospheric mantle. This process leads to characteristic, age-dependent magnetization of modern ocean floor and back-arc basins. Off-axis magmatism is generally restricted to a few kilometres away from the ridge, and as such, it is of similar age to the ridge itself. As the newly

Figure 19. Geochemical characteristics of oceanic terranes in British Columbia and Yukon indicate that all oceanic terranes group distinctly different tectonic environments. Northern Atlin (green) and Cache Creek (blue) terrane fields are plotted on Cabanis and Lecolle (1989) ternary plots to the far right for a, b, and c for comparison. **a)** Geochemical diversity in southern and central Cache Creek terrane (undivided) indicates that distinct tectonic environments are erroneously grouped together (Tardy et al., 2001; Lapierre et al., 2003). **b)** High-quality analyses indicate presence of ocean-island basalt, island-arc tholeiite, and back-arc-basin basalt environment magmas in Trembleur Lake area (Milidragovic and Grundy, 2019), suggesting similar relationships as Atlin and Cache Creek terranes in northern British Columbia. **c)** Reanalyses of Slide Mountain terrane rocks in the Sylvester allochthon (Nelson, 1993) indicate that they are characterized by island-arc tholeiite chemistry. **d)** Geochemical diversity of the Slide Mountain terrane in southern and central British Columbia indicates that distinct tectonic environments were erroneously grouped together (Tardy et al., 2001; Lapierre et al., 2003). Furthermore, rocks that were interpreted as MORBs are actually back-arc-basin basalt to island-arc tholeiite. **e)** Geochemical diversity of the Slide Mountain terrane in Yukon and British Columbia indicates that distinct tectonic environments were erroneously grouped together and that there are significant geochemical similarities between Slide Mountain, Atlin, and Cache Creek terranes.

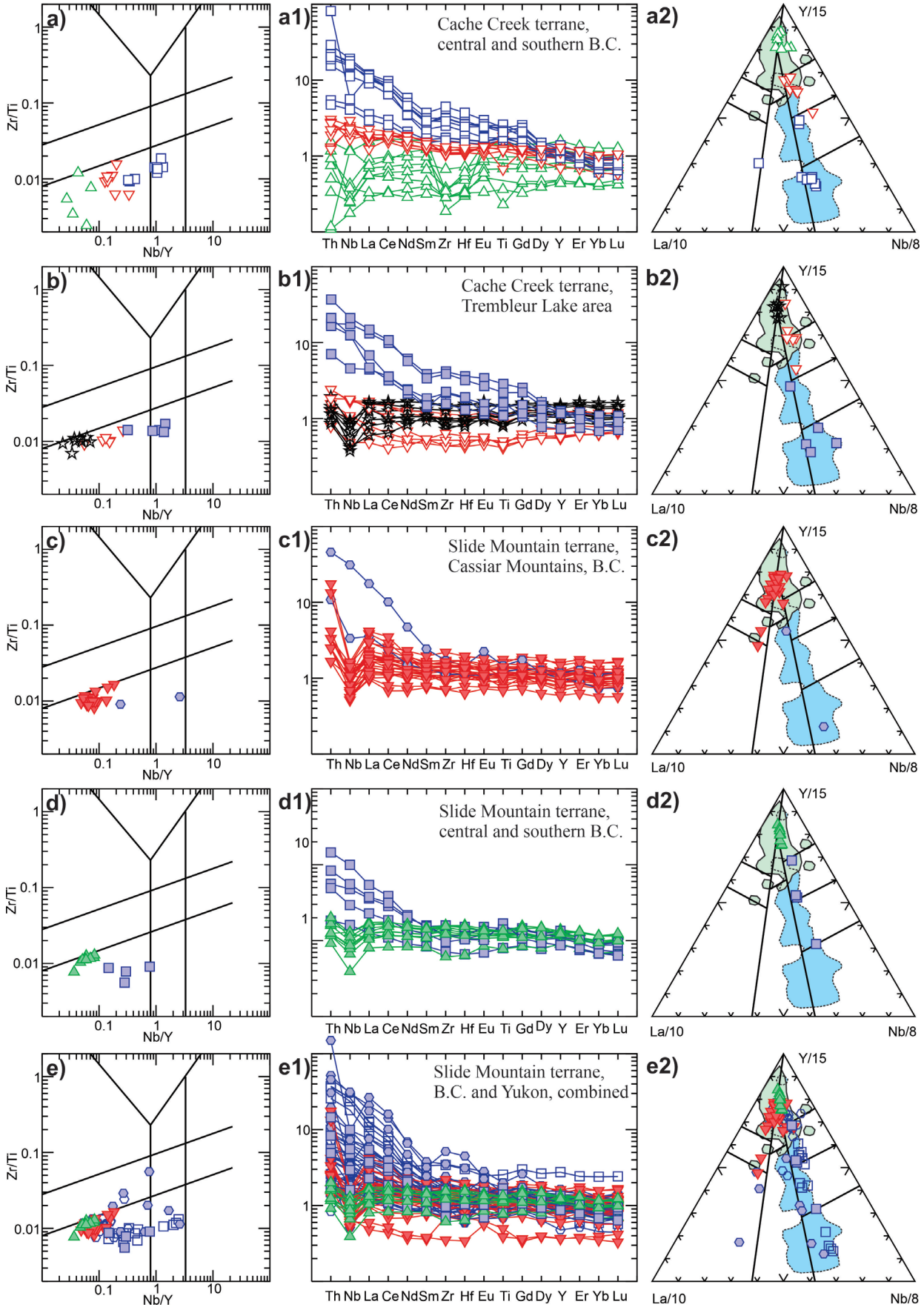
a)
a1)
Cache Creek terrane,
central and southern B.C.
a2)
b)
b1)
Cache Creek terrane,
Trembleur Lake area
b2)
c)
c1)
Slide Mountain terrane,
Cassiar Mountains, B.C.
c2)
d)
d1)
Slide Mountain terrane,
central and southern B.C.
d2)
e)
e1)
Slide Mountain terrane,
B.C. and Yukon, combined
e2)
Zr/Ti
Nb/Y
Th Nb La Ce Nd Sm Zr Hf Eu Ti Gd Dy Y Er Yb Lu
Y/15
La/10
Nb/8

formed crust moves away from the ridge, it may pass over mantle plumes or other enriched mantle sources, resulting in renewed magmatism that leads to formation of ocean-island basalt (e.g. Ishizuka et al., 2009). These ocean-island basalts are in stratigraphic contact with the underlying ocean crust; ocean islands are distinct from the ocean floor and are unrelated to the ridge. Environments such as the North Fiji Basin are distinct, as the plume component is directly sampled during back-arc ridge development (e.g. Eissen et al., 1994).

On a broad scale, formation of ophiolites at spreading centres results in lateral age dependency of crustal rocks (i.e. laterally diachronous), rather than long-term vertical stratification. Transform faults juxtapose different age domains, but this does not result in vertical stratification. Rifting of arcs or continents and opening of ocean basins does not create vertical stratification of ophiolite on top of rifted basement. This is because spreading centres create new crust above upwelling and melting mantle (Fig. 14). Dykes related to early rifts can intrude into the rifted basement and overlying sedimentary rocks (Reston and Manatschal, 2011), and continent-derived sediments may interfinger with parts of the ophiolite (van Staal et al., 2013), but the ophiolite and its mantle can never have a continental basement. This simple scenario may be complicated by having several generations of rifts in the same basin (Kurth et al., 1998), but new ridges still create new oceanic crust.

The concepts described above should form guiding principles for understanding ophiolites in any ancient orogenic belt, including the Canadian Cordillera. In the case of the Atlin terrane, ophiolitic rocks yielded ages ranging from ca. 264 Ma to 245 Ma. This indicates that the Atlin terrane spreading centres were active over about 19 Ma, generating as much as 570 km to 1700 km of back-arc-basin crust (assuming 3 cm/a to 8.8 cm/a continuous spreading, equivalent to Mariana Trough and Parece Vela back-arc basins respectively: Stern et al., 1996; Ohara et al., 2003). The actual width of this back-arc basin could be significantly less if extension was oblique, or if Atlin terrane ophiolites were generated during episodic extension. Even if episodic extension is assumed, the present extent of the Atlin terrane requires significant shortening of this basin in order to bring the various ages of ophiolites together. This suggests that the Atlin terrane is composite and comprises related, but widely separated fragments of a much larger back-arc basin (Fig. 16). For now, the present authors' data are not detailed enough to reliably delineate the individual ophiolitic components. Detailed studies of individual ophiolite massifs, however, do show significant promise in delineating distinctly different mantle domains (Canil et al., 2006; Corriveau, 2018; McGoldrick et al., 2018; Lawley et al., 2020), which may facilitate identification of distinct ophiolites.

The interpretation of the Slide Mountain and Yukon-Tanana terranes in Yukon poses significant challenges if the new perspective of ophiolite and back-arc basin development is considered. Most studies have interpreted that rifting of the Yukon-Tanana terrane in the Late Devonian to Early Carboniferous led to departure of the Yukon-Tanana terrane from the Laurentian margin and opening of the Slide Mountain Ocean as a peri-continental back-arc basin (Slide Mountain terrane). Rifting occurred either continuously or episodically over ca. 100 Ma, forming several ophiolitic sequences. Ophiolite generation started with Late Devonian Finlayson Assemblage boninites (Piercey et al., 2001), Early Permian Harzbugite Peak Complex island-arc tholeiite basalts (*see* 'Harzburgite Peak complex' section; Canil and Johnston, 2003; Canil et al., 2019), Early Permian Campbell Range Formation EMORB–island-arc tholeiite–MORB-ocean-island basalt (Piercey et al., 2012), and ending with formation of Middle Permian island-arc tholeiite ophiolites (*see* 'Slide Mountain and Yukon-Tanana terranes' section, Colpron et al., 2005; van Staal et al., 2018; Parsons et al., 2019). The Late Devonian boninites and Early Permian Campbell Range Formation were interpreted to be in stratigraphic continuity with the continentally derived or contaminated volcanic and plutonic suites (Piercey et al., 2001, 2003, 2006, 2012; Murphy et al., 2006). Piercey et al. (2001) interpreted these boninites to have formed in a ridge environment in a continental arc setting. Although a continental setting is certainly not typical for boninite generation (e.g. Falloon and Crawford, 1991; Sobolev and Danyushevsky, 1994; Deschamps et al., 2003), there is emerging evidence that many intraoceanic arcs originate on or near continental crust (e.g. Falloon et al., 2014; Tapster et al., 2014); however, the present authors are not aware of any cases where active continental arc magmatism is intimately associated with formation of boninite-dominated spreading ridges as envisioned by Piercey et al. (2001).

Recent boninites in the southwest Pacific Ocean form in: 1) a back-arc ridge propagating into an arc front, 2) along intersection of a back-arc spreading centre and a subduction zone-terminating transform fault, or 3) along the intersection of a back-arc spreading centre and incipient subduction zone that was formerly a transform fault (Fig. 16; e.g. Deschamps et al., 2003). Generation of boninites in spreading centres (e.g. Stern and Bloomer, 1992; Bédard et al., 1998; Deschamps et al., 2003; Schroetter et al., 2003) moves existing crust away from the spreading centre and requires that boninites are not built on continental basement, nor can extensive continentally derived plutons and related volcanic rocks be emplaced on top. As such, the current interpretation of the Yukon-Tanana terrane as Devonian to Permian arc built on older continental margin (e.g. Colpron et al., 2007) is not consistent with the known oceanic setting of recent and ancient boninites, or with their occurrence in suprasubduction zone spreading ridge environments.

The Yukon-Tanana and Slide Mountain terranes in Yukon underwent further back-arc spreading during the Early to Middle Permian, resulting in EMORB–island-arc tholeiite–MORB–ocean-island basalt magmatism in the Campbell Range Formation (Piercey et al., 2012). This phase of ridge development has been interpreted to have occurred

in a highly oblique environment, resulting in formation of an arc-perpendicular ridge and arc-parallel transform faults (Nelson, 1993; Piercey et al., 2012) and emplacement of a significant volume of ultramafic and mafic intrusions (Murphy et al., 2006). The association of island-arc tholeiite–MORB with mafic-ultramafic rocks is most consistent with obducted ophiolitic complexes (Zagorevski and van Staal, 2011), similar to other Slide Mountain terrane ophiolites such as Harzburgite Peak, Clinton Creek, Midnight Dome, and Dunite Peak complexes (*see* 'Slide Mountain and Yukon-Tanana terranes' section; Canil and Johnston, 2003; van Staal et al., 2018; Canil et al., 2019; Parsons et al., 2019), rather than with stratigraphic or intrusive contacts (e.g. Murphy et al., 2006).

The Slide Mountain terrane ophiolite and back-arc-basin development poses similar challenges in British Columbia. In its type locality at Sliding Mountain, the presence of Mississippian and Early Permian volcanic rocks (Struik and Orchard, 1985) suggests spreading over more than 60 Ma and sedimentation over 100 Ma. This probably generated a basin that was significantly wider than 500 to 1000 km, even if rifting was episodic, oblique, and slow. Thus, significant shortening of this basin is required to explain the overall narrow exposure of the belt of Slide Mountain terrane. This implies that the individual thrust sheets at Sliding Mountain likely represent originally widely separated parts of a much larger back-arc basin (e.g. Harms and Murchey, 1992). Similar, or longer magmatic history and tectonostratigraphic relationships has been identified in other parts of the Slide Mountain terrane in British Columbia (Monger et al., 1991), indicating that the composition and tectonic setting of the Slide Mountain terrane as a whole must be re-evaluated (e.g. van Staal et al., 2018; Parsons et al., 2019).

Implications for terrane definitions and sutures

Ophiolitic rocks in the Cordillera have been generally grouped into 'oceanic' terranes that comprise ophiolites, chert, limestone, and/or siliciclastic rocks, as well as ocean-island basalt to enriched mid-ocean-ridge basalt volcanic rocks (e.g. Nelson, 1993; Piercey et al., 2001, 2004, 2012; Lapierre et al., 2003; Murphy et al., 2006). This has resulted in significant challenges for stratigraphic nomenclature, terrane definitions, and tectonic reconstructions in the Cordillera. This problem is exemplified in the Atlin and Cache Creek terranes, which were grouped as a single terrane prior to this study. From a historical perspective, grouping 'oceanic' rocks into a single terrane made sense in the absence of direct age constraints, and in the context of scientific thought at the time (Fig. 4a). That is, ophiolites were generally accepted to represent mid-ocean ridges (e.g. Monger et al., 1991). As such, it was natural to assume that oceanic plateau-like sequences were built on top of older ophiolitic ocean floor. Cache Creek terrane carbonate rocks were thus interpreted to represent atolls on top of oceanic plateaus that were coeval with deep-water oceanic sediments such as chert and shale (Monger et al., 1991).

Recent data clearly demonstrate that this simple model is inconsistent with the newly established relationships (Fig. 4b). Atlin terrane ophiolitic rocks formed in a suprasubduction zone, broadly arc-related oceanic environment, rather than in a normal mid-ocean-ridge setting (*see* Fig. 12, English et al., 2010; Bickerton, 2013; McGoldrick et al., 2017). Precise U-Pb zircon constraints on Atlin terrane ophiolitic sequences indicate that they range from Middle Permian to Middle Triassic (ca. 264 Ma to 245 Ma; e.g. Gordey et al., 1998; Mihalynuk et al., 2003; N. Joyce, R. Friedman, and A. Bogatu, unpub. data, 2020). Hence, Atlin terrane ophiolites are much too young to be the basement to the Cache Creek terrane carbonate platform that initiated by the Early Carboniferous (Monger and Ross, 1971; Monger, 1977a, b; Golding, 2018). The Cache Creek terrane carbonate platform is also highly unusual because carbonate deposition occurred contemporaneously with, or episodically alternated with, magmatic and/or volcanic activity throughout much of its 100 Ma history, and did not form discrete postvolcanic capping carbonate atolls on top of quiescent ocean islands or plateaus. The carbonate platform appears to have been buoyant throughout its history, as indicated by shallow-water facies carbonate rocks and fossils. Its demise largely coincides with the global Permo-Triassic mass extinction, rather than reflecting thermal subsidence. Furthermore, the majority of the oceanic sedimentary rocks are too young (i.e. Middle Triassic to Early Jurassic Kedahda Formation and equivalents: e.g. Cordey et al., 1991; Mihalynuk et al., 2003, 2004b) to represent basinal facies coeval with the Paleozoic carbonate platform. Instead, these sedimentary rocks appear to unconformably overlie both Atlin and Cache Creek terranes and as such represent marine overlap assemblages (Zagorevski et al., 2018), rather than 'oceanic' (i.e. ocean floor) stratigraphy.

The historical grouping of unrelated tectonostratigraphic units (Atlin and Cache Creek terranes) into a single 'oceanic' terrane has negatively impacted stratigraphic nomenclature, terrane definitions, and tectonic reconstructions. For example, Middle Permian to Middle Triassic arc-related ophiolitic basalts were correlated with predominantly Carboniferous within-plate basalts and included within a singular Nakina Formation (Cui et al., 2017; Yukon Geological Survey, 2019). From a stratigraphic perspective, this has created significant confusion because it required that the Nakina Formation ranges from Early Carboniferous to Middle Triassic, was characterized by distinctly different chemistry at different times (Fig. 15d), and contained intimately associated, but seemingly incompatible rock types (shallow-water carbonate platform and ocean-floor mantle). From a terrane definition perspective, the Nakina Formation grouped rocks that originated in distinctly different tectonic environments into a single terrane, and failed to recognize that a fundamental suture exists between them (Fig. 3). This

further led to misinterpretation of steep Teslin, Nahlin, and King Salmon faults as terrane boundaries (e.g. Silberling et al., 1992), rather than recognizing them as younger faults that cut across a previously unidentified shallow-dipping terrane boundary. The interpretation of Teslin, Nahlin, and King Salmon faults as terrane boundaries has had a cascading impact on terrane definitions as correlative sequences on either side of these faults were separated into different terranes and their linkages were either not evaluated or they were ignored. For example, Hart (1997) suggested a correlation between Joe Mountain Formation of Stikinia and the Atlin terrane ophiolitic rocks (Cache Creek terrane in Hart, 1997); Monger et al. (1991) suggested that provenance of the Late Triassic Kedahda Formation may provide a link to Stikinia; and, Gabrielse (1998) suggested that Sinwa Formation of Stikinia stratigraphically overlies the Kutcho complex. These proposed correlations contradicted the existing terrane framework and were not properly tested, yet recent work supports these correlations (*see* 'Cache Creek and Atlin terranes section', English and Johnston, 2005; Schiarizza, 2012; Bickerton, 2013; Bordet et al., 2019).

Grouping of unrelated tectonostratigraphic units into a single 'oceanic' terrane resulted in unrealistic tectonic models and reconstructions. Examples include misidentification of vast tracts of accretionary prisms or mélange, proposed obduction of the subducting plate (Mihalynuk et al., 1994), unattributed orogenic episodes (e.g. Tahltanian Orogeny: Logan et al., 2000), and misattribution of provenance of terranes on the basis of fossils in unrelated terranes. Previous models generally inferred that Atlin terrane ophiolitic rocks are far-travelled and exotic to Laurentia (i.e. derived from Paleo-Tethys Ocean: e.g. Johnston and Borel, 2007). This inference was based on 'Tethyan' conodonts, fusulinids, and ammonoids that were collected from the Cache Creek carbonate platform (Fig. 20; e.g. Aitken, 1959; Monger, 1975, 1977b; Orchard et al., 2001; Sano et al., 2001, 2003). Detailed re-evaluation of fusulinids and ammonoids was not possible during this study; however, fusulinids (Fig. 20) are highly sensitive to water temperature and depth. The maximum depth range of fusulinids in the Late Paleozoic is estimated to be about 10 m to 40 m (*see* Davydov, 2014 for an overview), consistent with shallow-water, lagoonal carbonate facies inferred for parts of Horsefeed Formation within the Cache Creek terrane (Monger, 1975; Sano et al., 2003). In contrast, ophiolites generally represent oceanic spreading centres with water depths of about 3 km to 5 km (e.g. Ohara et al., 2003; Tucholke et al., 2008). As such, miscorrelation between carbonate platform (basalts intercalated with the Horsefeed Formation) and ophiolite (volcanic and hypabyssal crustal section) led to attribution of a Tethyan affinity to the unrelated deep-water spreading centres. In fact, there is no evidence that these ophiolitic rocks are in any way formed in the Tethyan realm from a fossil perspective. In addition, detailed re-evaluation of existing conodont collections indicates that the Cache Creek terrane carbonate platform (as defined herein) lacks the characteristic Tethyan realm faunal assemblage (Golding, 2018). Hence, the carbonate platform most likely represents a warmer paleoenvironment or paleolatitude than the adjacent terranes, a view that was originally advocated by Monger and Ross (1971), but subsequently abandoned (Monger, 1977b; Orchard et al., 2001; Sano et al., 2001, 2003).

The definition of the 'oceanic' Slide Mountain terrane shares many of the same problems described above for the Atlin and Cache Creek terranes. From a stratigraphic perspective, grouping of 'oceanic' elements has resulted in a confusing nomenclature that combines units with distinctly different chemistry formed in tectonically unrelated arc and within-plate oceanic environments (e.g. Campbell Range Formation: Piercey et al., 2012; *see* Parsons et al., 2019 for further discussion). From a tectonic perspective, grouping of unrelated oceanic rocks has also resulted in implausible tectonic models that require suprasubduction ophiolite generation in a subducting plate or continental setting, obduction of the subducting plate, multiple episodes of ridge formation on top of the same continental basement, high-pressure metamorphism of the arc, and unexplained orogenic episodes (*see* van Staal et al., 2018; Parsons et al., 2019 for a review).

CONCLUSIONS

Ophiolites form a major and very recognizable component of the Canadian Cordillera. The present investigation of ophiolite complexes in the northern Canadian Cordillera indicates they do not represent long-lived ocean basins far removed from subduction zones. Instead, they formed in suprasubduction zone settings, likely shortly before collisions with adjacent buoyant terranes. Canadian Cordillera ophiolites have been previously grouped together with

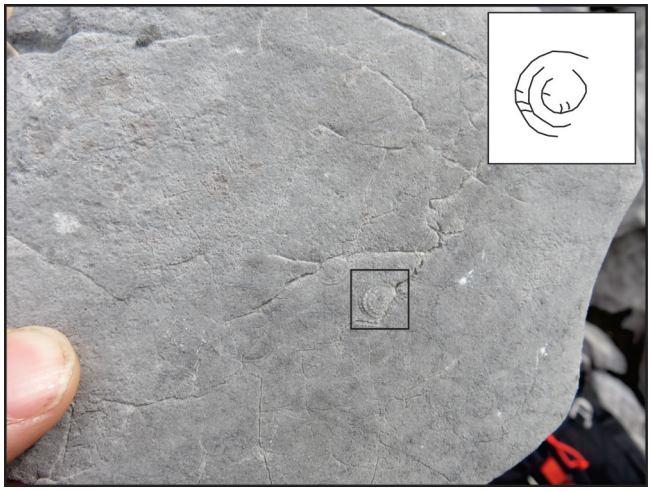

Figure 20. Fusulinids such as this one lived in shallow, warm seas. Inset: outline of fusulinid test wall. Their presence was initially attributed to paleo-environment or paleolatitude (Monger and Ross, 1971), but subsequently ascribed to paleolongitude. Photograph by A. Zagorevski. NRCan photo 2019-734

marine sedimentary rocks and geochemically unrelated volcanic rocks into 'oceanic' terranes. This flawed grouping resulted in significant problems with stratigraphic nomenclature and failed to recognize the presence of fundamentally distinct terranes. This, in turn, led to the definition of incorrect terrane boundaries that cut and displace older, more realistic tectonic boundaries. The sum of these errors has had a cascading effect on the creation of tectonic models that are based on an upside-down tectonostratigraphy, where the upper plates in subduction zone systems (i.e. ophiolites) were interpreted as the subducting plate. The present authors' investigations in northern British Columbia and Yukon indicate that all 'oceanic' terranes and their boundaries should be re-evaluated (e.g. van Staal et al., 2018; Parsons et al., 2019). The present investigation of ophiolites also revealed some unexpected results with respect to the development of ophiolites. For example, most of the north Cordilleran ophiolite complexes preserve evidence of extensive tectonically accommodated extension in magmatically productive environments. Such environments are recognized in modern and ancient environments (e.g. Ohara et al., 2003; Miranda and Dilek, 2010; Tani et al., 2011), but not on the scale observed in the northern Cordillera.

ACKNOWLEDGMENTS

This project was funded by the Geo-mapping for Energy and Minerals program with co-operative funding and support from the British Columbia Geological Survey and Yukon Geological Survey. Discovery Helicopters (Atlin) and Capital Helicopters (Whitehorse) are gratefully acknowledged for efficient and safe service and logistical support. This manuscript was reviewed and improved by J. Cutts and N. Rogers.

REFERENCES

Abbott, G., 1983. Origin of the Clinton Creek asbestos deposit; *in* Yukon Exploration and Geology 1982: Exploration and Geological Services Division; Indian and Northern Affairs Canada, Yukon, p. 18–25.

Aitken, J.D., 1959. Atlin map-area, British Columbia; Geological Survey of Canada, Memoir 307, 89 p. https://doi.org/10.4095/100528

Anonymous, 1972. Penrose field conference on ophiolites; Geotimes, v. 17, p. 22–24.

Ash, C.H., 1994. Origin and tectonics setting of ophiolitic ultramafic and related rocks in the Atlin area, British Columbia (NTS 104N); British Columbia Ministry of Energy, Mines and Petroleum Resources, Bulletin, v. 94, 54 p.

Ash, C.H., 2004. Geology of the Atlin area, Northwestern British Columbia; British Columbia Ministry of Energy and Mines, British Columbia Geological Survey, Geoscience Map 2004-4, scale 1:25 000.

Baragar, W.R.A., 1954. Report on the Betts Pond area on the Burlington Peninsula, Newfoundland; Newfoundland and Labrador Geological Survey, Assessment File 2E/13/0091, 8 p.

Bédard, J.H., Lauziere, K., Tremblay, A., and Sangster, A., 1998. Evidence for forearc seafloor-spreading from the Betts Cove Ophiolite, Newfoundland; oceanic crust of boninitic affinity; Tectonophysics, v. 284, p. 233–245. https://doi.org/10.1016/S0040-1951(97)00182-0

Bédard, J.H., Lauziere, K., Tremblay, A., Sangster, A., Douma, S.L., and Dec, T., 2000. Betts Cove Ophiolite and its cover rocks, Newfoundland; Geological Survey of Canada, Bulletin 550, 76 p. https://doi.org/10.4095/211642

Bédard, J.H.J., Zagorevski, A., and Corriveau, A.S., 2016. Fractional crystallization, impregnation and sulphide saturation recorded in Mesozoic arc-related cumulates at King Mountain, Cache Creek Ophiolite, northern British Columbia; American Geophysical Union Fall Meeting 2016, San Francisco, California, December 12–16, 2016, abstract V31D-04.

Bénard, A., Arculus, R.J., Nebel, O., Ionov, D.A., and McAlpine, S.R.B., 2017. Silica-enriched mantle sources of subalkaline picrite-boninite-andesite island arc magmas; Geochimica et Cosmochimica Acta, v. 199, p. 287–303. https://doi.org/10.1016/j.gca.2016.09.030

Beranek, L.P. and Mortensen, J.K., 2011. The timing and provenance record of the Late Permian Klondike Orogeny in northwestern Canada and arc-continent collision along western North America; Tectonics, v. 30, TC5017, 5 p. https://doi.org/10.1029/2010TC002849

Bickerton, L., 2013. The northern Cache Creek terrane: record of Middle Triassic arc activity and Jurassic-Cretaceous terrane imbrication; M.Sc. thesis, Simon Fraser University, Vancouver, British Columbia, 89 p.

Bickerton, L., Colpron, M., and Gibson, D., 2013. Cache Creek terrane, Stikinia, and overlap assemblages of eastern Whitehorse (NTS 105D) and western Teslin (NTS 105C) map areas; *in* Yukon Exploration and Geology 2012, (ed.) K.E. MacFarlane, M.G. Nordling, and P.J. Sack; Yukon Geological Survey, p. 1–17.

Bloodgood, M.A., Rees, C.J., and Lefebure, D.V., 1989a. Geology of the Atlin area, NTS 104N/11W, 12E; British Columbia Geological Survey Branch, Open File 1989-15, scale 1:50 000.

Bloodgood, M.A., Smyth, W.R., Rees, C.J., and Lefebure, D.V., 1989b. Geology and mineralization of the Atlin area, northwestern British Columbia (104N/11W and 12E); *in* Geological Fieldwork 1988; British Columbia Ministry of Energy, Mines and Petroleum Resources, Paper 1989-1, p. 311–322.

Bordet, E., 2017. Updates on the Middle Triassic-Middle Jurassic stratigraphy and structure of the Teslin Mountain and east Lake Laberge areas, south-central Yukon; *in* Yukon Exploration and Geology 2016, (ed.) K.E. MacFarlane and L.H. Weston; Yukon Geological Survey, p. 1–24.

Bordet, E., 2018. Bedrock geology map of the Teslin Mountain and east Lake Laberge areas; Yukon Geological Survey, Open File 2018-1, scale 1:50 000.

Bordet, E., Crowley, J.L., and Piercey, S.J., 2019. Geology of the eastern Lake Laberge area (105E), south-central Yukon; Yukon Geological Survey, Open File 2019-1, 120 p.

Breitsprecher, K. and Mortensen, J.K., 2004. BCAge 2004A – a database of isotopic age determinations for rock units from British Columbia; British Columbia Ministry of Energy and Mines, Geological Survey, Open File 2004-3 (release 3.0).

Brooker, R.A., Rudnick, R.L., James, R.H., Blundy, J.D., and Nakamura, E., 2004. Trace elements and Li isotope systematics in Zabargad peridotites: evidence of ancient subduction processes in the Red Sea mantle; Chemical Geology, v. 212, p. 179–204. https://doi.org/10.1016/j.chemgeo.2004.08.007

Cabanis, B. and Lecolle, M., 1989. Le diagramme La/10-Y/15-Nb/8: un outil pour la discrimination des séries volcaniques et la mise en évidence des processus de mélange et/ou de contamination crustale. The La/10-Y/15-Nb/8 diagram: a tool for distinguishing volcanic series and discovering crustal mixing and/or contamination; Comptes Rendus de l'Académie des Sciences, Série 2, Mécanique, Physique, Chimie, Sciences de l'Univers, Sciences de la Terre, v. 309, p. 2023–2029.

Canil, D. and Johnston, S.T., 2003. Harzburgite Peak: A large mantle tectonite massif in ophiolite from southwest Yukon; *in* 2002 Yukon Exploration and Geology; (ed.) D.S. Emond and L.L. Lewis; Exploration and Geological Services Division, Yukon Region, Indian and Northern Affairs Canada, p. 77–84.

Canil, D., Johnston, S.T., Evers, K., Shellnutt, J.G., and Creaser, R.A., 2003. Mantle exhumation in an early Paleozoic passive margin, northern Cordillera, Yukon; The Journal of Geology, v. 111, p. 313–327. https://doi.org/10.1086/373971

Canil, D., Mihalynuk, M.G., Mackenzie, J.M., Johnston, S.T., Ferreira, L., and Grant, B., 2004. Heavy mineral sampling of stream sediments for diamond and other indicator minerals in the Atlin-Nakina area (104N, 104K); *in* Geological Fieldwork 2003; British Columbia Ministry of Energy and Mines, British Columbia Geological Survey Paper 2004-1, p. 19–26.

Canil, D., Johnston, S.T., and Mihalynuk, M., 2006. Mantle redox in Cordilleran ophiolites as a record of oxygen fugacity during partial melting and the lifetime of mantle lithosphere; Earth and Planetary Science Letters, v. 248, p. 106–117. https://doi.org/10.1016/j.epsl.2006.04.038

Canil, D., Johnston, S.T., d'Souza, R.J., and Heaman, L.M., 2015. Protolith of ultramafic rocks in the Kluane Schist, Yukon, and implications for arc collisions in the northern Cordillera; Canadian Journal of Earth Sciences, v. 52, p. 431–443. https://doi.org/10.1139/cjes-2014-0138

Canil, D., Grundy, R., and Johnston, S.T., 2019. Thermal history of the Donjek harzburgite massif in ophiolite from Yukon, Canada with implications for the cooling of oceanic mantle lithosphere; Lithos (Oslo), v. 328–329, p. 33–42. https://doi.org/10.1016/j.lithos.2019.01.001

Cannat, M., Sauter, D., Escartin, J., Lavier, L., and Picazo, S., 2009. Oceanic corrugated surfaces and the strength of the axial lithosphere at slow spreading ridges; Earth and Planetary Science Letters, v. 288, p. 174–183. https://doi.org/10.1016/j.epsl.2009.09.020

Childe, F.C. and Thompson, J.F.H., 1997. Geological setting, U-Pb geochronology, and radiogenic isotopic characteristics of the Permo-Triassic Kutcho Assemblage, north-central British Columbia; Canadian Journal of Earth Sciences, v. 34, p. 1310–1324. https://doi.org/10.1139/e17-104

Colpron, M. and Nelson, J.L., 2011. A digital atlas of terranes for the northern Cordillera; British Columbia Ministry of Energy and Mines, British Columbia Geological Survey, GeoFile 2011-11.

Colpron, M., Gladwin, K., Johnston, S.T., Mortensen, J.K., and Gehrels, G.E., 2005. Geology and juxtaposition history of the Yukon-Tanana, Slide Mountain, and Cassiar terranes in the Glenlyon area of central Yukon; Canadian Journal of Earth Sciences, v. 42, p. 1431–1448. https://doi.org/10.1139/e05-046

Colpron, M., Nelson, J.L., and Murphy, D.C., 2006. A tectonostratigraphic framework for the pericratonic terranes of the northern Canadian Cordillera; *in* Paleozoic Evolution and Metallogeny of Pericratonic Terranes at the Ancient Pacific Margin of North America, Canadian and Alaskan Cordillera, (ed.) M. Colpron and J. Nelson; Geological Association of Canada, Special Paper, v. 45, p. 1–23.

Colpron, M., Nelson, J.L., and Murphy, D.C., 2007. Northern Cordilleran terranes and their interactions through time; GSA Today, v. 17, p. 4–10. https://doi.org/10.1130/GSAT01704-5A.1

Colpron, M., Carr, S., Hildes, D., and Piercey, S., 2017. Geophysical, geochemical and geochronological constraints on the geology and mineral potential of the Livingstone Creek area, south-central Yukon (NTS 105E/8); *in* Yukon Exploration and Geology 2016, (ed.) K.E. MacFarlane and L.H. Weston; Yukon Geological Survey, p. 47–86.

Cordey, F., Gordey, S.P., and Orchard, M.J., 1991. New biostratigraphic data for the northern Cache Creek Terrane, Teslin map area, southern Yukon; *in* Current Research, Part E; Geological Survey of Canada, Paper 91-1E, p. 67–76. https://doi.org/10.4095/132629

Corriveau, A.S., 2018. Caractérisation pétrologique et géochimique des roches mantelliques du terrane de Cache Creek Nord, Cordillère nord-américaine; M.Sc. thesis, Université du Québec / Institut national de la recherche scientifique, Québec, Quebec, 211 p.

Cui, Y., Miller, D., Schiarizza, P., and Diakow, L.J., 2017. British Columbia digital geology; British Columbia Ministry of Energy, Mines and Petroleum Resources, British Columbia Geological Survey, Open File 2017-8, 9 p.

Cutts, J.A., Zagorevski, A., McNicoll, V., and Carr, S., 2012. Tectono-stratigraphic setting of the Moreton's Harbour Group and its implications for the evolution of the Laurentian Margin; Canadian Journal of Earth Sciences, v. 49, p. 111–127. https://doi.org/10.1139/e11-040

Davydov, V., 2014. Warm water benthic Foraminifera document the Pennsylvanian-Permian warming and cooling events; the record from the Western Pangea tropical shelves; Palaeogeography, Palaeoclimatology, Palaeoecology, v. 414, p. 284–295. https://doi.org/10.1016/j.palaeo.2014.09.013

de Keijzer, M., Williams, P.F., and Brown, R.L., 1999. Kilometre-scale folding in the Teslin Zone, northern Canadian Cordillera, and its tectonic implications for the accretion of the Yukon-Tanana Terrane to North America; Canadian Journal of Earth Sciences, v. 36, p. 479–494. https://doi.org/10.1139/e98-096

Deschamps, A., Larter, R.D., Lallemand, S., and Leat, P.T., 2003. Geodynamic setting of Izu-Bonin-Mariana boninites; Geological Society Special Publications, v. 219, p. 163–185. https://doi.org/10.1144/GSL.SP.2003.219.01.08

Devine, F.A.M., 2002. U-Pb geochronology, geochemistry, and tectonic implications of oceanic rocks in the northern Cache Creek terrane, Nakina area, northwestern British Columbia; B.Sc. thesis, University of British Columbia, Vancouver, British Columbia, 50 p.

Dilek, Y., 2003. Ophiolite concept and its evolution; Geological Society of America, Special Paper 373, p. 1–16. https://doi.org/10.1130/0-8137-2373-6.1

Dilek, Y. and Furnes, H., 2009. Structure and geochemistry of Tethyan ophiolites and their petrogenesis in subduction rollback systems; Lithos, v. 113, p. 1–20. https://doi.org/10.1016/j.lithos.2009.04.022

Dilek, Y. and Furnes, H., 2014. Ophiolites and their origins; Elements, v. 10, p. 93–100. https://doi.org/10.2113/gselements.10.2.93

Eissen, J.-P., Auzende, J.-M., Nohara, M., Cotten, J., Hirose, K., and Urabe, T., 1994. North Fiji Basin basalts and their magma sources; part I, incompatible element constraints; Marine Geology, v. 116, p. 153–178. https://doi.org/10.1016/0025-3227(94)90174-0

English, J.M., 2004. Convergent margin tectonics in the North American Cordillera: implications for continental growth and orogeny; Ph.D. thesis, University of Victoria, Victoria, British Columbia, 193 p.

English, J.M. and Johnston, S.T., 2005. Collisional orogenesis in the northern Canadian Cordillera: implications for Cordilleran crustal structure, ophiolite emplacement, continental growth, and the terrane hypothesis; Earth and Planetary Science Letters, v. 232, p. 333–344. https://doi.org/10.1016/j.epsl.2005.01.025

English, J.M., Mihalynuk, M.G., and Johnston, S.T., 2010. Geochemistry of the northern Cache Creek Terrane and implications for accretionary processes in the Canadian Cordillera; Canadian Journal of Earth Sciences, v. 47, p. 13–34. https://doi.org/10.1139/E09-066

Falloon, T.J. and Crawford, A.J., 1991. The petrogenesis of high-calcium boninite lavas dredged from the northern Tonga Ridge; Earth and Planetary Science Letters, v. 102, p. 375–394. https://doi.org/10.1016/0012-821X(91)90030-L

Falloon, T.J., Meffre, S., Crawford, A.J., Hoernle, K., Hauff, F., Bloomer, S.H., and Wright, D.J., 2014. Cretaceous fore-arc basalt from the Tonga arc: geochemistry and implications for the tectonic history of the SW Pacific; Tectonophysics, v. 630, p. 21–32. https://doi.org/10.1016/j.tecto.2014.05.007

Gabrielse, H., 1969. Geology of Jennings River map-area, British Columbia (104-O); Geological Survey of Canada, Paper 68-55, 37 p. https://doi.org/10.4095/102349

Gabrielse, H., 1998. Geology of the Cry Lake and Dease Lake map areas, north-central British Columbia; Geological Survey of Canada, Bulletin 504, 147 p. https://doi.org/10.4095/210074

Gabrielse, H., Mortensen, J.K., Parrish, R.R., Harms, T.A., Nelson, J.L., and van der Heyden, P., 1993. Late Paleozoic plutons in the Sylvester allochthon, north-central British Columbia; *in* Radiogenic age and isotopic studies, report 7; Geological Survey of Canada, Paper 93-2, p. 107–118. https://doi.org/10.4095/193340

Gabrielse, H., Haggart, J.W., Murphy, D.C., Mortensen, J.K., Enkin, R.J., and Monger, J.W.H., 2006. Cretaceous and Cenozoic dextral orogen-parallel displacements, magmatism, and paleogeography, north-central Canadian Cordillera; Geological Association of Canada Special Paper, v. 46, p. 255–276.

Gilotti, J.A., McClelland, W.C., van Staal, C.R., and Petrie, M.B., 2017. Detrital zircon evidence for eclogite formation by basal subduction erosion; an example from the Yukon-Tanana composite arc, Canadian Cordillera; Geological Society of America, Special Paper, v. 526, p. 173–189. https://doi.org/10.1130/2017.2526(09)

Golding, M., 2018. Heterogeneity of conodont faunas in the Cache Creek Terrane, Canada; significance for tectonic reconstructions of the North American Cordillera; Palaeogeography, Palaeoclimatology, Palaeoecology, v. 506, p. 208–216. https://doi.org/10.1016/j.palaeo.2018.06.038

Golding, M.L., Orchard, M.J., and Zagorevski, A., 2017. Conodonts from the Stikine Terrane in northern British Columbia and southern Yukon; Geological Survey of Canada, Open File 8278, 23 p. https://doi.org/10.4095/304273

Gordey, S.P. and Stevens, R.A., 1994. Preliminary interpretation of bedrock geology of the Teslin area (105C), southern Yukon; Geological Survey of Canada, Open File 2886, scale 1:250 000. https://doi.org/10.4095/205239

Gordey, S.P., McNicoll, V.J., and Mortensen, J.K., 1998. New U-Pb ages from the Teslin area, southern Yukon, and their bearing on terrane evolution in the northern Cordillera; *in* Radiogenic age and isotopic studies, report 11; Geological Survey of Canada, Current Research 1998-F, p. 129–148. https://doi.org/10.4095/210064

Harms, T.A. and Murchey, B.L., 1992. Setting and occurrence of late Paleozoic radiolarians in the Sylvester Allochthon, part of a proto-Pacific ocean floor terrane in the Canadian Cordillera; Palaeogeography, Palaeoclimatology, Palaeoecology, v. 96, p. 127–139. https://doi.org/10.1016/0031-0182(92)90063-B

Hart, C.J.R., 1997. A transect across northern Stikinia: geology of the northern Whitehorse map area, southern Yukon Territory (105D/13-16); Exploration and Geological Services Division, Yukon, Indian and Northern Affairs Canada, Bulletin 8, 112 p.

Ildefonse, B., Blackman, D.K., John, B.E., Ohara, Y., Miller, D.J., MacLeod, C.J., Abe, N., Abratis, M., Andal, E.S., Andreani, M., Awaji, S., Beard, J.S., Brunelli, D., Charney, A.B., Christie, D.M., Delacour, A.G., Delius, H., Drouin, M., Einaudi, F.,. . . Zhao, X., 2007. Oceanic core complexes and crustal accretion at slow-spreading ridges; Geology, v. 35, p. 623–626. https://doi.org/10.1130/G23531A.1

Ishizuka, O., Yuasa, M., Taylor, R.N., and Sakamoto, I., 2009. Two contrasting magmatic types coexist after the cessation of back-arc spreading; Chemical Geology, v. 266, p. 274–296. https://doi.org/10.1016/j.chemgeo.2009.06.014

Jobin-Bevans, L.S., 1995, Petrology, geochemistry and origin of ultramafic bodies within the Cache Creek terrane, southern Yukon; B.Sc. thesis, University of Manitoba, Winnipeg, Manitoba, 227 p.

Johnston, S.T. and Borel, G.D., 2007. The odyssey of the Cache Creek Terrane, Canadian Cordillera: implications for accretionary orogens, tectonic setting of Panthalassa, the Pacific Superswell, and break-up of Pangea; Earth and Planetary Science Letters, v. 253, p. 415–428. https://doi.org/10.1016/j.epsl.2006.11.002

Johnston, S.T., Canil, D., and Heaman, L.H., 2007. Permian exhumation of the Buffalo Pitts orogenic peridotite massif, northern Cordillera, Yukon; Canadian Journal of Earth Sciences, v. 44, p. 275–286. https://doi.org/10.1139/e06-078

Kimura, G. and Ludden, J., 1995. Peeling oceanic crust in subduction zones; Geology, v. 23, p. 217–220. https://doi.org/10.1130/0091-7613(1995)023%3c0217:POCISZ%3e2.3.CO%3b2

Kurth, M., Sassen, A., Suhr, G., and Mezger, K., 1998. Precise ages and isotopic constraints for the Lewis Hills (Bay of Islands Ophiolite): preservation of an arc-spreading ridge intersection; Geology, v. 26, p. 1127–1130. https://doi.org/10.1130/0091-7613(1998)026%3c1127:PAAICF%3e2.3.CO%3b2

Lapierre, H., Bosch, D., Tardy, M., and Struik, L.C., 2003. Late Paleozoic and Triassic plume-derived magmas in the Canadian Cordillera played a key role in continental crust growth; Chemical Geology, v. 201, p. 55–89. https://doi.org/10.1016/S0009-2541(03)00224-9

Lawley, C.J.M., Pearson, D.G., Waterton, P., Zagorevski, A., Bédard, J.H., Jackson, S.E., Petts, D.C., Kjarsgaard, B.A., Zhang, S., and Wright, D., 2020. Element and isotopic signature of re-fertilized mantle peridotite as determined by nanopowder and olivine LA-ICPMS analyses; Chemical Geology, v. 536, article no. 119464, 17 p. https://doi.org/10.1016/j.chemgeo.2020.119464

Lissenberg, C.J. and van Staal, C.R., 2006. Feedback between deformation and magmatism in the Lloyds River Fault Zone, an example of episodic fault reactivation in an accretionary setting, Newfoundland Appalachians; Tectonics, v. 25, article no. TC4004, 18 p. https://doi.org/10.1029/2005TC001789

Lissenberg, C.J., Bédard, J.H., and van Staal, C.R., 2004. The structure and geochemistry of the gabbro zone of the Annieopsquotch Ophiolite, Newfoundland; implications for lower crustal accretion at spreading ridges; Earth and Planetary Science Letters, v. 229, p. 105–123. https://doi.org/10.1016/j.epsl.2004.10.029

Logan, J.M. and Iverson, O., 2013. Dease Lake Geoscience Project: geochemical characteristics of Tsaybahe, Stuhini and Hazelton volcanic rocks, northwestern British Columbia (NTS 104I, J); *in* Geoscience BC Summary of Activities 2012; Geoscience BC, Report 2013-1, p. 11–32.

Logan, J.M., Drobe, J.R., and McClelland, W.C., 2000. Geology of the Forrest Kerr-Mess Creek area, northwestern British Columbia (NTS 104B/10,15 & 104G/2 & 7W); British Columbia Ministry of Energy and Mines, Energy and Minerals Division, Geological Survey Branch, Bulletin 104, 163 p.

MacLeod, C.J., Searle, R.C., Murton, B.J., Casey, J.F., Mallows, C., Unsworth, S.C., Achenbach, K.L., and Harris, M., 2009. Life cycle of oceanic core complexes; Earth and Planetary Science Letters, v. 287, p. 333–344. https://doi.org/10.1016/j.epsl.2009.08.016

Manatschal, G., Montanini, A., Sauter, D., Karpoff, A.M., Masini, E., Mohn, G., Lagabrielle, Y., Piccardo, G.B., Tribuzio, R., and Dick, H.J.B., 2011. The Chenaillet Ophiolite in the French/Italian Alps: an ancient analogue for an oceanic core complex; Lithos, v. 124, p. 169–184. https://doi.org/10.1016/j.lithos.2010.10.017

McGoldrick, S., Zagorevski, A., and Canil, D., 2017. Geochemistry of volcanic and plutonic rocks from the Nahlin ophiolite with implications for a Permo-Triassic arc in the Cache Creek terrane, northwestern British Columbia; Canadian Journal of Earth Sciences, v. 54, p. 1214–1227. https://doi.org/10.1139/cjes-2017-0069

McGoldrick, S., Canil, D., and Zagorevski, A., 2018. Constrasting thermal and melting histories for segments of mantle lithosphere in the Nahlin Ophiolite, British Columbia, Canada; Contributions to Mineralogy and Petrology, v. 173, p. 25. https://doi.org/10.1007/s00410-018-1450-9

Mihalynuk, M.G., and Cordey, F., 1997. Potential for Kutcho Creek volcanogenic massive sulphide mineralization in the northern Cache Creek Terrane; a progress report; *in* Geological Fieldwork 1996; BC Ministry of Energy, Mines and Petroleum Resources, p. 157–170.

Mihalynuk, M.G., and Smith, M.T., 1992. Highlights of 1991 mapping in the Atlin-West map area (104N/12); *in* Geological Fieldwork 1991; BC Ministry of Energy, Mines and Petroleum Resources, Paper 1992-1, p. 221–228.

Mihalynuk, M.G., Smith, M.T., Gabites, J.E., Runkle, D., and Lefebure, D., 1992. Age of emplacement and basement character of the Cache Creek Terrane as constrained by new isotopic and geochemical data; Canadian Journal of Earth Sciences, v. 29, p. 2463–2477. https://doi.org/10.1139/e92-193

Mihalynuk, M.G., Nelson, J., and Diakow, L.J., 1994. Cache Creek Terrane entrapment: oroclinal paradox within the Canadian Cordillera; Tectonics, v. 13, p. 575–595. https://doi.org/10.1029/93TC03492

Mihalynuk, M.G., Mountjoy, K.J., Smith, M.T., Currie, L.D., Gabites, J.E., Tipper, H.W., Orchard, M.J., Poulton, T.P., and Cordey, F., 1999. Geology and mineral resources of the Tagish Lake area (NTS 104M/8, 9, 10E, 15 and 104N/12W), northwestern British Columbia; British Columbia Ministry of Energy and Mines, Energy and Minerals Division, Geological Survey Branch, Bulletin 105, 217 p.

Mihalynuk, M.G., Johnston, S.T., Lowe, C., Cordey, F., English, J.M., Devine, F.A.M., Larson, K., and Merran, Y., 2002. Atlin TGI, Part II: preliminary results from the Atlin Targeted Geoscience Initiative, Nakina area, Northwest British Columbia; *in* Geological Fieldwork 2001; British Columbia Ministry of Energy and Mines, Paper 2002-1, p. 5–18.

Mihalynuk, M.G., Johnston, S.T., English, J.M., Cordey, F., Villeneuve, M.E., Rui, L., and Orchard, M.J., 2003. Atlin TGI, Part II: regional geology and mineralization of the Nakina area (NTS 104N/2W and 3); *in* Geological Fieldwork 2002; British Columbia Ministry of Energy and Mines, Paper 2003-1, p. 9–37.

Mihalynuk, M.G., Erdmer, P., Ghent, E.D., Cordey, F., Archibald, D.A., Friedman, R.M., and Johannson, G.G., 2004a. Coherent French Range blueschist; subduction to exhumation in <2.5 m.y.; Geological Society of America Bulletin, v. 116, p. 910–922. https://doi.org/10.1130/B25393.1

Mihalynuk, M.G., Fiererra, L., Robertson, S., Devine, F.A.M., and Cordey, F., 2004b. Geology and new mineralization in the Joss'alun belt, Atlin area; *in* Geological Fieldwork 2003; British Columbia Ministry of Energy and Mines, Paper 2004-1, p. 61–82.

Mihalynuk, M., Zagorevski, A., and Cordey, F., 2012. Geology of the Hoodoo Mountain area (NTS 104B/14); *in* Geological Fieldwork 2011; BC Ministry of Forests, Mines and Lands, Paper 2012-1, p. 45–67.

Mihalynuk, M.G., Zagorevski, A., Milidragovic, D., Tsekhmistrenko, M., Friedman, R.M., Joyce, N., Camacho, A., and Golding, M., 2018. Geologic and geochronologic update of the Turtle Lake area, NTS 104M/16, northwest British Columbia; *in* Geological Fieldwork 2017; British Columbia Ministry of Energy, Mines and Petroleum Resources, British Columbia Geological Survey, Paper 2018-1, p. 83–128.

Milidragovic, D. and Grundy, R., 2019. Geochemistry and petrology of rocks in the Decar area, central British Columbia: petrologically constrained subdivision of the Cache Creek complex; *in* Geological Fieldwork 2018; British Columbia Ministry of Energy and Mines, British Columbia Geological Survey, Paper 2019-1, p. 55–77.

Milidragovic, D., Zagorevski, A., and Chapman, J.B., 2017. The Mount Hickman ultramafic complex: an Fe-rich Alaskan-type ultramafic intrusion; *in* Geological Fieldwork 2016; British Columbia Ministry of Energy and Mines, British Columbia Geological Survey, Paper 2017-1, p. 117–132.

Milidragovic, D., Grundy, R., and Schiarizza, P., 2018. Geology of the Decar area north of Trembleur Lake, NTS 93K/14; *in* Geological Fieldwork 2017; British Columbia Ministry of Energy, Mines and Petroleum Resources, British Columbia Geological Survey, Paper 2018-1, p. 129–142.

Miranda, E.A. and Dilek, Y., 2010. Oceanic core complex development in modern and ancient oceanic lithosphere: gabbro-localized versus peridotite-localized detachment models; The Journal of Geology, v. 118, p. 95–109. https://doi.org/10.1086/648460

Monger, J., 1975. Upper Paleozoic rocks of the Atlin Terrane, northwestern British Columbia and south-central Yukon; Geological Survey of Canada, Paper 74-47, 63 p. https://doi.org/10.4095/102554

Monger, J.W.H., 1977a. Upper Paleozoic rocks of northwestern British Columbia; *in* Report of Activities, Part A; Geological Survey of Canada, Paper 77-1A, p. 255–262.

Monger, J.W.H., 1977b. Upper Paleozoic rocks of the western Canadian Cordillera and their bearing on Cordilleran evolution; Canadian Journal of Earth Sciences, v. 14, p. 1832–1859. https://doi.org/10.1139/e77-156

Monger, J.W.H. and Ross, C.A., 1971. Distribution of fusulinaceans in the western Canadian Cordillera; Canadian Journal of Earth Sciences, v. 8, p. 259–278. https://doi.org/10.1139/e71-026

Monger, J.W.H., Wheeler, J.O., Tipper, H.W., Gabrielse, H., Harms, T., Struik, L.C., Campbell, R.B., Dodds, C.J., Gehrels, G.E., and O'Brien, J., 1991. Part B. Cordilleran terranes; *in* Chapter 8 *of* Geology of the Cordilleran Orogen in Canada, (ed.) H. Gabrielse and C.J. Yorath; Geological Survey of Canada, Geology of Canada, no. 4, p. 281–327 (*also* Geological Society of America, The Geology of North America, v. G-2). https://doi.org/10.4095/134091

Monzier, M., Danyushevsky, L.V., Crawford, A.J., Bellon, H., and Cotten, J., 1993. High-Mg andesites from the southern termination of the New Hebrides island arc (SW Pacific); Journal of Volcanology and Geothermal Research, v. 57, p. 193–217. https://doi.org/10.1016/0377-0273(93)90012-G

Mortensen, J.K., 1990. Geology and U-Pb geochronology of the Klondike District, west-central Yukon Territory; Canadian Journal of Earth Sciences, v. 27, p. 903–914. https://doi.org/10.1139/e90-093

Murphy, D.C., Colpron, M., Mortensen, J.K., Piercey, S.J., Orchard, M.J., Gehrels, G.E., and Nelson, J.L., 2006. Mid-Paleozoic to early Mesozoic tectonostratigraphic evolution of Yukon-Tanana and Slide Mountain terranes and affiliated overlap assemblages, Finlayson Lake massive sulphide district, southeastern Yukon; Geological Association of Canada, Special Paper 45, p. 75–105.

Murphy, D.C., van Staal, C.R., and Mortensen, J.K., 2008. Windy McKinley terrane, Stevenson Ridge area (115JK), western Yukon: composition and proposed correlations, with implications for mineral potential; *in* Yukon Exploration and Geology 2007, (ed.) D.S. Emond, L.R. Blackburn, R.P. Hill, and L.H. Weston; Yukon Geological Survey, p. 225–235.

Murphy, D.C., Mortensen, J.K., and van Staal, C.R., 2009. Windy-McKinley terrane, western Yukon: new data bearing on its composition, age, correlation and paleotectonic settings; *in* Yukon Exploration and Geology 2008, (ed.) L.H. Weston, L.R. Blackburn, and L.L. Lewis; Yukon Geological Survey, p. 195–209.

Nelson, J.L., 1993. The Sylvester Allochthon: upper Paleozoic marginal-basin and island-arc terranes in northern British Columbia; Canadian Journal of Earth Sciences, v. 30, p. 631–643. https://doi.org/10.1139/e93-048

Nelson, J.L. and Bradford, J.A., 1993. Geology of the Midway-Cassiar area, northern British Columbia (104O, 104P); British Columbia Ministry of Energy, Mines and Petroleum Resources, Mineral Resources Division, Geological Survey Branch, Bulletin 83, 100 p.

Nelson, J.L. and Colpron, M., 2007. Tectonics and metallogeny of the British Columbia, Yukon and Alaskan Cordillera, 1.8 Ga to the present; *in* A Synthesis of Major Deposit-Types, District Metallogeny, the Evolution of Geological Provinces, and Exploration Methods, (ed.) W.D. Goodfellow; Geological Association of Canada, Mineral Deposits Division, Special Publication 5, p. 755–791.

Nelson, J.L., Colpron, M., Colpron, M., Piercey, S.J., Dusel-Bacon, C., Murphy, D.C., Roots, C.F., and Nelson, J.L., 2006. Paleozoic tectonic and metallogenetic evolution of pericratonic terranes in Yukon, northern British Columbia and eastern Alaska; Geological Association of Canada, Special Paper 45, p. 323–360.

Nelson, J.L., Colpron, M., and Israel, S., 2013. The Cordillera of British Columbia, Yukon, and Alaska; tectonics and metallogeny; *in* Tectonics, Metallogeny, and Discovery: The North American Cordillera and Similar Accretionary Settings; Society of Economic Geologists, Special Publication 17, p. 53–109.

North American Commission on Stratigraphic Nomenclature, 2005. North American Stratigraphic Code; North American Commission on Stratigraphic Nomenclature; American Association of Petroleum Geologists Bulletin, v. 89, p. 1547–1591. https://doi.org/10.1306/07050504129

Ohara, Y., Fujioka, K., Ishii, T., and Yurimoto, H., 2003. Peridotites and gabbros from the Parece Vela backarc basin: unique tectonic window in an extinct backarc spreading ridge; Geochemistry Geophysics Geosystems, v. 4, no. 7, article no. 8611, 22 p. https://doi.org/10.1029/2002GC000469

Orchard, M.J., Struik, L.C., Cordey, F., Rui, L., Bamber, E.W., Mamet, B., Struik, L.C., Sano, H., Taylor, H.J., and MacIntyre, D.G., 2001. Biostratigraphic and biogeographic constraints on the Carboniferous to Jurassic Cache Creek Terrane in central British Columbia; Canadian Journal of Earth Sciences, v. 38, p. 551–578. https://doi.org/10.1139/e00-120

Parsons, A.J., Ryan, J.J., and Coleman, M., 2017a. Report of activities, 2017: Dunite Peak area, Big Salmon Range, south-central Yukon: GEM2 Cordillera Project; Geological Survey of Canada, Open File 8307, 10 p. https://doi.org/10.4095/305966

Parsons, A.J., Ryan, J.J., Coleman, M., and van Staal, C.R., 2017b. The Slide Mountain ophiolite, Big Salmon Range, south-central Yukon: preliminary results from fieldwork; *in* Yukon Exploration and Geology Overview 2016, (ed.) K.E. MacFarlane and L.H. Weston; Yukon Geological Survey, p. 181–196.

Parsons, A.J., Zagorevski, A., Ryan, J.J., McClelland, W.C., van Staal, C.R., Coleman, M.J., and Golding, M.L., 2019. Petrogenesis of the Dunite Peak Ophiolite, south-central Yukon, and the distinction between upper-plate and lower-plate settings; a new hypothesis for the late Paleozoic-early Mesozoic tectonic evolution of the Northern Cordillera; Geological Society of America Bulletin, v. 131, p. 274–298. https://doi.org/10.1130/B31964.1

Pearce, J.A., 1996. A user's guide to basalt discrimination diagrams; *in* Trace Element Geochemistry of Volcanic Rocks: Applications for Massive Sulphide Exploration, (ed.) D.A. Wyman; Geological Association of Canada, Short Course Notes, v. 12, p. 79–113.

Pearce, J.A., 2014. Immobile element fingerprinting of ophiolites; Elements, v. 10, p. 101–108. https://doi.org/10.2113/gselements.10.2.101

Pearce, J.A., Dilek, Y., and Ernst, R.E., 2008. Geochemical fingerprinting of oceanic basalts with applications to ophiolite classification and the search for Archean oceanic crust; Lithos, v. 100, p. 14–48. https://doi.org/10.1016/j.lithos.2007.06.016

Piercey, S.J., Murphy, D.C., Mortensen, J.K., and Paradis, S., 2001. Boninitic magmatism in a continental margin setting, Yukon-Tanana Terrane, southeastern Yukon, Canada; Geology, v. 29, p. 731–734. https://doi.org/10.1130/0091-7613(2001)029%3c0731:BMIACM%3e2.0.CO%3b2

Piercey, S.J., Mortensen, J.K., and Creaser, R.A., 2003. Neodymium isotope geochemistry of felsic volcanic and intrusive rocks from the Yukon-Tanana Terrane in the Finlayson Lake region, Yukon, Canada; Canadian Journal of Earth Sciences, v. 40, p. 77–97. https://doi.org/10.1139/e02-094

Piercey, S.J., Murphy, D.C., Mortensen, J.K., and Creaser, R.A., 2004. Mid-Paleozoic initiation of the northern Cordilleran marginal backarc basin: geologic, geochemical, and neodymium isotope evidence from the oldest mafic magmatic rocks in the Yukon-Tanana Terrane, Finlayson Lake District, southeast Yukon, Canada; Geological Society of America Bulletin, v. 116, p. 1087–1106. https://doi.org/10.1130/B25162.1

Piercey, S.J., Colpron, M., Nelson, J.L., Colpron, M., Dusel-Bacon, C., Simard, R.-L., Roots, C.F., and Nelson, J.L., 2006. Paleozoic magmatism and crustal recycling along the ancient Pacific margin of North America, northern Cordillera; Geological Association of Canada, Special Paper 45, p. 281–322.

Piercey, S.J., Murphy, D.C., and Creaser, R.A., 2012. Lithosphere-asthenosphere mixing in a transform-dominated late Paleozoic backarc basin: implications for northern Cordilleran crustal growth and assembly; Geosphere, v. 8, p. 716–739. https://doi.org/10.1130/GES00757.1

Raymond, L.A., 1984. Classification of melanges; *in* Melanges: Their Nature, Origin, and Significance, (ed.) L.A. Raymond; Geological Society of America Special Paper 198, p. 7–20. https://doi.org/10.1130/SPE198-p7

Read, P.B., 1984. Geology, Klastline River East, Ealue Lake West, Cake Hill West and Stikine Canyon East, British Columbia; Geological Survey of Canada, Open File 1080, scale 1:50 000. https://doi.org/10.4095/129893

Reston, T. and Manatschal, G., 2011. Rifted margins: building blocks of later collision; *in* Arc-Continent Collision, (ed.) D. Brown and P.D. Ryan; Springer-Verlag, Berlin, Heidelberg, p. 3–21. https://doi.org/10.1007/978-3-540-88558-0_1

Robinson, P.T., Malpas, J., Dilek, Y., and Zhou, M., 2008. The significance of sheeted dike complexes in ophiolites; GSA Today, v. 18, p. 4–11. https://doi.org/10.1130/GSATG22A.1

Rollinson, H., 2009. New models for the genesis of plagiogranites in the Oman ophiolite; Lithos, v. 112, p. 603–614. https://doi.org/10.1016/j.lithos.2009.06.006

Ryan, W.B.F., Carbotte, S.M. Coplan, J., O'Hara, S., Melkonian, A., Arko, R., Weissel, R.A., Ferrini, V., Goodwillie, A., Nitsche, F., Bonczkowski, J., and Zemsky, R., 2009. Global Multi-Resolution Topography synthesis; Geochemistry Geophysics Geosystems, v. 10, no. 3, article no. Q03014. http://doi.org/10.1029/2008GC002332

Ryan, J.J., Zagorevski, A., Williams, S.P., Roots, C., Ciolkiewicz, W., Hayward, N., and Chapman, J.B., 2013a. Geology, Stevenson Ridge (northeast part), Yukon; Geological Survey of Canada, Canadian Geoscience Map 117 (2nd preliminary edition), scale 1:100 000. https://doi.org/10.4095/292408

Ryan, J.J., Zagorevski, A., Williams, S.P., Roots, C., Ciolkiewicz, W., Hayward, N., and Chapman, J.B., 2013b. Geology, Stevenson Ridge (northwest part), Yukon; Geological Survey of Canada, Canadian Geoscience Map 116 (2nd preliminary edition), scale 1:100 000. https://doi.org/10.4095/292407

Ryan, J.J., Zagorevski, Z., Roots, C.F., and Joyce, N., 2014. Paleozoic tectonostratigraphy of the northern Stevenson Ridge area, Yukon; Geological Survey of Canada, Current Research 2014-4, 16 p. https://doi.org/10.4095/293924

Ryan, J.J., Westberg, E.E., Williams, S.P., and Chapman, J.B., 2016. Geology, Mount Nansen-Nisling River area, Yukon; Geological Survey of Canada, Canadian Geoscience Map 292 (preliminary edition), scale 1:100 000. https://doi.org/10.4095/298835

Ryan, J.J., Zagorevski, A., and Piercey, S.J., 2018. Geochemical data of Yukon-Tanana and Slide Mountain Terranes and their successor rocks in Yukon and northern British Columbia; Geological Survey of Canada, Open File 8500, 11 p. https://doi.org/10.4095/313250

Sano, H., Struik, L.C., Rui, L., and MacIntyre, D.G., 2001. Facies interpretation of Middle Carboniferous to Lower Permian Pope succession limestone of Cache Creek Group, Fort St. James, central British Columbia; Canadian Journal of Earth Sciences, v. 38, p. 535–550. https://doi.org/10.1139/e01-009

Sano, H., Igawa, T., and Onoue, T., 2003. Atlin TGI, Part V: carbonate and siliceous rocks of the Cache Creek Terrane, southern Sentinel Mountain, NTS 104N/5E and 6W; *in* Geological Fieldwork 2002, British Columbia Ministry of Energy and Mines, Paper 2003-1, p. 57–64.

Schiarizza, P., 2012. Geology of the Kutcho Assemblage between the Kehlechoa and Tucho rivers, northern British Columbia (NTS 104I/01, 02); *in* Geological Fieldwork 2011, British Columbia Ministry of Energy, Mines and Petroleum Resources, Paper 2012-1, p. 75–98.

Schroetter, J.-M., Page, P., Bédard, J.H., Tremblay, A., and Bécu, V., 2003. Forearc extension and sea-floor spreading in the Thetford Mines ophiolite complex; Geological Society Special Publications, v. 218, p. 231–251. https://doi.org/10.1144/GSL.SP.2003.218.01.13

Shervais, J.W., 1982. Ti-V plots and the petrogenesis of modern and ophiolitic lavas; Earth and Planetary Science Letters, v. 59, p. 101–118. https://doi.org/10.1016/0012-821X(82)90120-0

Silberling, N.J., Jones, D.L., Monger, J.W.H., and Coney, P.J., 1992. Lithotectonic terrane map of the North American Cordillera; U.S. Geological Survey, Miscellaneous Investigations Series Map 2176, 2 sheets, scale 1:5 000 000.

Sobolev, A.V. and Danyushevsky, L.V., 1994. Petrology and geochemistry of boninites from the north termination of the Tonga Trench; constraints on the generation conditions of primary high-Ca boninite magmas; Journal of Petrology, v. 35, p. 1183–1211. https://doi.org/10.1093/petrology/35.5.1183

Stern, R.J. and Bloomer, S.H., 1992. Subduction zone infancy; examples from the Eocene Izu-Bonin-Mariana and Jurassic California arcs; Geological Society of America Bulletin, v. 104, p. 1621–1636. https://doi.org/10.1130/0016-7606(1992)104%3c1621:SZIEFT%3e2.3.CO%3b2

Stern, R.J., Bloomer, S.H., Martinez, F., Yamazaki, T., and Harrison, T.M., 1996. The composition of back-arc basin lower crust and upper mantle in the Mariana Trough; a first report; The Island Arc, v. 5, p. 354–372. https://doi.org/10.1111/j.1440-1738.1996.tb00036.x

Stern, R.J., Reagan, M., Ishizuka, O., Ohara, Y., and Whattam, S., 2012. To understand subduction initiation, study forearc crust; to understand forearc crust, study ophiolites; Lithosphere, v. 4, p. 469–483. https://doi.org/10.1130/L183.1

Struik, L.C. and Orchard, M.J., 1985. Late Paleozoic conodonts from ribbon chert delineate imbricate thrusts within the Antler Formation of Slide Mountain Terrane, central British Columbia; Geology, v. 13, p. 794–798. https://doi.org/10.1130/0091-7613(1985)13%3c794:LPCFRC%3e2.0.CO%3b2

Struik, L.C., Schiarizza, P., Orchard, M.J., Cordey, F., Sano, H., MacIntyre, D.G., Lapierre, H., and Tardy, M., 2001. Imbricate architecture of the upper Paleozoic to Jurassic oceanic Cache Creek Terrane, central British Columbia; Canadian Journal of Earth Sciences, v. 38, p. 495–514. https://doi.org/10.1139/e00-117

Sun, S.S. and McDonough, W.F., 1989. Chemical and isotopic systematics of oceanic basalts: implications for mantle composition and processes; Geological Society Special Publications, v. 42, p. 313–345. https://doi.org/10.1144/GSL.SP.1989.042.01.19

Tani, K., Dunkley, D.J., and Ohara, Y., 2011. Termination of backarc spreading: zircon dating of a giant oceanic core complex; Geology, v. 39, p. 47–50. https://doi.org/10.1130/G31322.1

Tapster, S., Roberts, N.M.W., Petterson, M.G., Saunders, A.D., and Naden, J., 2014. From continent to intra-oceanic arc: zircon xenocrysts record the crustal evolution of the Solomon island arc; Geology, v. 42, p. 1087–1090. https://doi.org/10.1130/G36033.1

Tardy, M., Lapierre, H., Struik, L.C., Bosch, D., and Brunet, P., 2001. The influence of mantle plume in the genesis of the Cache Creek oceanic igneous rocks: implications for the geodynamic evolution of the inner accreted terranes of the Canadian Cordillera; Canadian Journal of Earth Sciences, v. 38, p. 515–534. https://doi.org/10.1139/e00-104

Terry, J., 1977. Geology of the Nahlin ultramafic body, Atlin and Tulsequah map-areas, northwestern British Columbia; *in* Report of Activities, Part A; Geological Survey of Canada, Paper 77-1A, p. 263–266. https://doi.org/10.4095/102697

Tremblay, A., Robertson, A.H.F., Meshi, A., Bédard, J.H., Parlak, O., and Koller, F., 2009. Oceanic core complexes and ancient oceanic lithosphere: insights from Iapetan and Tethyan ophiolites (Canada and Albania); Tectonophysics, v. 473, p. 36–52. https://doi.org/10.1016/j.tecto.2008.08.003

Tucholke, B.E., Behn, M.D., Buck, W.R., and Lin, J., 2008. Role of melt supply in oceanic detachment faulting and formation of megamullions; Geology, v. 36, p. 455–458. https://doi.org/10.1130/G24639A.1

van Staal, C.R., Chew, D.M., Zagorevski, A., McNicoll, V., Hibbard, J., Skulski, T., Castonguay, S., Escayola, M.P., and Sylvester, P.J., 2013. Evidence of Late Ediacaran hyperextension of the Laurentian Iapetan margin in the Birchy Complex, Baie Verte Peninsula, northwest Newfoundland: implications for the opening of Iapetus, formation of peri-Laurentian microcontinents and Taconic–Grampian orogenesis; Geoscience Canada, v. 40, p. 94–117. https://doi.org/10.12789/geocanj.2013.40.006

van Staal, C.R., Zagorevski, A., McClelland, W.C., Escayola, M., Ryan, J., Parsons, A.J., and Proenza, J.A., 2018. Age and setting of Permian Slide Mountain terrane ophiolitic ultramafic-mafic complexes in the Yukon: implications for late Paleozoic-early Mesozoic tectonic models in the northern Canadian Cordillera; Tectonophysics, v. 744, p. 458–483. https://doi.org/10.1016/j.tecto.2018.07.008

Watson, K.D. and Mathews, W.H., 1944. The Tuya-Teslin area, northern British Columbia; British Columbia Department of Mines, Bulletin 17, 11 p.

Yukon Geological Survey, 2019. Yukon Digital Bedrock Geology; Yukon Geological Survey. http://www.geology.gov.yk.ca/update_yukon_bedrock_geology_map.html [accessed December 25, 2019]

Zagorevski, A., 2018. Geochemical data of the northern Cache Creek, Slide Mountain, and Stikine Terranes and their overlap assemblages, British Columbia and Yukon; Geological Survey of Canada, Open File 8395, 12 p. https://doi.org/10.4095/308496

Zagorevski, A. and van Staal, C.R., 2011. The record of Ordovician arc–arc and arc–continent collisions in the Canadian Appalachians during the closure of Iapetus; *in* Arc-Continent Collision, Frontiers in Earth Sciences, (ed.) D. Brown and P.D. Ryan; Springer-Verlag, Berlin, Heidelberg, p. 341–371.

Zagorevski, A., Rogers, N., McNicoll, V., Lissenberg, C.J., van Staal, C.R., and Valverde-Vaquero, P., 2006. Lower to Middle Ordovician evolution of peri-Laurentian arc and back-arc complexes in the Iapetus: constraints from the Annieopsquotch Accretionary Tract, central Newfoundland; Geological Society of America Bulletin, v. 118, p. 324–342. https://doi.org/10.1130/B25775.1

Zagorevski, A., Corriveau, A.S., McGoldrick, S., Bédard, J.H., Canil, D., Golding, M.L., Joyce, N., and Mihalynuk, M.G., 2015. Geological framework of ancient oceanic crust in northwestern British Columbia and southwestern Yukon, GEM 2 Cordillera; Geological Survey of Canada, Open File 7957, 12 p. https://doi.org/10.4095/297273

Zagorevski, A., Mihalynuk, M.G., McGoldrick, S., Bédard, J.H., Golding, M., Joyce, N.L., Lawley, C., Canil, D., Corriveau, A.S., Bogatu, A., and Tremblay, A., 2016. Geological framework of ancient oceanic crust in northwestern British Columbia and southwestern Yukon, GEM 2 Cordillera; Geological Survey of Canada, Open File 8140, 15 p. https://doi.org/10.4095/299196

Zagorevski, A., Mihalynuk, M.G., Joyce, N.J., and Anderson, R.G., 2017. Late Cretaceous magmatism in the Atlin-Tagish area, northern British Columbia (104M, 104N); *in* Geological Fieldwork 2016; British Columbia Ministry of Energy, Mines and Natural Gas, British Columbia Geological Survey, Paper 2017-1, p. 133–152.

Zagorevski, A., Soucy La Roche, R., Golding, M., Joyce, N., Regis, D., and Coleman, M., 2018. Stikinia bedrock, British Columbia and Yukon; GEM-2 Cordillera Project, report of activities 2018; Geological Survey of Canada, Open File 8485, 12 p. https://doi.org/10.4095/311325

APPENDIX A

This section is intended to provide an overview of usage of some nomenclature in this manuscript. It is not intended to be an exhaustive description of all existing nomenclature.

CACHE CREEK TERRANE

Horsefeed Formation (clarified)

The Horsefeed Formation is described in detail by Monger (1975) and comprises thick, massive, crinoidal and fusulinid calcarenitic limestone. Monger (1975) noted that the Horsefeed Formation locally contains lenses of mafic to felsic volcanic rocks. The larger exposures of these volcanic rocks were subsequently included in the Nakina Formation (e.g. Cui et al., 2017; Yukon Geological Survey, 2019). In contrast to the Nakina Formation, volcanic rocks that are unequivocally in stratigraphic continuity with the Horsefeed Formation are commonly vesicular, haematized, olivine porphyritic, intimately associated with Carboniferous and rarely Permian limestone, and characterized by within-plate chemical characteristics (Fig. 15, *see* text). The present authors propose that these volcanic rocks should be retained in the Horsefeed Formation. Although it may be possible to formally define volcanic members within the Horsefeed Formation (e.g. volcanic rocks at Alfred Butte, Yukon), lenses of these volcanic rocks are generally too small and discontinuous to warrant formal units.

ATLIN TERRANE

Nakina suite (modified)

The Nakina Formation was originally defined by Monger (1975). Herein, this unit is retained on the basis of its historical significance and widespread usage (e.g. Cui et al., 2017; Yukon Geological Survey, 2019), however its definition is modified, and its rank is changed from Nakina Formation to Nakina suite to be more consistent with the traditionally included lithologies and the stratigraphic code (North American Commission on Stratigraphic Nomenclature, 2005). As originally defined, the Nakina Formation has created a significant degree of confusion in regional mapping. Much of Nakina Formation, regionally and in its type locality on Nakina Lake, is dominated by aphyric, variably fragmented, sometimes flow-banded basalt. Complex structural relationships in the type locality led Monger (1975) to correlate these basalts with similar basalt that is intercalated with the Mississippian Horsefeed Formation limestone, and to assign a Mississippian age to the Nakina Formation. Several studies clearly indicate that the Mississippian basalts are intercalated with the carbonate platform, whereas regionally extensive basalts associated with ultramafic rocks are Middle Permian to Middle Triassic. Apart from age, differences between these basalts include petrography (olivine porphyritic versus aphyric or clinopyroxene porphyritic), distinctly different rock associations (carbonate platform versus ophiolite), radically different geochemical characteristics (ocean-island basalt and/or continental rift versus island-arc tholeiite and/or back-arc tholeiite), and distinctly different ages (Carboniferous versus Middle Permian to Middle Triassic). The contact between these distinctly different basalt units is a fault and there is no stratigraphic continuity as was originally interpreted (Monger, 1975; Monger et al., 1991). Basalts that are intercalated with the carbonate platform do not generally form regionally mappable, continuous units and are herein included in the Horsefeed Formation (*see* 'Horsefeed formation (clarified)' section). Basalts that form part of the ophiolite succession are regionally mappable, and as such, the present authors retain Nakina Formation for these basalt units. Although this change could cause some confusion, the name is retained because of its widespread usage for these very voluminous rocks and consistency with the type locality. As originally defined and applied, Nakina Formation is generally massive and structureless, often rubbly-weathering basalt. Detailed investigations indicate that many localities of Nakina Formation include a significant proportion of hypabyssal (basaltic dykes, diabase, microgabbro). In some cases, coarse intrusive rocks (gabbro and layered gabbro cumulate rocks) have been included in the Nakina Formation (*see* 'King Mountain suite (new)' section). A rank of suite is much more appropriate for rocks that include a significant proportion of hypabyssal intrusions and are not stratified. The North American Commission on Stratigraphic Nomenclature does not definitively recognize usage of geochemistry in the definition of lithodemes; however, the Nakina suite is easily distinguished from the Horsefeed Formation volcanic rocks on the basis of major and trace elements (Fig. 15c, d). Unlike many petrographic observations, which can form part of stratigraphic definitions, high-quality geochemical analyses are rapid (more rapid than many fossil analyses and as rapid as cutting thin sections for example), can be carried out during mapping using portable XRF devices (e.g. Mihalynuk et al., 2012), do not have to carry any genetic connotations (i.e. a certain sample plotting in a particular field on a tectonic discrimination diagram or having a particular trace-element ratio does not have to carry any genetic connotations), and provide quantitative and reproducible data. As such, geochemical characteristics can be easily used to differentiate Nakina suite from other volcanic rocks in the area. Nakina suite and associated intrusive rocks yield Middle Permian to Middle Triassic U-Pb crystallization ages and fossils.

Dozy Marmot suite (new)

Present extent of the Nakina suite includes a significant proportion of intrusive rocks (e.g. Cui et al., 2017; Yukon Geological Survey, 2019). These genetically related intrusive rocks were previously included in the Nakina suite, in part because hypabyssal intrusive suites were mapped as volcanic rocks, and in part because intrusive complexes were not named and were thus included in the Nakina suite due to lack of any other stratigraphic options. Studies of oceanic crust and ophiolitic rocks recognize distinct pseudostratigraphy (zones: e.g. Anonymous, 1972; Dilek, 2003; Dilek and Furnes, 2009) that is very useful in regional and detailed mapping (e.g. Bédard et al., 1998, 2000; Lissenberg et al., 2004; Lissenberg and van Staal, 2006; Zagorevski et al., 2006; Cutts et al., 2012). Hypabyssal rocks are abundant north of Letain Lake along Dozy Marmot Ridge. In this locality, Gabrielse (1998) recognized an intrusive complex consisting of gabbro intruding into basalt. The present authors' examination of these localities indicated that the Dozy Marmot Ridge is underlain by a sheeted dyke–sill complex consisting of numerous basalt, diabase, and microgabbro dykes intruding each other. The present authors proposed to include these hypabyssal rocks in the Dozy Marmot suite (new) and this ridge is designated as the type locality. The Dozy Marmot suite thus consists of mafic sills and dykes (equivalent to sheeted dyke zone of ophiolite: Anonymous, 1972), the boundary with the Nakina suite is not observed in this locality, but the present authors propose a ratio of 1:1 for the proportion of hypabyssal to volcanic rocks as an acceptable mapping boundary between Dozy Marmot and Nakina suites. A supplementary type locality is designated on Union Mountain (Atlin), where very fine- to fine-grained gabbro dykes intrude each other with local screens of basalt and radiolarian chert. Radiolarian chert from Union Mountain locality yielded Late Permian radiolaria (F. Cordey, unpub. report, 2017).

King Mountain suite (new)

The present extent of the Nakina suite includes a significant proportion of isotropic to layered cumulate gabbro (e.g. Cui et al., 2017; Yukon Geological Survey, 2019). Recognizing these rocks as a separate unit within ophiolite pseudostratigraphy is critical for establishing regional map relationships. Plutonic rocks are abundant on the flanks of King Mountain, where Gabrielse (1998) recognized layered gabbro on fresh exposures in an alpine glacier cirque. This area also includes lesser pyroxenite, hornblendite, gabbro pegmatite, quartz diorite, and isotropic gabbro. To the northeast, gabbroic rocks grade into layered ultramafic cumulate rocks consisting of websterite, dunite, and harzburgite. The present authors propose inclusion of these intrusive rocks, and other localities of Atlin terrane ultramafic cumulate rocks in the King Mountain suite (new) with King Mountain designated as the type locality. In the Cry Lake area, the King Mountain suite is areally extensive, however, it becomes only a minor component of the Atlin terrane to the north and west of Dease Lake, where cumulate sections are only locally identified (Terry, 1977; Jobin-Bevans, 1995; Canil et al., 2004). King Mountain suite quartz diorite yielded a ca. 255 Ma U-Pb zircon crystallization age, whereas cumulate gabbro from Hardluck Peak–Peridotite Peak massif yielded ca. 264 Ma and ca. 255 Ma U-Pb zircon crystallization ages (N. Joyce, unpub. data, 2020)

Nahlin suite (reinstated and modified)

Ultramafic rocks are generally assigned to the Cache Creek complex in British Columbia, and to the Nahlin formation of the Cache Creek complex in Yukon (e.g. Cui et al., 2017; Yukon Geological Survey, 2019). Many authors have pointed out numerous problems with using Cache Creek "complex" or "group". These were mainly based on the lack of discernible stratigraphy, which is a result of using common nomenclature across terrane boundaries and overlap assemblages. The present authors propose to reinstate the original Nahlin suite nomenclature of Terry (1977) for all ultramafic rocks in the Atlin terrane, with the exception of known ultramafic cumulate rocks ('King Mountain suite (new)' section). As the Nahlin suite contains a diversity of rock types with different, but related genetic connotations, 'suite' rather than 'formation' or 'group' is appropriate for these rocks. The inaccessible, but spectacularly exposed Nahlin Mountain would thus continue to serve as the type locality; however, there are excellent exposures throughout the Atlin terrane, including easily accessible exposures on Monarch Mountain on the outskirts of Atlin (e.g. Bloodgood et al., 1989a, b; Ash, 1994, 2004), which can serve as a supplementary locality.

Kutcho complex (modified)

The Kutcho Formation (assemblage) is described in detail in Gabrielse (1998) and Schiarizza (2012). Since Kutcho Formation includes a significant proportion of cogenetic intrusive rocks (Schiarizza, 2012), Kutcho 'complex' is more appropriate than 'formation', and is an accepted stratigraphic term unlike 'assemblage'. Kutcho complex type locality is the remote Kutcho Creek–Letain Creek area about 100 km east-southeast of Dease Lake.

OVERLAP

Kedahda Formation (clarified)

The Kedahda Formation (Watson and Mathews, 1944; Gabrielse, 1969; Monger, 1975) is retained herein on the basis of its historical significance and widespread usage (e.g. Cui et al., 2017; Yukon Geological Survey, 2019), however, the present authors clarify and correct its age and

stratigraphic context. The Kedahda Formation is generally accepted to be characterized by variably, but generally highly folded chert, argillite, wacke, and minor limestone. Locally, siliciclastic rocks and epiclastic rocks are abundant (Aitken, 1959; Gabrielse, 1969; Monger, 1975). Specifically, these authors have noted characteristic fresh hornblende, feldspar, clinopyroxene, quartz, epidote, and biotite-bearing wackes. Watson and Mathews (1944) identified Permian fauna in limestone exposures that are spatially associated with the Kedahda Formation chert and siliciclastic rocks and could not identify any obvious unconformities. As such, they assigned a Permian age to the Kedahda Formation and this was subsequently expanded to Carboniferous to Permian as Kedahda Formation equivalents were identified in adjacent areas (Gabrielse, 1969, 1998; Monger, 1975). Most authors have inferred that Kedahda either underlies or is interbedded or interfingered with the Paleozoic limestone and a depositional model was developed to address the occurrence of shallow carbonate limestone in deep-water chert (e.g. Fig. 8.69 in Monger et al., 1991). The inferred conformable relationship between the Paleozoic limestone and Kedahda Formation has created a significant degree of confusion in regional stratigraphic relationship, in part because there are both Paleozoic and Mesozoic limestone units.

Numerous collections of Kedahda Formation chert and limestone have yielded Middle to Late Triassic, as well as some Early Jurassic radiolaria and conodonts (Cordey et al., 1991; Mihalynuk et al., 2002, 2003). As a result of a very extensive study of these rocks in Yukon, chert, argillite, and wacke that yielded Middle Triassic to Early Jurassic fossils (Cordey et al., 1991) were excluded from the Kedahda Formation and assigned to a separate unit (Yukon Geological Survey, 2019). Although Paleozoic fossils have been recovered from some chert, the vast majority of Kedahda Formation is not Paleozoic. Paleozoic chert localities should be re-investigated to evaluate whether they constitute their own unit or whether they should be included in other Paleozoic units (e.g. Nakina suite or Horsefeed Formation).

It is the view of the present authors that Kedahda Formation should be restricted to Middle Triassic to Early Jurassic chert, argillite, wacke, and minor limestone. This restriction would not change the current distribution of the Kedahda Formation, except in Yukon, where Middle Triassic to Early Jurassic rocks have been previously excluded from the Kedahda Formation (Cordey et al., 1991; Yukon Geological Survey, 2019).

The base of the Kedahda formation is generally not preserved, an angular unconformity between Horsefeed and Kedahda formations was reported by Monger (1975) in the Nakina Lake area. In this area, the basal contact of the Kedahda formation is marked by discontinuous, but locally very thick breccia-conglomerate and relationships indicate that the unconformity cuts through Late Permian to Upper Mississippian carbonate. The present authors have sampled volcanogenic wacke and associated chert from several localities for petrography, U-Pb zircon provenance, and fossils; results confirm that siliciclastic rocks interbedded with Late Triassic chert have predominantly Late Triassic zircon provenance. The mineral modes of the siliciclastic sediments are consistent with derivation from Late Triassic Stuhini Group and correlatives consistent with inferences made by Monger et al. (1991). These results also indicate that Late Triassic (Rhaetian) Kedahda Formation locally unconformably overlies Permian Teslin Formation (Mount Farnsworth) and this relationship is likely also exposed at Hall Lake, where Monger (1975) and Aitken (1959) observed hornblende-bearing wacke in stratigraphic contact with the Permian Teslin Formation.

The present authors' results also indicate that some of the rocks that have been included in the Kedahda Formation are Early Jurassic. This is consistent with inferences made by Monger et al. (1991) that parts of the Kedahda Formation may be correlative with the Laberge Group.

Sinwa Formation

The Sinwa Formation (Hancock Member of the Aksala Formation in Yukon) is a Late Triassic limestone that caps the Stuhini Group (Lewes River Group in Yukon). The present authors do not intend to modify Sinwa Formation; however, it is worth pointing out that Sinwa Formation has been historically restricted to occur only below the Nahlin Fault, which was interpreted as a terrane boundary. Since the Nahlin Fault is not a terrane boundary, Late Triassic limestone of the Kedahda Formation may be correlative with the Sinwa Formation. Kedahda Formation may simply represent different, but coeval, carbonate-chert facies within the same basin.